CURVATURE MICROSTRIP SENSOR

USHASRI KRISHNAN

A project report submitted in partial fulfilment of the requirements for the award of the degree of Bachelor (Hons.) of Electrical and Electronic Engineering

Faculty of Engineering and Science
Universiti Tunku Abdul Rahman

May 2016

DECLARATION

I hereby declare that this project report is based on my original work except for citations and quotations which have been duly acknowledged. I also declare that it has not been previously and concurrently submitted for any other degree or award at UTAR or other institutions.

Signature : _____________________________

Name : Ushasri Krishnan

ID No. : 1300978

Date : _____________________________

APPROVAL FOR SUBMISSION

I certify that this project report entitled **"CURVATURE MICROSTRIP SENSOR"** was prepared by **USHASRI KRISHNAN** has met the required standard for submission in partial fulfilment of the requirements for the award of Bachelor of Engineering (Hons.) Electrical and Electronic Engineering at Universiti Tunku Abdul Rahman.

Approved by,

Signature : _______________________

Supervisor : Dr. Lee Kim Yee

Date : _______________________

The copyright of this report belongs to the author under the terms of the copyright Act 1987 as qualified by Intellectual Property Policy of University Tunku Abdul Rahman. Due acknowledgement shall always be made of the use of any material contained in, or derived from, this report.

© 2016, Ushasri Krishnan. All right reserved.

Specially dedicated to

my beloved grandmother, mother and father

ACKNOWLEDGEMENTS

I would like to thank everyone who had contributed to the successful completion of this project. I would like to express my gratitude to my research supervisor, Dr. Lee Kim Yee for his invaluable advice, guidance and his enormous patience throughout the development of the research.

In addition, I would also like to express my gratitude to my loving parent and friends who had helped and given me encouragement.

CURVATURE MICROSTRIP LINE

ABSTRACT

In this project, curvature mictostrip was used as a sensor for permittivity measurement of a sample. The design of the microstrip is simple as compared to any other in planar transmission line. Since the design parameters in microstrip is based on the effective permittivity between the substrate and sample placed on it. As for an unknown sample, the permittivity is obtained for a 50 ohm characterized microstrip line. The substrate used is FR - 4 and RT Duroid 6006 with a dielectric constant of 4.3 and 6.15 ± 0.15 respectively which the frequency range falls between 150 kHz to 8 GHz. The design of the microstrip line was interpreted through using AWR Design Environment. For a condition when the sensor is covered by air, then the ideal width of the strip ,w, is 3.1370 mm for FR - 4 substrate while for the RT Duroid 6006 substrate, the width is taken as 0.9316 mm. Beside this, the length of the microstrip line is taken as 40 mm and 70 mm for each substrate. The magnitude and phase response for reflection coefficient and transmission coefficient are done by using Vector Network Analzer (VNA) to the microstrip line with a specified permittivity of the sample. Comparison of the measured data and calculated data provided by AWR simulation will be carried out. Based on the obtained results, there is no sequential order of performance in associated with the curvature effect of the sensor aimed at different sample permittivity and followed by the different line length of the sensor.

TABLE OF CONTENTS

LIST OF TABLES

LIST OF FIGURES

LIST OF SYMBOLS / ABBREVIATIONS

w	width of the microstrip line
t	thickness of the conductor
ε_r	relative permittivity of the substrate Fm^{-1}
h	height of the substrate
TEM	transverse electromagnetic field
ε_o	absolute permittivity 8.854 x 10^{12} Fm^{-1}
$\hat{\varepsilon}$	complex permittivity Fm^{-1}
ε'	real permittivity Fm^{-1}
ε''	imaginary permittivity Fm^{-1}
$\varepsilon_e(f)$	frequency dependant effective dielectric constant
$\varepsilon_e(0)$	effective dielectric constant of the line at DC
$G(f)$	function of frequency of varies form
Γ	reflection coefficient
τ	transmission coefficient
Zc	impedance of the cable, 50 Ω
Zo	characteristic impedance of the microstrip line
ε_{eff}	effective permittivity Fm^{-1}

CHAPTER 1

INTRODUCTION

1.1 Background of Microstrip Line

The main root for the existence of microstrip is based on the development given by Rumsey and Jamieson in early 1940s. It all started from the coaxial cable with a flat conductor. Simultaneously, the concept of conductor which two slabs was also developed by Hewlett Packard Company. Then Barrett concluded that from thick centre conductor to thin centre conductor could be used which results a small effect on the properties of the transmission line. So, that's how the existence of the stripline came. Stripline is basically placing a metallic strip in between two metal clad dielectric sheets. From here the advancement is grown and microstrip line model was introduced by the IIT (Institute of Technology) Federal Telecommunications Laboratories in Nutley New Jersey, Grieg and Engelmann, around 1952. The difference was removing one of the stripline's ground planes. Eventually, the application of the microstrip has been grown in several fields such as in microwave transmission line, printed microwave circuit, microwave monolithically integrated circuits (MMICs) and also radio frequency integrated circuits (RFICs).

Figure 1.1 shows the evolution of the stripline transmission line. From round coaxial conductor line followed by the square shaped conductor line. Then a rectangular shaped conductor line introduced and enhanced to stripline.

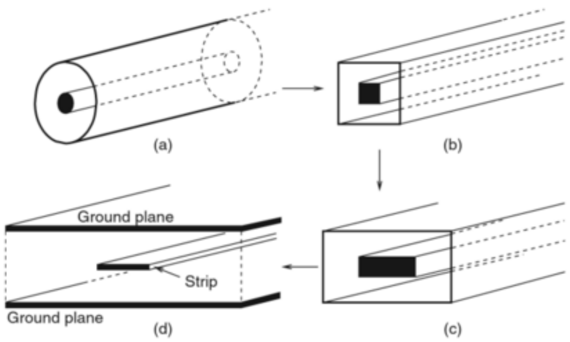

Figure 1.1 Evolution of stripline where (a) coaxial conductor, (b) squared shaped conductor, (c) rectangular shaped conductor and (d) stripline

1.2 Microstrip Line Structure

The structure of a microstrip line consists of a single conductor trace placed on top side of a dielectric substrate and for the bottom side is a single ground which is illustrated in Figure 1.2. The width (w) of the conductor with a thickness (t) placed on top of the substrate of specified relative dielectric constant (ε_r). The height of the dielectric substrate is denoted as (h).

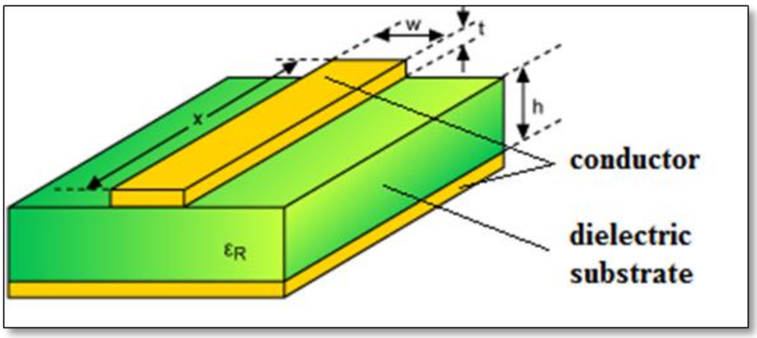

Figure 1.2 Geometry of microstrip structure

This microstrip does not support pure transverse electromagnetic field (TEM) as of the structure is identified as an inhomogeneous type due to fact of the electromagnetic (EM) field lines in the microstrip line are not entirely in the substrate but also propagate external part of the substrate shown in Figure 1.3. This is considered to Quasi transverse electromagnetic field (TEM) which explains that their propagation velocities are dependable on both material properties as such permeability and permittivity as well as the physical dimension of the microstrip.

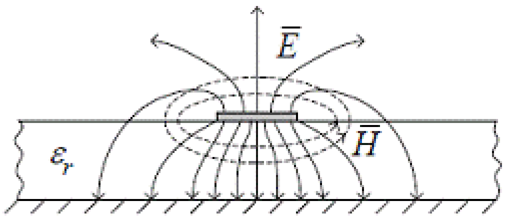

Figure 1.3 propagation of EM field lines

1.3 Microstrip Line for Permittivity Measurement

Planar transmission line has greater flexibility and compact in terms of design when compared to the coaxial lines. Due to advancement in fabrication process, high resolution and high accuracy pattern design of the planar transmission line have been introduced. Beside this, the planar type, the sensor can be designed into either single or double port network in measuring both the transmission and reflection coefficients. (David M. Pozar, 2012)

Coming to this project, the microstrip line is selected to measure the permittivity of the sample within broadband of the microwave frequency signal. For the conceptual view, most of the planar transmission lines: coplanar, stripline, microstrip and coplanar waveguide are similar. The differences in these types are seen in the number of strips on the surface of substrate and the direction of the electromagnetic (EM) wave to the ground. This project a curvature microstrip line is selected to measure the permittivity. The parameter of the length of the line is considered while designing the curvature microstrip.

1.4 Problem Statement

The motivation of this project is to develop a curvature microstrip line using a flexible substrate for broadband permittivity measurement. RT Duroid is chosen due to having low loss factor and ability to produce high level of accuracy in data. However, flat microstrip line that has been developed is only restricted to flat surface of the sample. For curve shaped sample, this flat microstrip does not comply. As a result, for this project the design of curvature microstrip line has been proposed using RT Duroid 6006 which is flexible to amend in curve shaped to certain extend.

1.5 Aim and Objective

In this project, the main aim and objective are

a) To design and construct a 50 Ω curvature microstrip line using RT-Duroid 6006 board for permittivity measurement with different lengths of the transmission line have been shown in accordance to the selective material chosen as a sample filled having of respective permittivity respectively

b) To analyse the performance of the microstrip towards different lengths in the transmission line.

c) To examine the curvature effect of the microstrip sensor of different line lengths towards different permittivity samples.

1.6 Thesis Overview

Chapter 1 focuses on the outline of the brief introduction of microstrip line sensor based on the evolution of the existence and the basic geometry structure. The main objective of this thesis has been stated in this as well.

Coming to chapter 2 is mainly on the literature review on the measurement of dielectric constant and how is it dependant towards the frequency. Alongside with this, the measurement procedures that have been taken in place for planar circuit method in both resonant method and non- resonant method respectively have been explained. On top of that, a brief explanation on the microstrip method has been highlighted in terms of the impedance matching based on the width of the substrate. Appropriate journals have been featured primarily on the permittivity measurement for microstrip line sensor.

For Chapter 3 is on the methodology process involved in the preparation of the sensors for both different substrates. Listing of the dielectric liquid samples which are used for the experiment is also provided with the respective permittivity. Subsequently for chapter 4 is the assortment of the results obtained for the laboratory session. In terms of chapter 5 emphasized on the closure of this thesis followed by the recommendation in refers to enhancement that can be done in further.

CHAPTER 2

LITERATURE REVIEW

2.1 Dielectric Constant Measurement

The occurrence of the interaction of a material with the electric field applied on it and respectively is called as dielectric constant. At times, it is also known as permittivity. The equivalent equation is consisting of both real part and imaginary part of the permittivity. For the real part is signifying as energy storage and energy dissipation for the imaginary part. From the equation, the energy storage is taken as the energy exchange between the field and material thus it operates internally which in turn is considered as the lossless. Coming to the imaginary part is a loss of energy as of it is an absorption of energy.

$$\varepsilon = \varepsilon' + j\,\varepsilon'' \tag{2.1}$$

While relative permittivity ε_r is dimensionless unit

$$\varepsilon_r = \frac{\varepsilon}{\varepsilon_o} = \frac{\varepsilon' + j\,\varepsilon'}{\varepsilon_o} = \varepsilon_r' + j\,\varepsilon_r'' \tag{2.2}$$

where,

ε_o is absolute permittivity 8.854 x 10^{12} F / M

ε_r' is the relative dielectric constant (real) and ε_r'' is the loss factor (imaginary.

Difference in the physical phenomena of the material is related to the presence of the permittivity. The main mechanisms of it are of as such ionic conduction, dipolar relaxation, atomic polarization and electronic polarization. (L.F Chen, C.K Ong, C.P. Neo, V.V Varadan, V.K. Varadan, 2004).

Figure 2.1 shows the graph of permittivity based on various dielectric mechanism based on microscopic level. In the dielectric material, the charges will move opposite in direction when it became polarized to compensate. In the graph, it can be seen that at dipole relaxation and ionic conduction have high interaction at microwave frequency. On contrary, at the atomic and electronic polarization, are weak and almost constant at the microwave range of frequency. Therefore, for different materials, the magnitude of each mechanism is different.

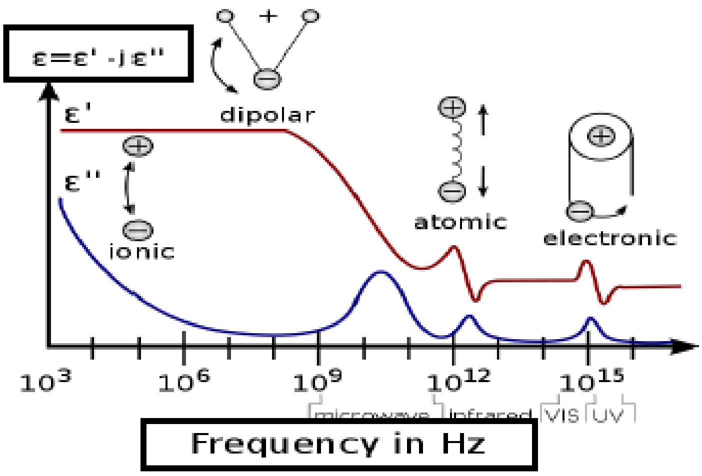

Figure 2.1 Graph of dielectric mechanism over frequency

2.1.1 Dependence on frequency effect

Keeping the fact of the microstrip does not support pure TM wave and its propagation constant is not a linear function of frequency. Consequently, the effective dielectric constant changes along with the frequency. (David M. Pozar, 2012) There would not be a uniform flow of current across the width of the single conductor. In this manner, the distribution varies in accordance with frequency.

The variation of frequency is crucial condition needed to be considered in order to satisfy the parameters of the transmission line. In the microstrip line, the frequency variation of the effective dielectric constant is more significant. For instance, a change in the effective dielectric constant taken in place, and subsequently, result on the effect on the phase delay is shown. Likewise, the difference in the parameters of the transmission line with respect to the frequency variation leads to propagate differently.

$$\varepsilon_e(f) = \varepsilon_r - \frac{\varepsilon_r - \varepsilon_e(0)}{1 + G(f)} \tag{2.3}$$

where

$\varepsilon_e(f)$ is the frequency dependant effective dielectric constant

$\varepsilon_e(0)$ is the effective dielectric constant of the line at DC

$G(f)$ is the function of frequency of varies form

2.1.2 Relationship between of Dipole Moment and Loss Factor

The loss factor of the dielectric material is determined by the presence of the frequency of the EM wave and the conductivity of the dielectric material. Besides this, it is co-related the strength in the interaction of the molecules in the dielectric material. For instance, having strong strength in the interaction of the molecules in the dielectric material tends the EM wave to have slow speed of propagation in turn lead to have high energy dissipation. Dipole moment is based on the strength of the interaction of the molecules.

According to Solomons Fryhle, atoms with different electronegativity form a covalent bond. In this, the electron pairs are not shared equally between two different atoms. Polar convent bond is when the electron pair move towards the atom which of higher electronegativity. Thus, partial positive charge and partial negative charge are created on deficient in electron and rich in electron respectively. A molecule with partial negative and positive charge is present then it is called as dipole moment.

Dipole – dipole interaction is occurred in the contact of one molecule to other molecule of having dipole moment.

2.2 Planar Circuit Method

In practice, these types of transmission lines are widely used in RF and microwave networks. Among all, the common planar circuit design is the microstrip line. Having the fact of easy design and compact, the test sample is used either as substrate or superstrate for dielectric permittivity measurements based on the physical properties of the sample. (M. F. S. Kashif Saeed, Matthew B. Byrne, Ian C. Hunter)

2.2.1 Non-resonant Method

In this method, it has higher accuracy rate over a wide range of frequency band. Thus, as for this main essential factor, it requires lesser sample of frequency. The non-resonant includes two primary methods which are the reflection method and transmission / reflection method.

2.2.1.1 Reflection Method

The basic principle of the reflection properties of a segment in the transmission line are used in determining the measurement of electromagnetic properties of a sample. Nevertheless, for different types of transmission line, the placement of the sample would be different with one and another. From the fundamental of electromagnetic propagation, it is known that if the wave propagation in two different medium, then wave is partially transmitted through and reflected back due to the fact of having different dielectric constant and the characteristic impedance of the medium. As a result, during designing the microstrip line, the parameters of the length and width of the line, permittivity of the substrate were interpreted with the aim to create a matched condition with no reflection back. In contrary, the reflection is seen in input only if it is an unmatched condition.

By referring to the figure 2.2.1.1 shows the difference between the transmission with matched condition and unmatched condition. For the figure 2.2.1.1demonstrated the ideal transmission line with material having of dielectric constant as 1 and the 50 Ω value of the transmission line which is identical to the impedance value of the connected cable. As for this, there would be absence of reflection. Coming to the figure (b) is illustrated as when the dielectric constant is no longer 1 in turn the impedance of the transmission is not equivalent to the impedance of the cable. So, for this scenario, the impedance is thus calculated by means of measuring the reflection coefficient.

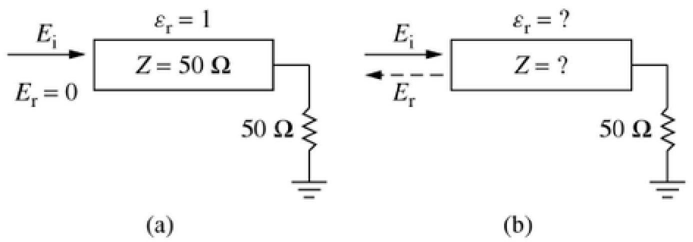

Figure 2.2.1.1 Condition of impedance in accorance to the transmission line

The formula is given as

$$\Gamma = \frac{|Zc - Zo|}{Zc + Zo} \tag{2.4}$$

$$\tau = \sqrt{1 - \Gamma} \tag{2.5}$$

where

Γ is the reflection coefficient

τ is the transmission coefficient

Zc is the impedance of the cable, 50 Ω

Zo is the characteristic impedance of the microstrip line, in Ω

2.2.1.2 Transmission / Reflection Method

For this method, it is determined through the concept of the existence of transmission and reflection in the electromagnetic propagation of waves. From the figure 2.2.1.2, demonstrates the reflection method for different impedance at the terminal.

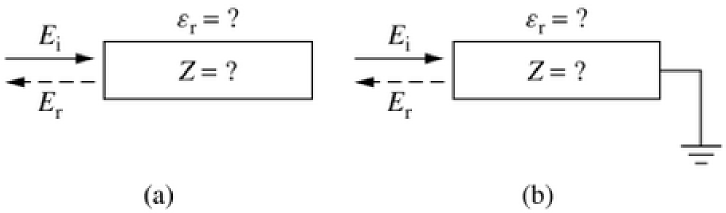

Figure 2.2.1.2 Condition of different impedance in a line

2.2.2 Resonant Method

For resonant method, it only provides results at discrete interval of frequency range in return, it more accurate. Resonator method and resonant perturbation method is used to determine the characteristic the electromagnetic properties of a material.

2.2.2.1 Resonator Method

In this method, the resonance is basically supported by the dielectric itself, thus the sample would act as a dielectric resonator. However, the level of accuracy is high, but there are several factors that falls under the drawback of this method. The first drawback is for one sample, single point of frequency is obtained. In terms of calculating the dielectric constant is tedious by only means the complicated Bessel functions is used. On top of that, the dimension of the sample required is needed to be large in size. Despite these disadvantages, it is commonly used in measuring the dielectric loss as well. Three mainly used techniques are

Table 2.2.2.1 Different technique with respective illustration of the sample placed in a planar circuit method

(i) Post resonance technique	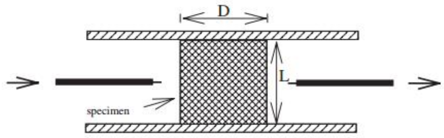
(ii) Cylindrical cavity resonance technique	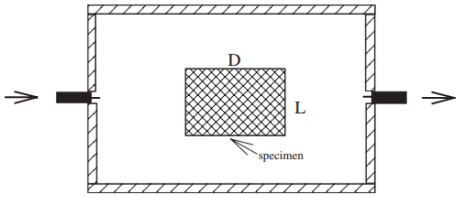
(iii) Waveguide reflection resonance technique	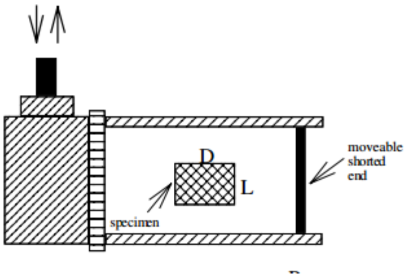

.

2.2.2.2 Resonant Perturbation Method

Regarding the resonant perturbation method, the resonance is supported by the metal walls of a metal cavity. Occurrence of the perturbation on the field distribution in the metal cavity is due the presence of samples in it. Well, the working principle is based on the presence of the shift in the resonant frequency and a decrease in the quality factor of the cavity when the sample is occupied (Jyh Sheen). The figure 2.2.2.2 shows the rectangular cavity.

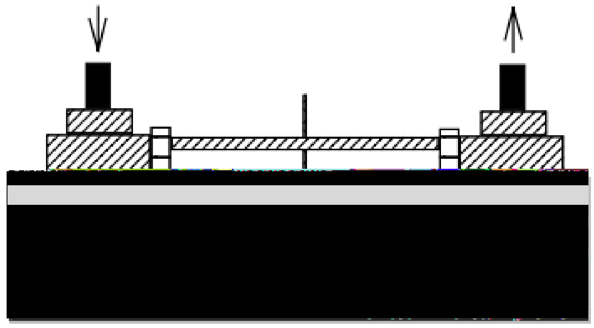

Figure 2.2.2.2 Illustration of resonant pertubation

2.3 Microstrip Line

2.3.1 Effective Dielectric Constant

Effective dielectric constant is known as the dielectric constant of a homogeneous medium that replaces the air and the dielectric substrate used in the microstrip design. However, the dielectric constant of a substrate will be greater than air. Due to this, the propagation velocity falls between the speed of radio waves in the substrate and the speed of radio waves in air. Therefore in most of the time, the effective dielectric constant is slightly less than the substrate dielectric constant because part of the fields from the microstrip conductor exists in the air.

According to Bahl and Trivedi, the effective dielectric constant can be calculated through the formula given below. Two cases are given based on the ratio of the width and thickness of the microstrip line when W/H is less than 1 and when W/H is greater than or equal to 1. This is an approximation made for the effective dielectric constant regardless the microstrip lines thickness and frequency dispersion as their effects are usually small.

$$\varepsilon_{eff} = \begin{Bmatrix} \frac{\varepsilon_r+1}{2}+\frac{\varepsilon_r-1}{2}\left[\left(1+12\left(\frac{h}{w}\right)\right)^{-1/2}+0.04\left(1+12\left(\frac{h}{w}\right)\right)^{2}\right], when \ \frac{w}{h}<1 \\ \frac{\varepsilon_r+1}{2}+\frac{\varepsilon_r-1}{2}\left[\left(1+12\left(\frac{h}{w}\right)\right)^{-1/2}\right], when \ \frac{w}{h}\geq 1 \end{Bmatrix} \quad (2.6)$$

Where

ε_{eff} is the effective permittivity Fm^{-1}

ε_r is the relative permittivity Fm^{-1}

h is the thickness of the substrate

w is the width of the microstrip line

2.3.2 Characteristic Impedance

The characteristic impedance of a microstrip line is based on the value of the dielectric constant and the physical parameters of such thickness of the substrate and the width of the conductor. It represented in the complex form, as from the basics, the real part of the impedance is identified as the resistance while the imaginary part is called as the reactance. The behaviour of reactance is due to the presence of the capacitors and inductors. For the period of AC, a significant variation of the reactance is displayed in which is dependent to the frequency. For the resistance part, the current is in phase with the voltage in both AC and DC regardless with the existence of the frequency.

Having the parameters of the microstrip line, the characteristic impedance is calculated as

$$Zo = \begin{cases} \dfrac{60}{\sqrt{\varepsilon_{eff}}} \ln\left(\dfrac{8h}{w} + \dfrac{w}{h}\right) & , when \quad \dfrac{w}{h} < 1 \\ \dfrac{1}{\sqrt{\varepsilon_{eff}}}\left(\dfrac{120\pi}{\left[\dfrac{w}{h} + 1.393 + 0.667 \ln\left(\dfrac{w}{h} + 1.444\right)\right]}\right) & , when \quad \dfrac{w}{h} \geq 1 \end{cases} \tag{2.7}$$

where

Zo is the characteristic impedance of the microstrip line, Ω

w is the width of the microstrip line

h is the thickness of the substrate

The main ratio is between the width of the line and thickness of the substrate is essential in determining the characteristic impedance. From the equation displayed, if the ratio is less than 1, the characteristic impedance is sensitive to the width of the microstrip. On the other hand, when the ratio is greater or equal to one, it is less sensitive.

2.3.3 Correlation of the width of substrate and matching impedance

The width of the microstrip plays a crucial role in designing a simple microstrip line. The width is dependant to the characteristic impedance of the microstrip line. In order to determine the optimum width of the microstrip line for the proper design of line, the impedance of the microstrip line has to match with the impedance of the coaxial cable transmission line. Hence, it is known as the matching impedance. The EM wave will totally transmit to the other medium if and only if the impedance of both the mediums is matched. If the impedance between the microstrip and the coaxial cable is partially matched, the EM wave would not be totally transmitted into the microstrip line. Partial EM wave will reflect back to the coaxial cable. Thus, the amplitude of the transmitted EM wave is very low.

2.4 Microstrip Method

It is known microstrip method is widely used in the characterization of the electromagnetic properties of materials because of having high accuracy in obtaining data.

2.4.1 Transmission Line Method

According to Hinojosa, the sample test used as a substrate for the microstrip line development determining the electromagnetic properties of the substrate sample are obtained from the transmission and reflection properties of the microstrip circuit. In fact, there would not be any air gap between the strip and substrate.

In terms of calculation, it is done through the S – parameter measurement at the microstrip planes labelled as P_1 and P_2 in the figure of measurement fixture below and the wave propagation was done in quasi TEM mode. It mainly includes two steps through using S- parameters: a) direct problem and b) inverse problem. Direct problem involves the computation of S -parameters at the access planes of the microstrip cell under test propagating only the quasi-TEM mode, according to the complex substrate properties as such μ_r and ε_r, the cell dimensions and the frequency. With these values are given, and then effective permittivity and permeability followed by the complex characteristics impedance are calculated. From here, the S- parameters can compute by the reflection / transmission method. For the inverse problem, is the iterative technique in which carries out the μ_r and ε_r alongside with the convergence of the S-parameters between measured values and calculated values obtained from the direct problem through the successive increment initial values.

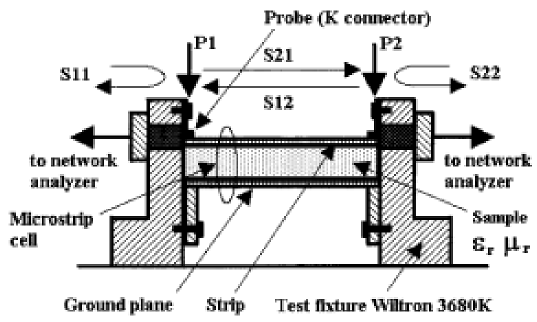

Figure 2.4.1Illustration of the transmision line method

In this method, it gives the accurate results when the length of the microstrip line is long. It works well in the condition of the transition effect of coax -to – microstrip where the permittivity of the substrate sample is known earlier, so that the characteristic impedance of the test section is designed around 50Ω.

2.4.2 Thin film Transmission / Reflection Method

In generally it works on the principle of the transmission / reflection method on the microstrip circuit with sample being placed on it. But, this method is inaccurate in the measuring the permittivity as due to it imposes a strict restriction on the dimensions of the sample which needed to fill up the entire cross section of the substrate. For thin films, it implies the propagation of the electromagnetic wave along the sample thickness, as a result the measurement sensitivity is low.

According to Queddelec, a broad band characterization method has been developed that can be applied to thin films and thick sample also. The method is based on the measurement of the S -parameters of reflection and transmission coefficient in determining the permittivity as well as permeability. In fact, the thin film does not entirely fill the cross section of the substrate indicated in the figure 2.4.2.

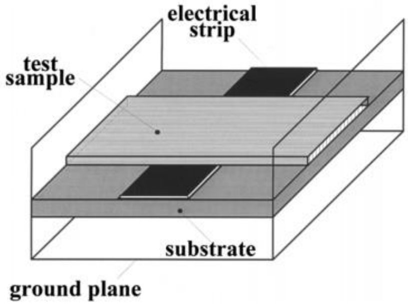

Figure 2.4.2Illustration of microstrip with sample placed

For the calculation of permittivity is done from the measured S- parameters with optimization procedure (direct problem) and the full wave analysis of the cell (inverse problem). The purpose of full wave analysis is to provide precise information of the material properties. For direct problem, function of permittivity and permeability is produced by first determining the dispersion characteristics of the microstrip line which is done through analyzing the cross section of it. The second step is calculating the S- parameters imposing continuity conditions on electromagnetic fields at the edge of the cell. Coming to the inverse problem is done by matching the calculated and measured values of the S- parameter through using the optimization procedure. Optimization procedure is the minimizing the function with several variables.

2.4.3 S-parameter measurements with three equidistant positions

For this method is done by three sets of S-parameter measurements of the microstrip line together along an obstacle in three equidistant positions over the line shown in the figure below. (Prasanth Moolakuzhy Narayanan, 2014). Criteria for the obstacle should exhibit a reflection and transmission loss within the range of 4–12 and 2–30 dB, respectively thus, a section of CER-10 copper-clad PCB was used. The obstacle is placed on the metal side of it is in touch with the trace of the microstrip line. The approach is done by using Line Network Network (LNN) calibration technique in which it delivers the electrical wavelength or the relative permittivity of the transmission line without direct connection (Heuermann Holger , 1997). The main advantage of this method is that it has minimum issues on the effect of sample connector non-reproducibility and impedance mismatch. But it can be applied for the measurement of which the frequency falls beyond the range of 4 GHz because of the placement of the obstacle produces error in the permittivity value. In short, with high permittivity in turn small error in the obstacle positioning will cause large error in the electrical length of the line. However, this problem is overcome through the use of high accuracy motor positioning method fixture with slots as it could eliminate the effect of impedance mismatch and calibration errors by self-calibration technique (I.Rolfes , 2007).

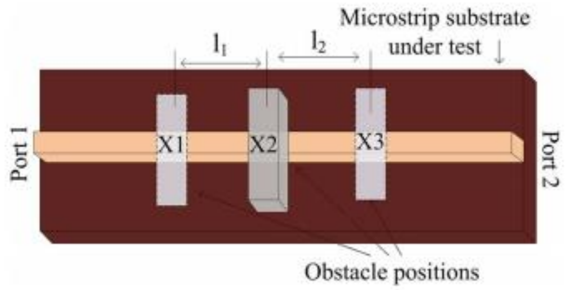

Figure 2.4.3 Diagram of three different position of sample on the line

2.4.4 Permittivity Measurement for Metamaterials

Metamerials are those materials engineered to have produce properties that don't occur naturally. According to Nesimoglu and Sabah, the characterization of metamatrials is through a technique of S-Shaped resonator (SSR) on the front side of the substrate and a feeding transmission line (FTL) on the back side of the substrate illustrated in the figure below. In one –sided SSR, the electric resonance (the coupling between the electric field and the gap creates electric resonance when the indicated EM wave excites the metamaterials) is successfully tuned by deforming the symmetry of the SSR (Nesimoglu Sabah Karaali, 2014). This method the SSR was excited using a 50 Ω feeding transmission line on the back side of the substrate and a grounding frame was inserted around the SSR. Thus the metamaterial can be excited and measured by using standard test equipment using coaxial SMA connectors. From the theory of MTMs, the real parts of the permittivity and permeability must be negative at a certain frequency region (V. G. Veselago, 1968).

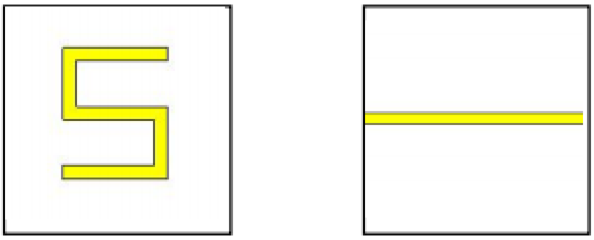

Figure 2.4.4 Diagram of the geometry of the microstrip line on both sides

2.5 Analysis of Curved Microstrip

For the recent days, most of the electronic systems often implemented in curved surfaces, therefore an analysis of the microstrip transmission line with curved substrate becomes a necessity. Researchers have made the analysis of microstrip transmission line in accordance to a shape of cylindrical surface (N. G. Alexopoiilos and A. Nakatzni, 1988) or elliptical surface (F. Medina ,M. Harno,1990). According to X. Q. Sheng, E. K. N, Yung, and C. H. Chan, to analysis the effect of the microstrip line with finite width curved substrate is done by applying the fast and accurate finite element boundary-integral method to simulate the field in the transmission line. Subsequently, in determining the characteristic parameters of the transmission line is by using the a super-resolution estimation of signal parameters via rotational invariance technique (ESPRIT) algorithm (R. Roy, A. Paulraj, and T. Kailath, 1986)

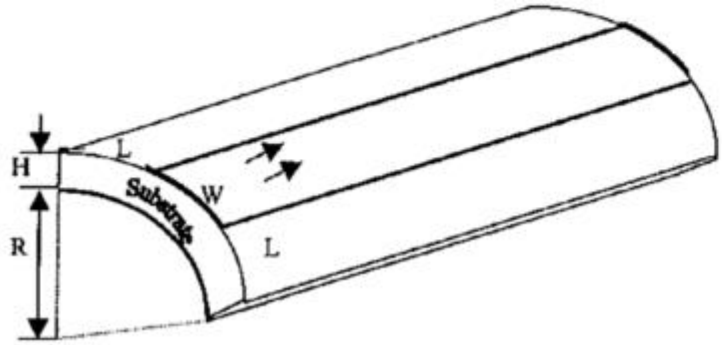

Figure 2.5.1 Microstrip line with finite –width curved surface: w – width , R - curvature of the substrate , H - substrate thickness, ε_r - dielectric relative permittivity

The current distribution is obtained from the method of fast and accurate finite-element boundary-integral method which is able to extract the propagation characteristics. Whereas to extract the characteristic parameters of transmission line by using (ESPRIT) algorithm as it has stability with respect to noise.

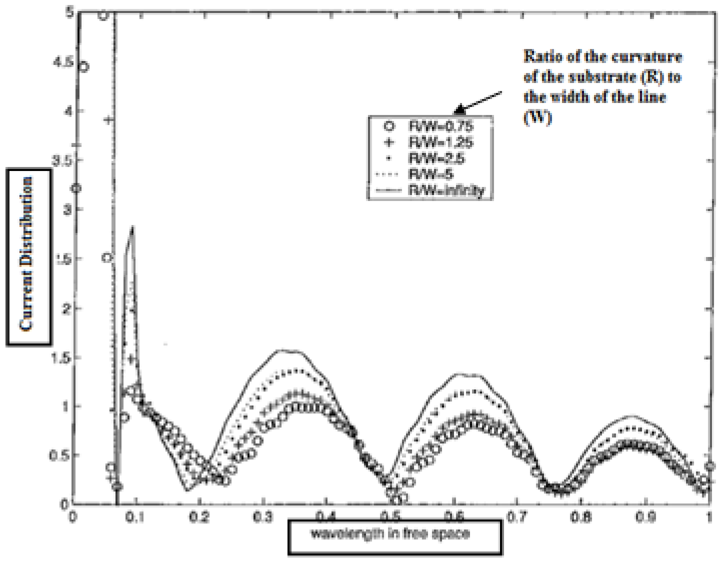

Figure 2.5.2 Graph of the current distribution of microstrip with different substrate curvatures

Figure 2.5.2 presents the distribution of the current on the curved microstrip. It can be seen that the current distribution on the line forms a standing wave beyond an appropriate reference plane. For the maximum values of the standing wave are not equal for different segments as it is caused by the radiation from the finite width of the substrate and the reflection from the finite length of the transmission line.

According to Weisshaar and Tripathi, the results obtained for the scattering parameters of the curved microstrip bend converge very fast with increasing number of higher order modes considered and have been shown to be consistent for large curvatures and bends with small angle.

Figure 2.5.3 shows the magnitudes of the scattering parameters of three different curved microstrip of 50 Ω. It can be seen that for all the three cases, an improvement in the transmission properties with respect to the right-angle and chamfered right-angle bends is evident for high frequencies.

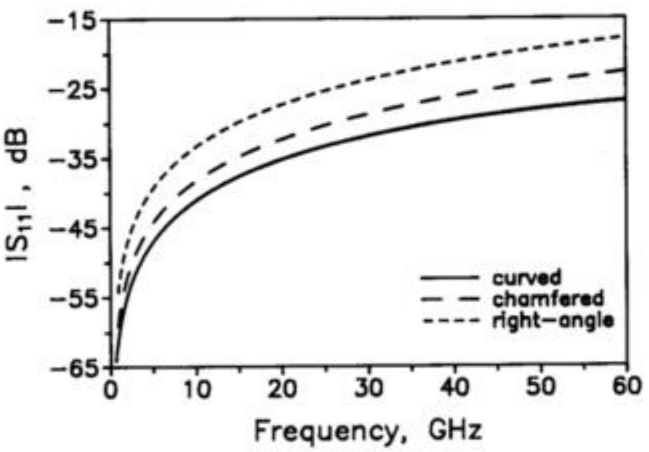

(a)

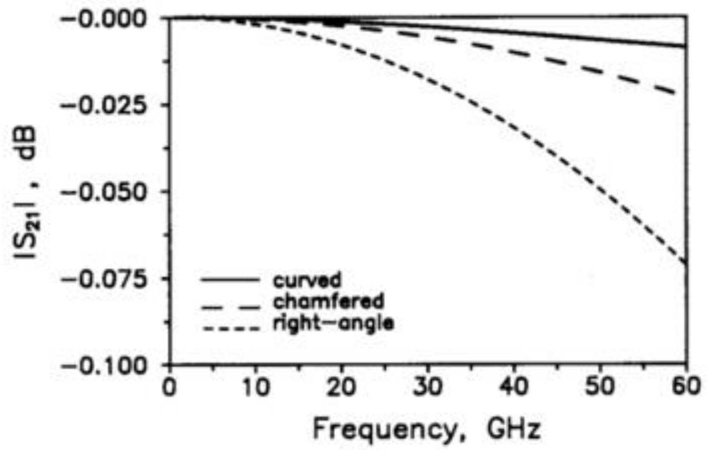

(b)

Figure 2.5.3 Graph Magnitude of (a) the reflection coefficient and (b) the transmission coefficient as a function of frequency for a curved microstrip with different angle bends in the line

CHAPTER 3

METHODOLOGY

3.1 Design of Microstrip Line

In terms of designing the sensors, the FR – 4 substrate and RT Duroid 6006 substrate was chosen independently. For FR – 4 substrate has higher losses and unable to bend when compared to the RT Duroid 6006 substrate. The formula and equations which define the characteristic impedance and effective dielectric constant were studied in order to obtain the optimum width for different length of microstrip line sensor. By means of using TXLine from AWR Design Environment software, the optimum width is attained. By setting the material parameters in regard to the dielectric constant, type of the conductor based on the required design. Thus, the optimum width for FR – 4 substrate is about 3.1370 mm while for the RT Duroid 6006 substrate, the width is taken as 0.9316 mm.

3.2 Construction of Microstrip Line

The construction of the microstrip line model is done in several steps ahead. The flow of preparation the microstrip is illustrated below. First task is the collection of appropriate materials needed as such FR4 substrate, RT Duroid 6006 substrate, launchers, sand paper. The following step is the printing of the microstrip line on the FR-4 and RT Duroid 6006 substrates and followed by the soldering of the launcher

3.2.1 Process of Fabrication

The process is started with a preparation of photomask with an assigned measurement of microstrip line required. Initially, the size of the microstrip line is drawn in AUTOCAD software and with this is later printed on the tracing paper by means of a laser printer. In the tracing paper, the black mark colour is used to avoid the contact of the ultraviolet (UV) light to pass through it. This in turn affects the resolution of design that being transferred to the surface of the microstrip line.

Once the preparation of photomask is done, the subsequent process is called as photolithography. It is the circuit is being transferred to FR-4 substrate and RT Duroid 6006 coated with photoresist. As from the purchasing, both the substrates are with photoresist is readily available and thus expedited the process. Followed by this step, is the alignment and exposure process. The tracing paper is placed on the substrate in result direct contact which lead the UV light can pass through the visible pattern from the tracing paper and expose the photoresist. Leaving for couple of minutes, the substrate is removed from the exposure machine. Then, the boards are submerged into a solution of sodium hydroxide, NaOH, in this procedure, it removes the exposure part photoresist and thus, the desired pattern is shown. Later, the board is placed on the rack to dry up. During this process, all the procedure taken in place are needed to avoid any direct contact from the sunlight as due to the reason that it is sensitive only towards the UV light.

The next phase is the etching process is done by placing the board into the chemical etching process filled in by solution of peroxy sulfuric. The presence of this solution is used to remove the copper. Once this is complete, the board is thoroughly cleaned up with water and set aside to dry up.

In the finishing step, manual cutter is used in the cutting of the board done in a rectangular in shape alongside with the size of the diameter of the microstrip line printed on. The edges of the board were smoothed via sandpaper.

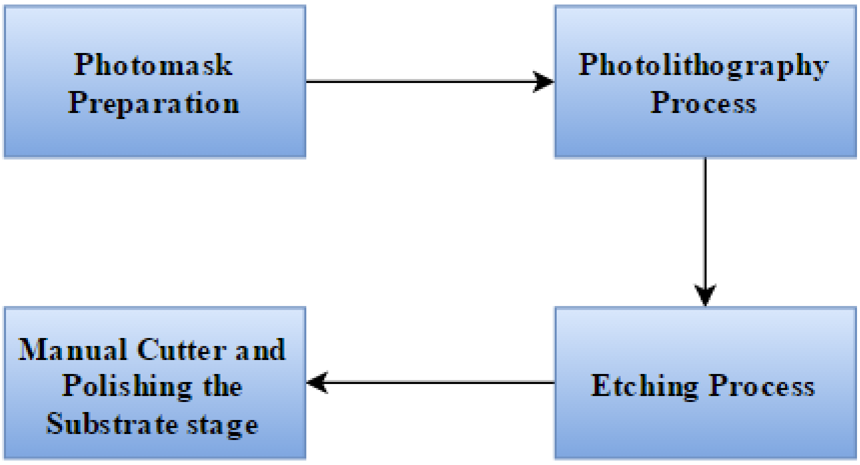

Figure 3.2.1 Flow chart of overall fabrication process

3.2.2 Process of Soldering Launcher

With the board is prepared, the connectors were soldered at the bottom of the microstrip line. Those connectors are placed exactly below the both ends of the line. But before that, the launchers are required to be selected based on the precise type for both the FR-4 board and RT Duroid 6006 respectively that needed to be soldered at the sides. The connectors needed to ensure that it is tightened towards the microstrip. Otherwise, there would not a connectivity if it is placed in lose.

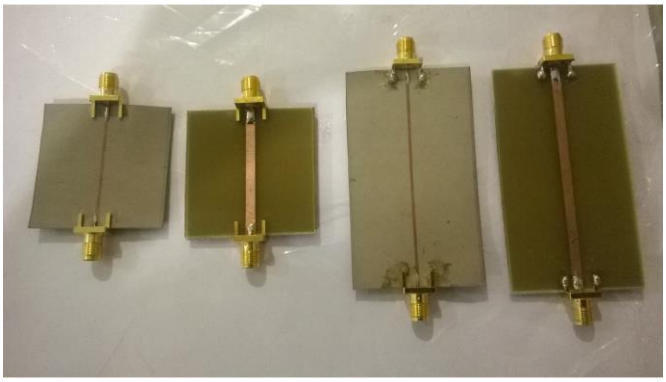

Figure 3.3.1 Image of the Microstrip sensors of 4 cm and 7 cm for FR -4 and RT Duroid 6006 substrates respectively

3.3 Measurement Setup

Once the fabrication and soldering processes are done, the sensor is then connected to VNA anlyzer. The microstrip line sensor is connected to the VNA by means of coaxial cable. Coming to temperature, it would be set in accordance to the laboratory with the standard value of 25° C and the frequency range of the EM wave lies from 150 kHz to 8 GHz.

In terms of the calibration, it is done before preceding the experiment. The standard calibration tools are (TOSM) – Through, Short, Open and Match. When this is done, the sample is placed in a plastic container. Then the experiment will be carried out having different samples on the microstrip line. The VNA is set as to magnitude of transmission coefficient mode. The waveform is the compared between the measured waveforms from the VNA analyzer and the simulated waveform from the AWR software.

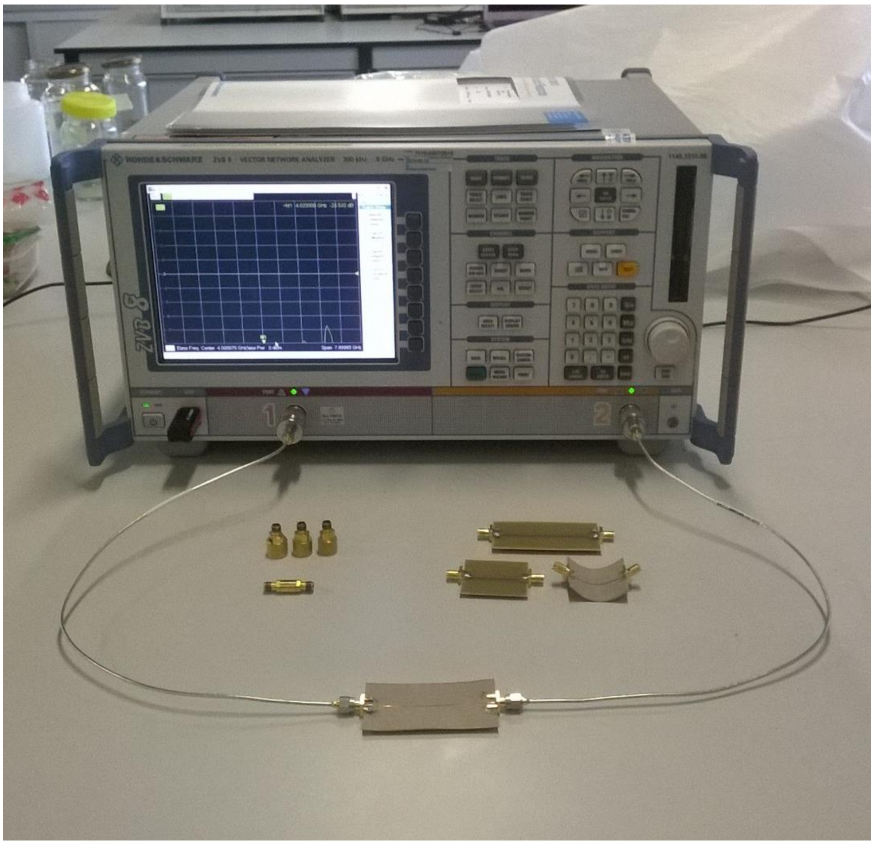

Figure 3.3.1 Image of Measurement setup that has been made during the experiment

3.4 Sample Preparation

To examine the performance towards different curvature effects with wide range samples have been chosen. In table 3.1 listed is the several types of liquid samples with respective permittivity. The reason of selecting this range was to first to analyse the extreme condition as such air and sample water of dielectric constant of 1 and 80 respectively. To avoid any hazardous type of liquid was taken as a preventive measure when conducting the experiment using the VNA network analyzer. Thus liquid sample of acetone, ethanol, methanol and glycerol were considered. Subsequently, for testing purpose sample permittivity is picked on different range among other samples as to cover wider scope.

For placing the sample on the microstrip line sensor, plastic bag was preferred during conducting the experiment. The reason behind this was restricted to have a thin layer between the sensor and the sample with the intention to minimize the interference throughout the experiment. In the figure 3.5.2 shows the placement of the sample on top of the microstrip sensor that has been sealed with the elastic rubber band. To prevent any leakage of sample in the course of the experiment so as to avoid the damage the equipment used. Beside this, the plastic bag is flexible as it is possible to place the sample on the sensor with the presence of certain bending angle effect.

Table 3.4.1 Liquid samples with respective dielectric constant

Liquid Sample	**Dielectric Constant**
Air	1
Acetone	20.7
Ethanol	24.3
Methanol	33.1
Glycerol	42.5
Water	80

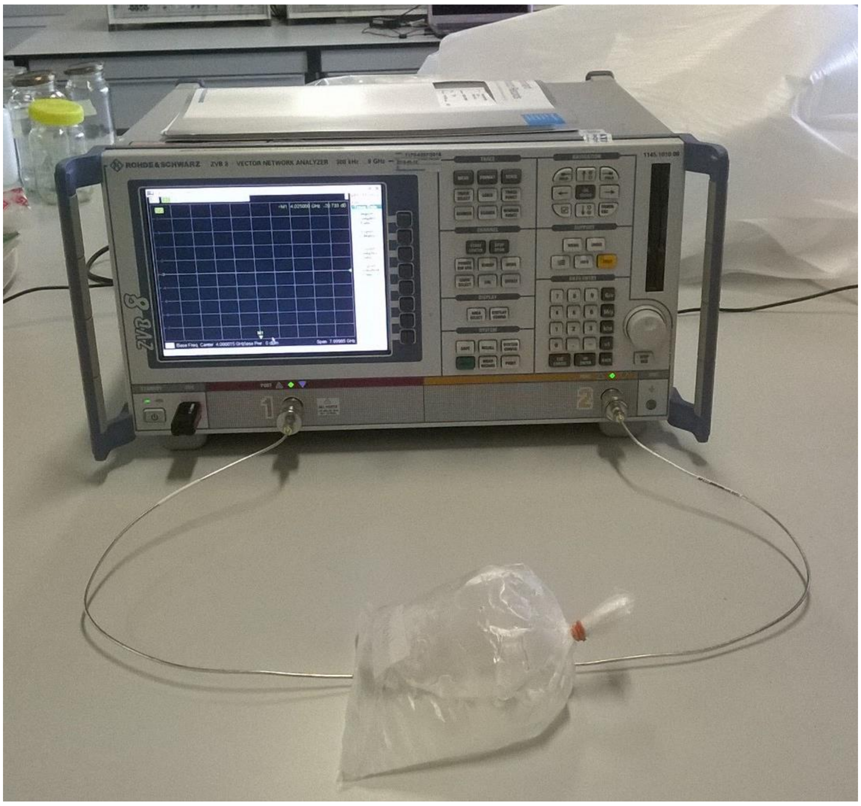

Figure 3.4.2 Demonstration on placement of sample on the sensor

3.5 Provision of the Curvature Effect

Since the main purpose is to examine the curvature effect of the microstrip sensor, certain bending angles were designated**.** Measurement of the bending angle is done with the purpose of applying the same bending angle for different line lengths of the sensor. Coming to analysing the result, it is convenient to examine the behaviour of the performance given in for each sample used in the experiment. Given that in the AWR Design Environment software, it is unable to generate the simulated data for different bending angles of the microstrip sensor as it is only restricted to flat surface. Therefore, the performance is just compared between the measured data from flat surface to different bending angle. The first bending angle was selected as it is close to flat surface which is about 20° angle and the next bending angle was to the extreme of 50° angle. The maximum bending angle is preferred at 50° as it has to comply with both the sensor line length and also to prevent the substrate snapped out seeing that the thickness of the RT Duroid 6006 substrate is thin.

CHAPTER 4

RESULTS AND DISCUSSIONS

4.1 Acquired Results

In this project, the RT Duroid 6006 substrate is used to design the microstrip line with relative permittivity of 6.15 ± 0.15. The height of the substrate between two conductor layers is about 0.635 mm. for the thickness of the conductor is taken as t is 0.0025 mm. The optimum width is taken as 0. 9316 mm. Two length conditions are taken to experiment of the permittivity measurement for the curvature microstrip line sensor which is about 40 mm and 70 mm respectively.

Comparison of the transmission coefficient from the measured value obtained from experimentally and with the simulated values attained from the AWR Design Environment. The main objective is to check the measurement of the permittivity taken in place for the curvature of the microstrip line.

4.2 Comparison of measured data for flat RT Duroid 6006 substrate with the different line length

For this section, the data displayed for the following samples are the magnitude response and the phase response. The comparison is made between the flat surface of RT Duroid 6006 substrate with transmission line length of 4 cm and 7cm respectively. In terms of the transmission coefficient, it can be seen that the magnitude response is lower for the case when the length of microstrip line is longer. This is due to when the length of the microstrip line is longer, it affect the EM wave propagation throughout the line. The major difference comes under the involvement of the loss factor towards the transmission line. As the frequency increases, the magnitude of reflection coefficient increases while it decreases for the transmission coefficient. As for the magnitude response for transmission coefficient, it can be interpreted that the range of magnitude of a selective frequency range lies in the same margin. For instance, at 3 GHz frequency, the margin of the magnitude response lies within the specified range with different line length of the sensor. This is applicable for all the samples used from air till sample water. Since there is difference in the line length of the sensor, there is shift in both of the phase responses.

a)

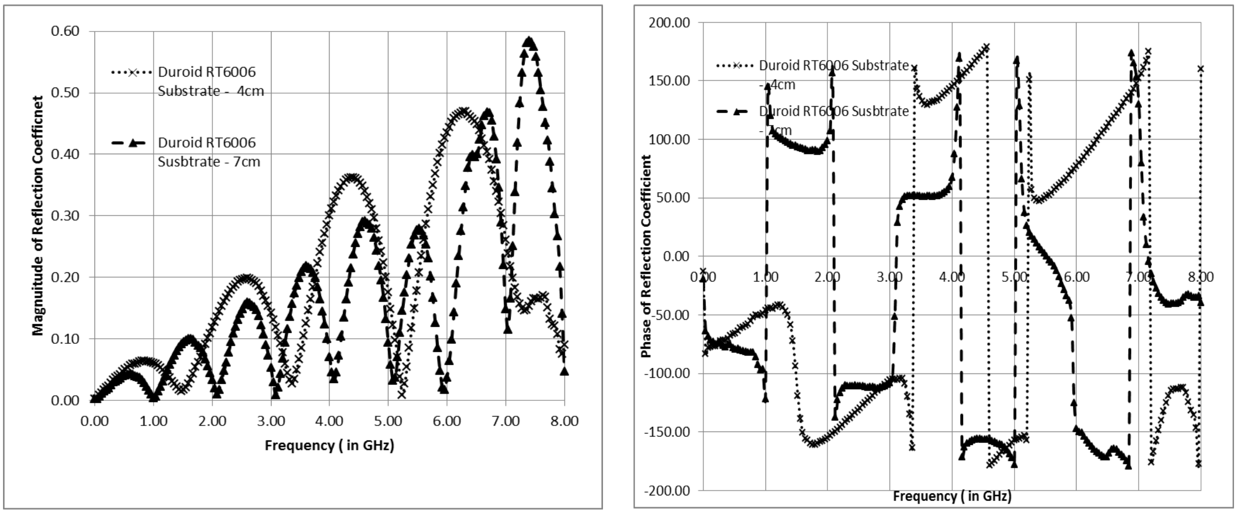

b)

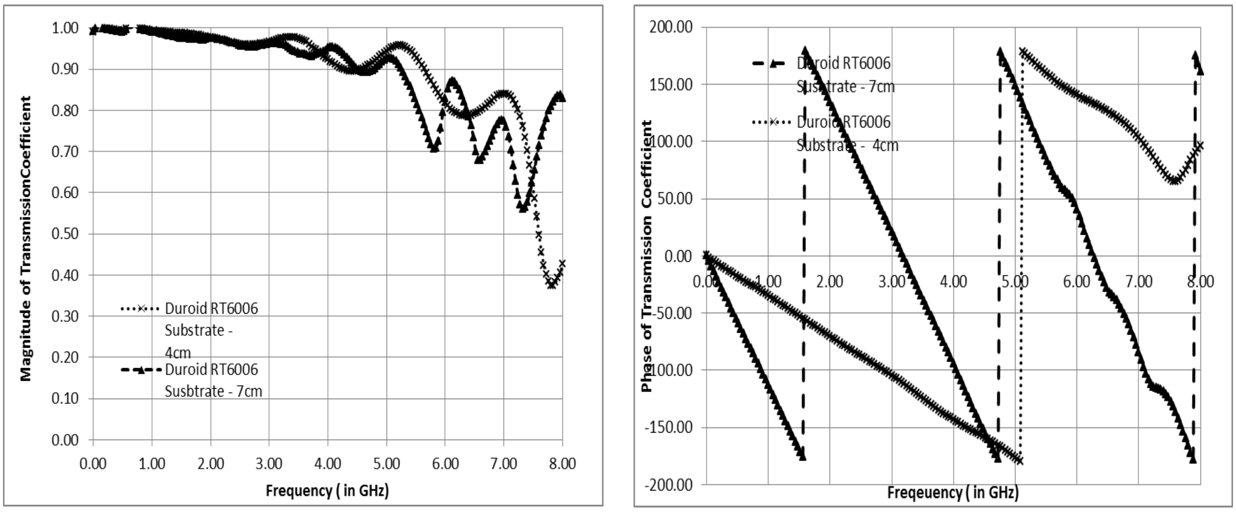

Figure 4.2.1 a) Reflection Coefficient & b) Transmission Coefficient for sample Air against frequency

a)

b)

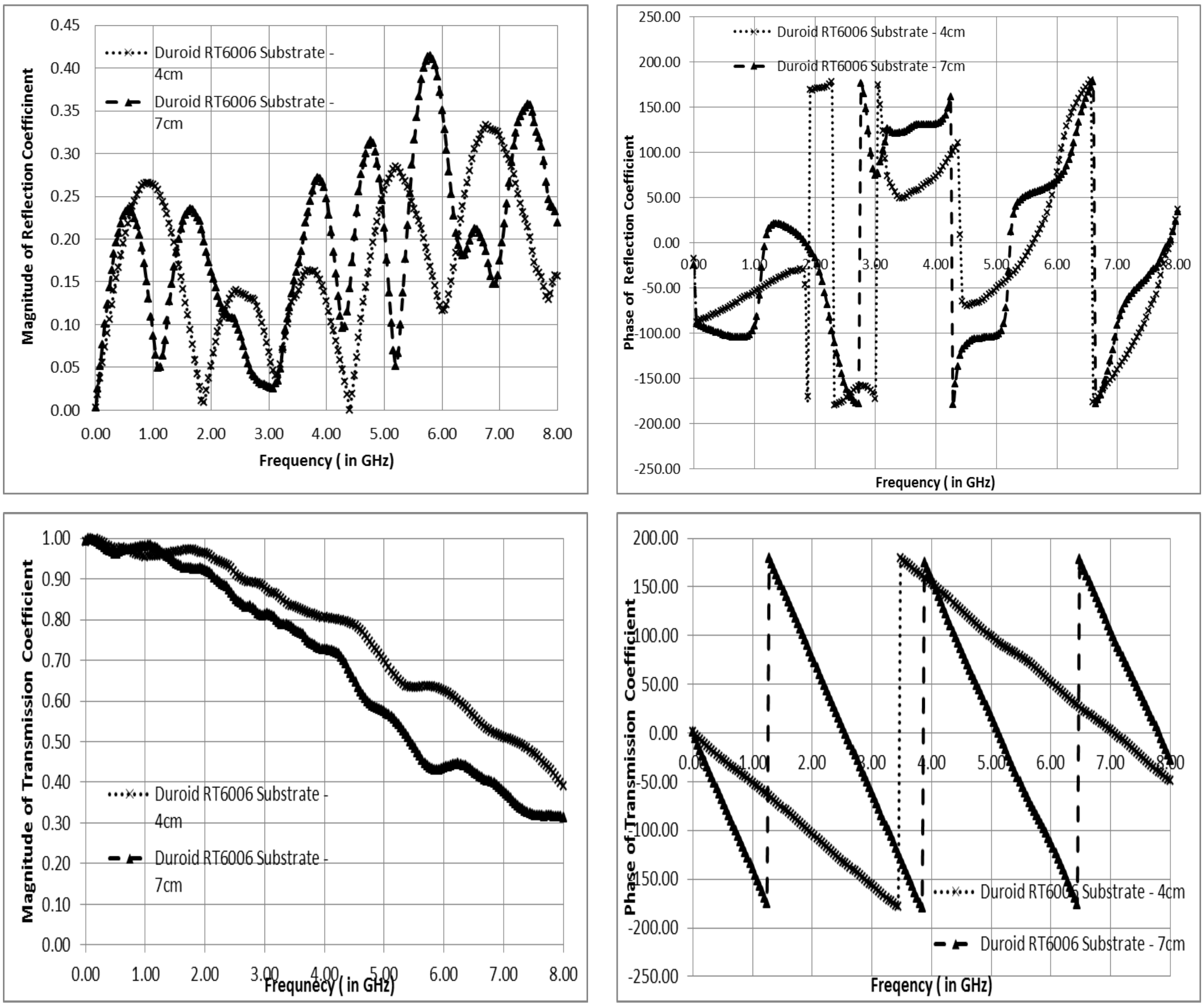

Figure 4.2.2 a) Reflection Coefficient & b) Transmission Coefficient for sample Acetone against frequency

a)

b)

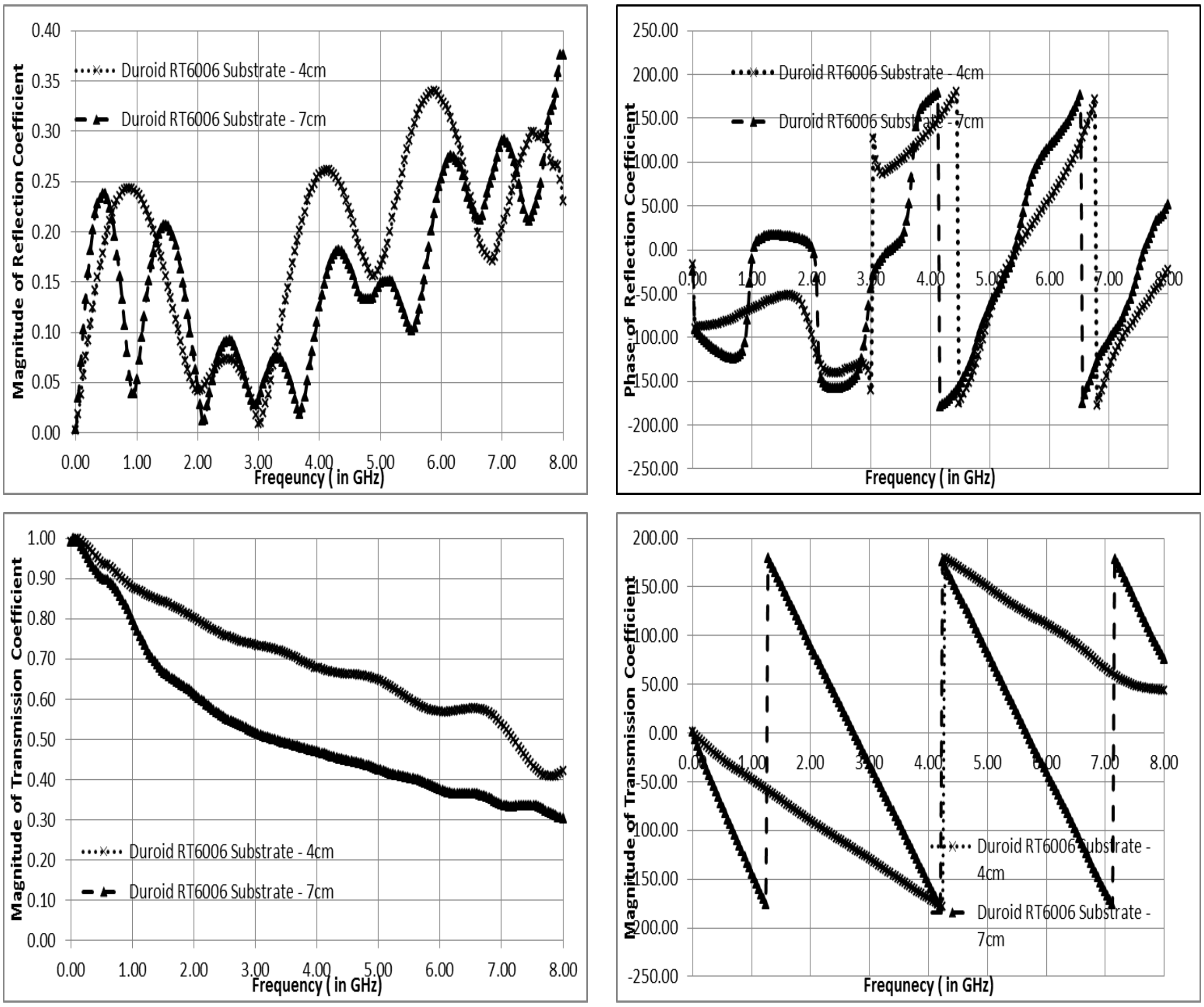

Figure 4.2.3 a) Reflection Coefficient & b) Transmission Coefficient for sample Ethanol against frequency

a)

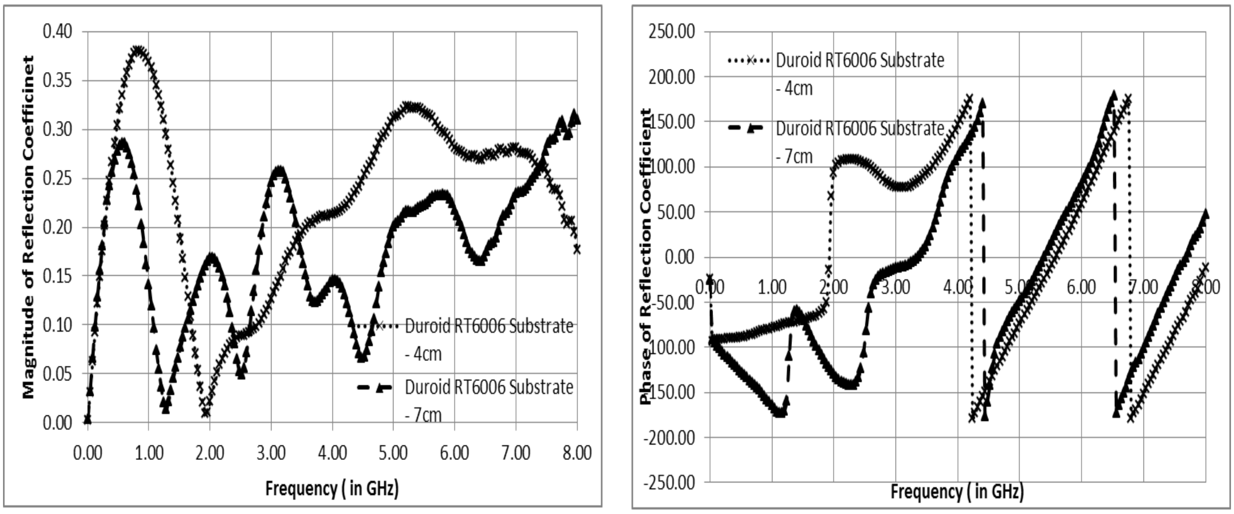

b)

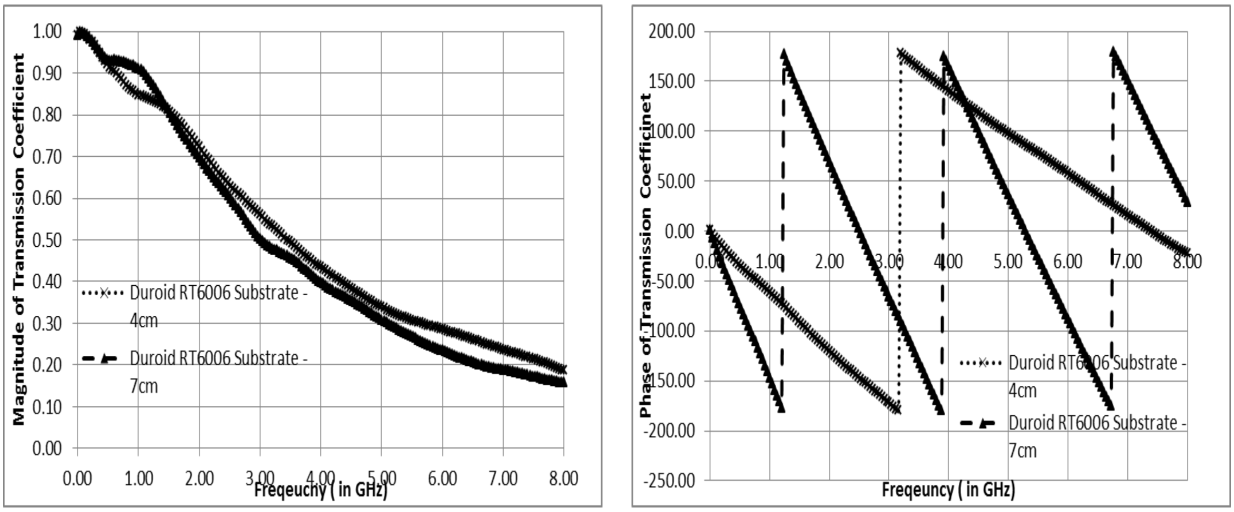

Figure 4.2.4 a) Reflection Coefficient & b) Transmission Coefficient for sample Methanol against frequency

a)

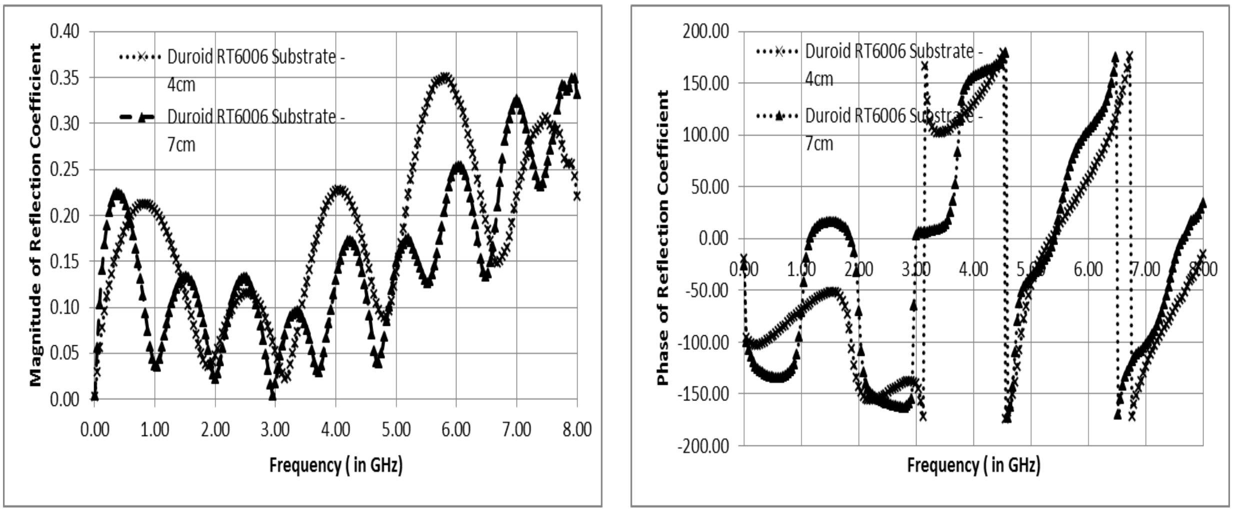

b)

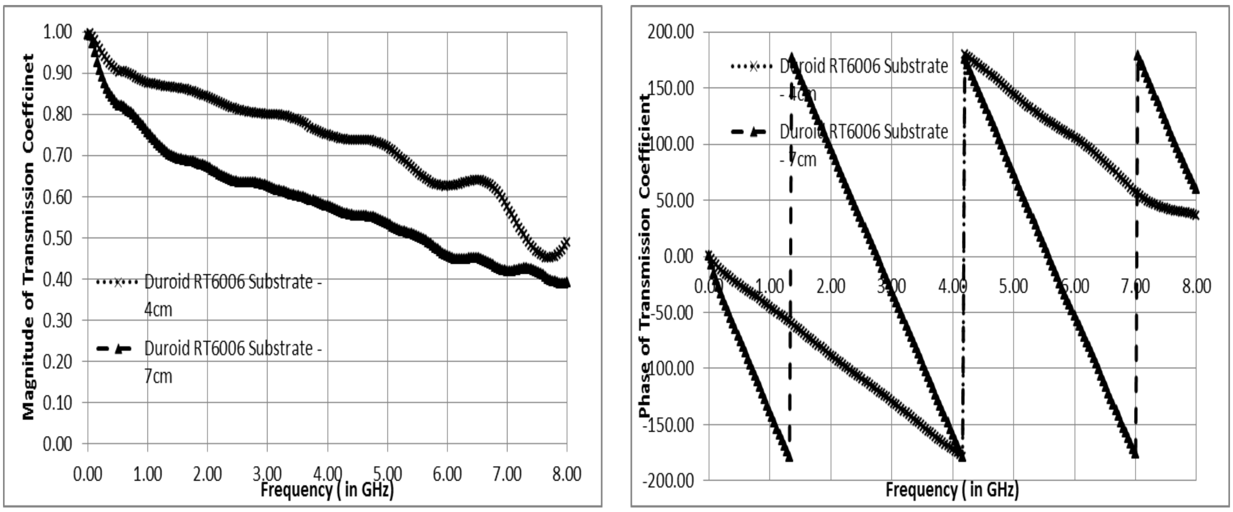

Figure 4.2.5 a) Reflection Coefficient & b) Transmission Coefficient for sample Glycerol against frequency

a)

b)

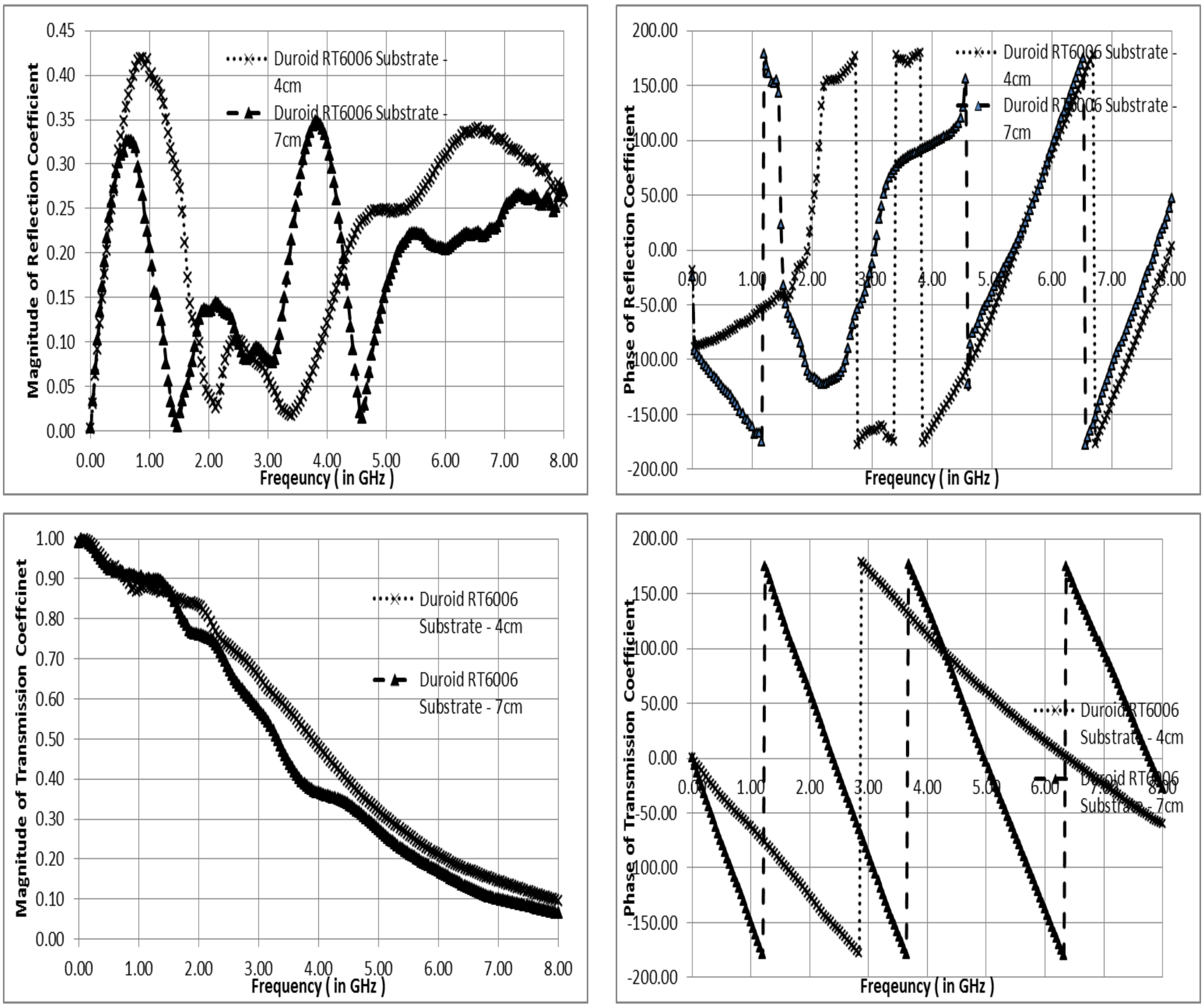

Figure 4.2.5 a) Reflection Coefficient & b) Transmission Coefficient for sample Water against frequency

4.3 Comparison of measured data for 20° RT Duroid 6006 substrate with the different line length

The performances of the transmission and reflection coefficient have been observed when there is presence of certain angle in the microstrip line sensor. At the first step, small bending angle is done which is about 20° at the centre of the sensor. For all the samples that being tested, it can be comprehended similar to the flat version but the range of magnitude response of reflection coefficient is slightly lower.

a)

b)

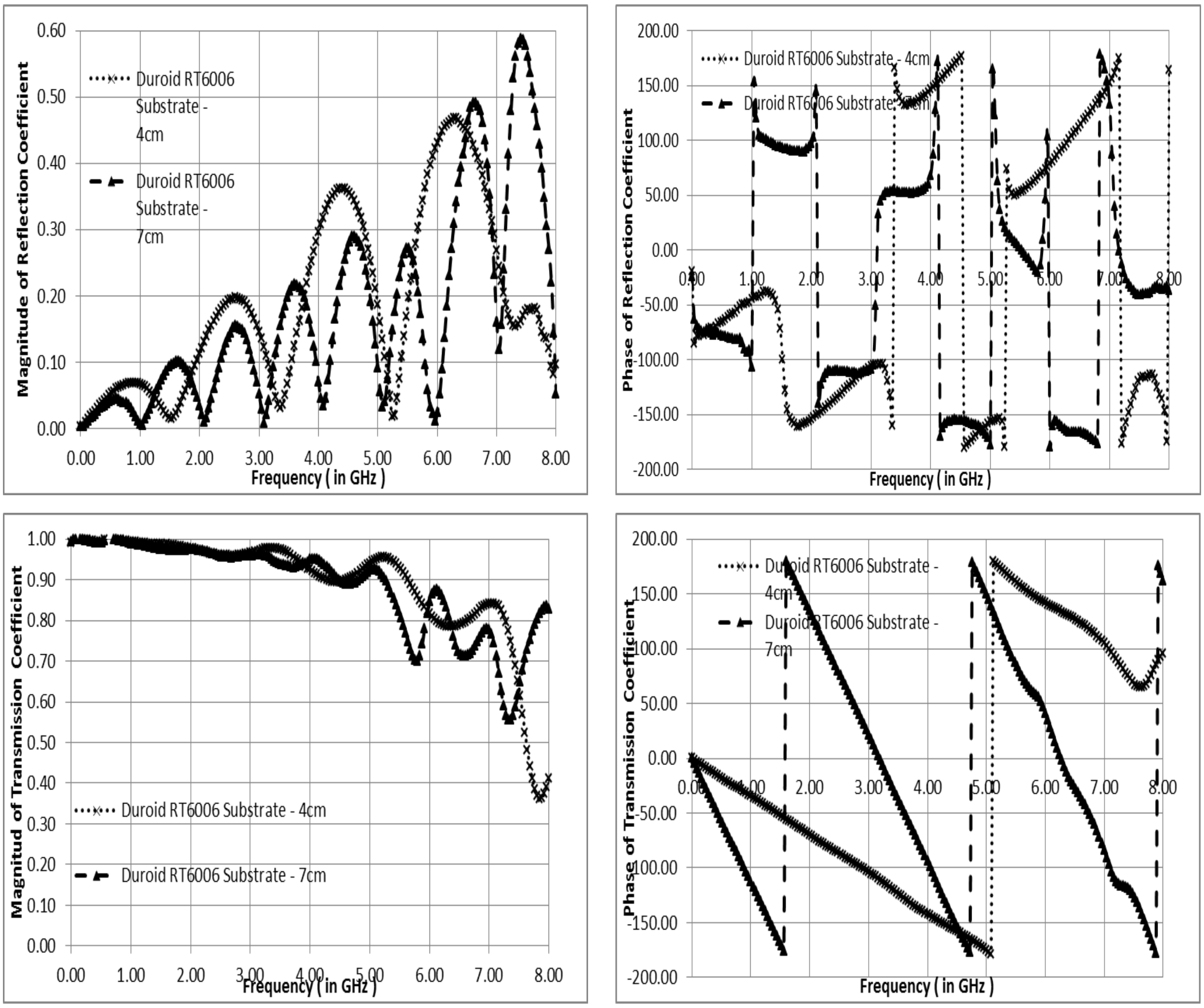

Figure 4.3.1 a) Reflection Coefficient & b) Transmission Coefficient for sample Air against frequency

a)

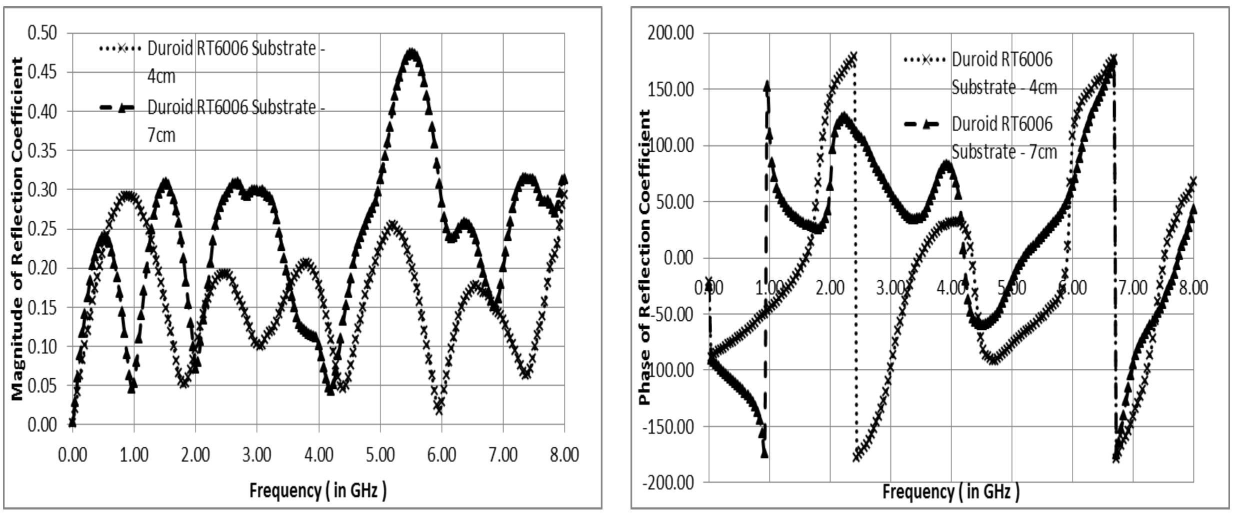

b)

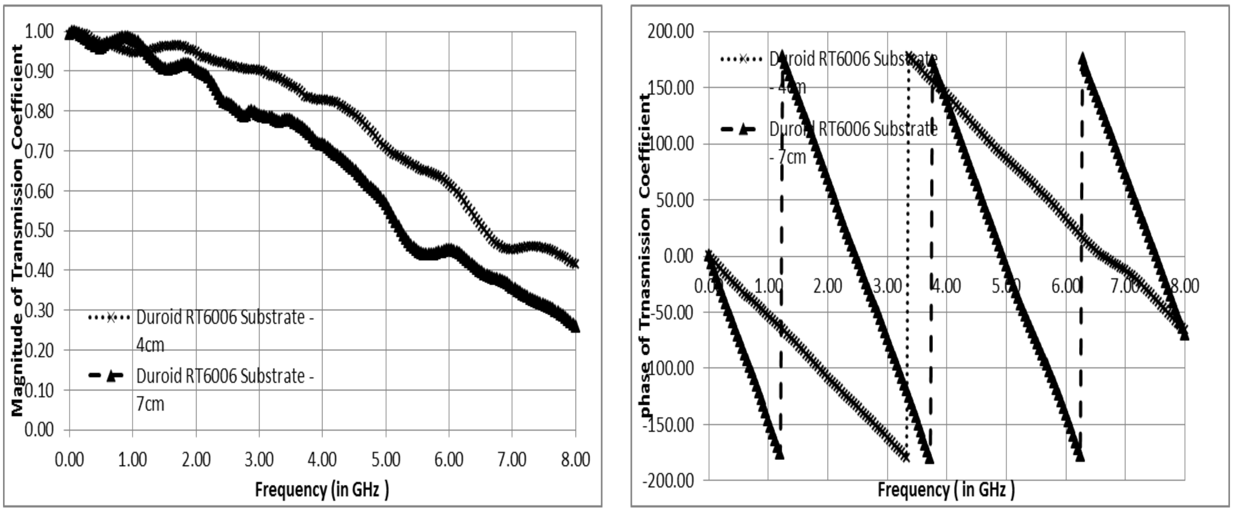

Figure 4.3.2 a) Reflection Coefficient & b) Transmission Coefficient for sample Acetone against frequency

a)

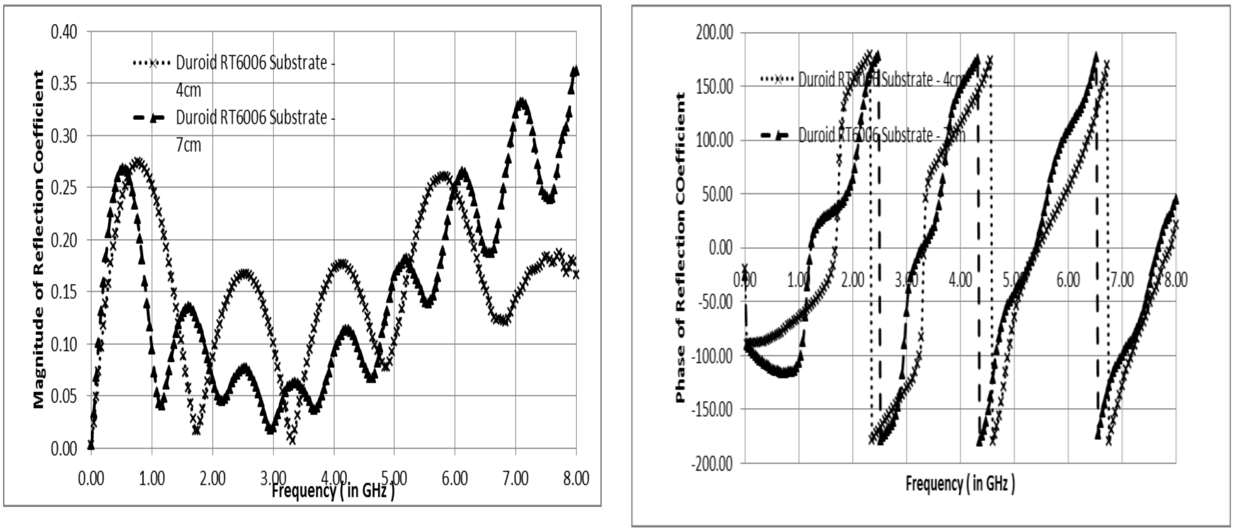

b)

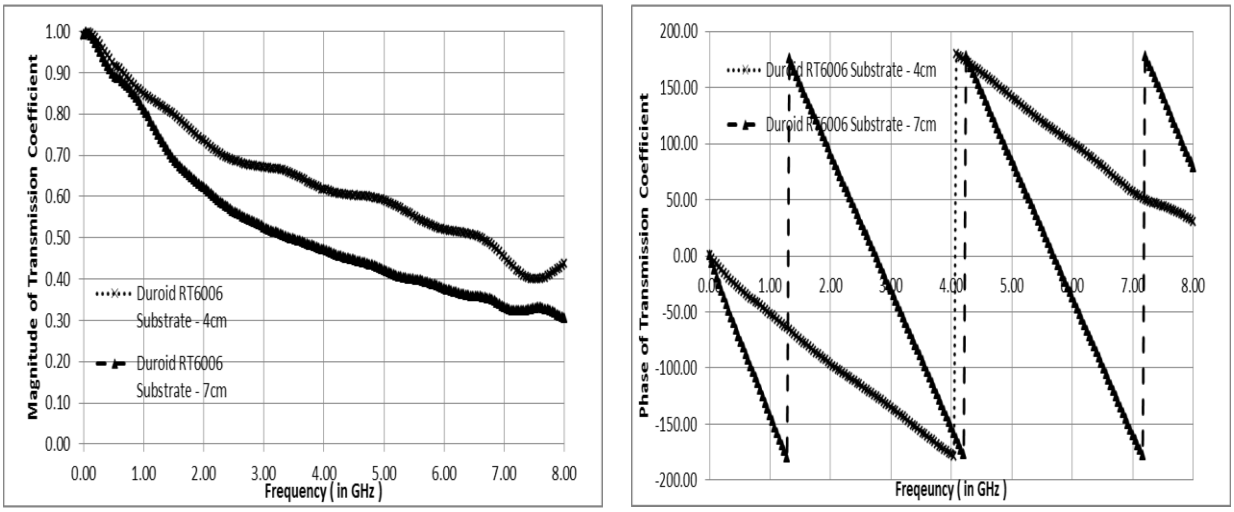

Figure 4.3.3 a) Reflection Coefficient & b) Transmission Coefficient for sample Ethanol against frequency

a)

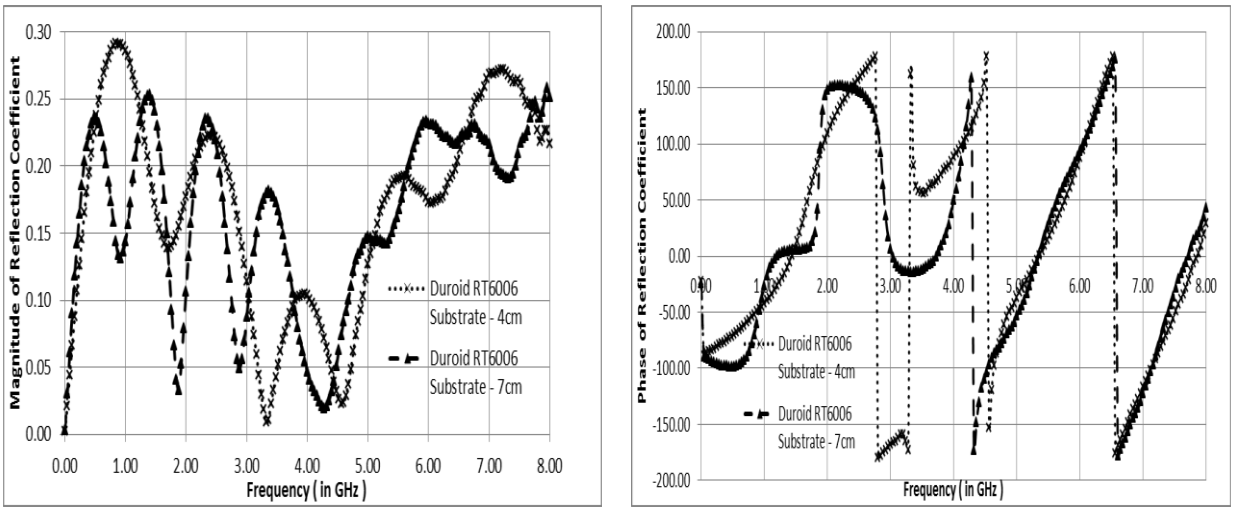

b)

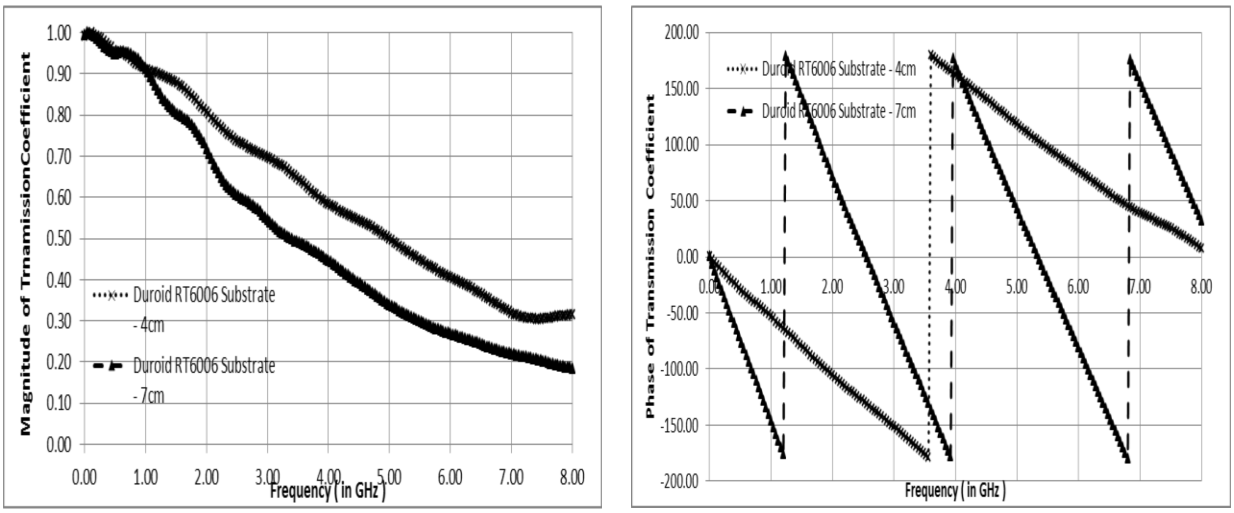

Figure 4.3.4 a) Reflection Coefficient & b) Transmission Coefficient for sample Methanol against frequency

a)

b)

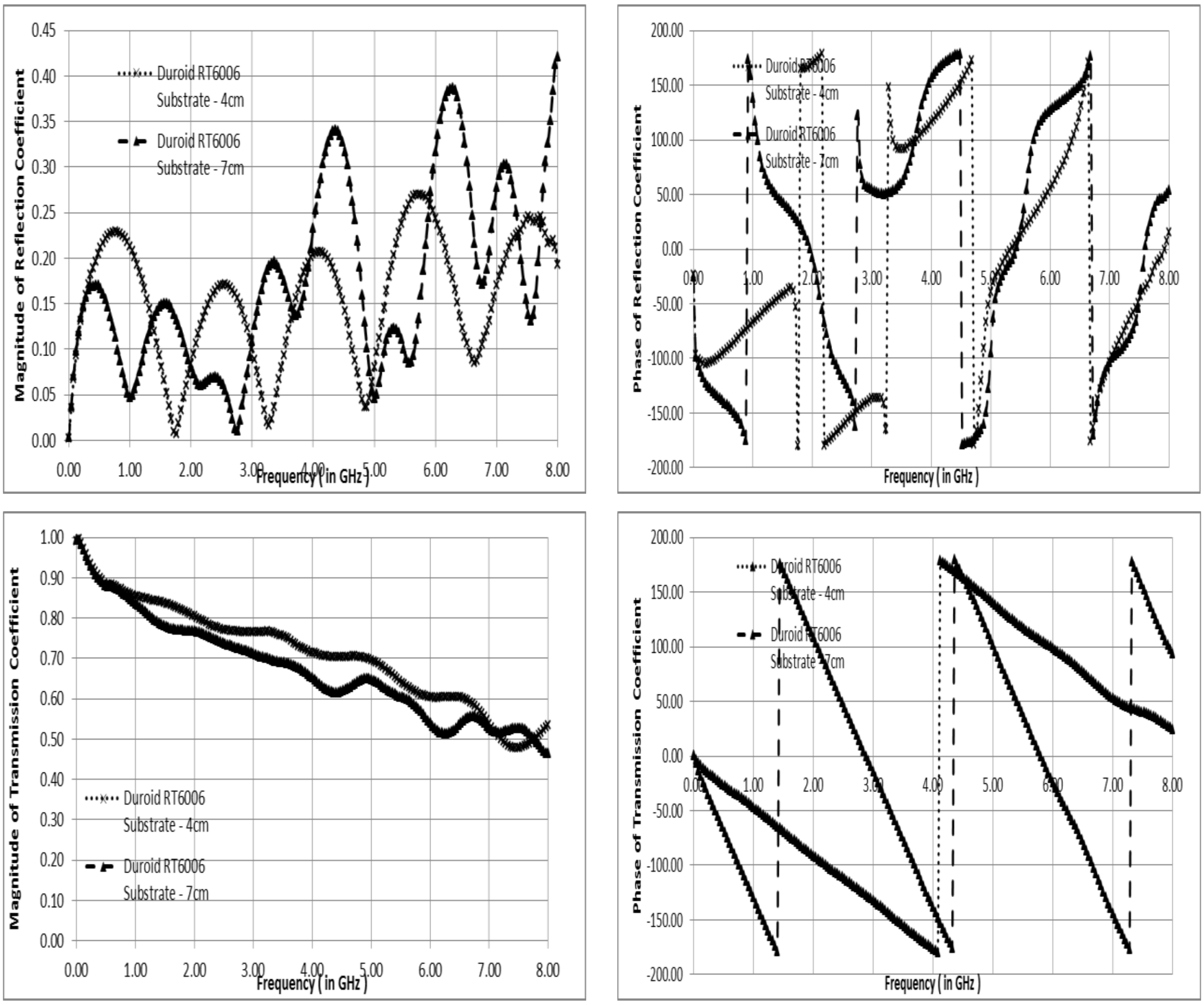

Figure 4.3.5 a) Reflection Coefficient & b) Transmission Coefficient for sample Glycerol against frequency

a)

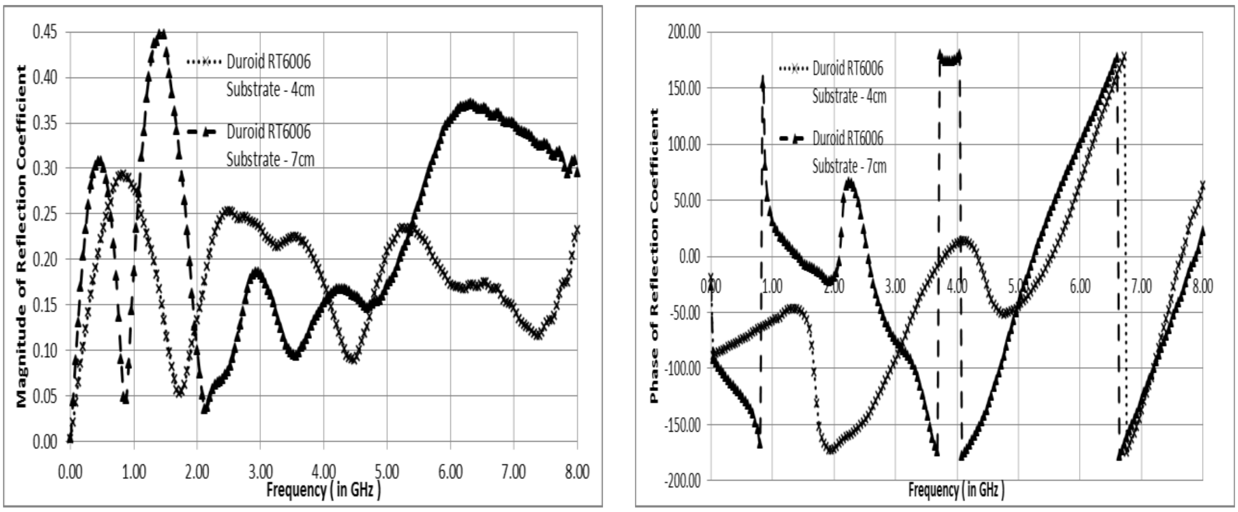

b)

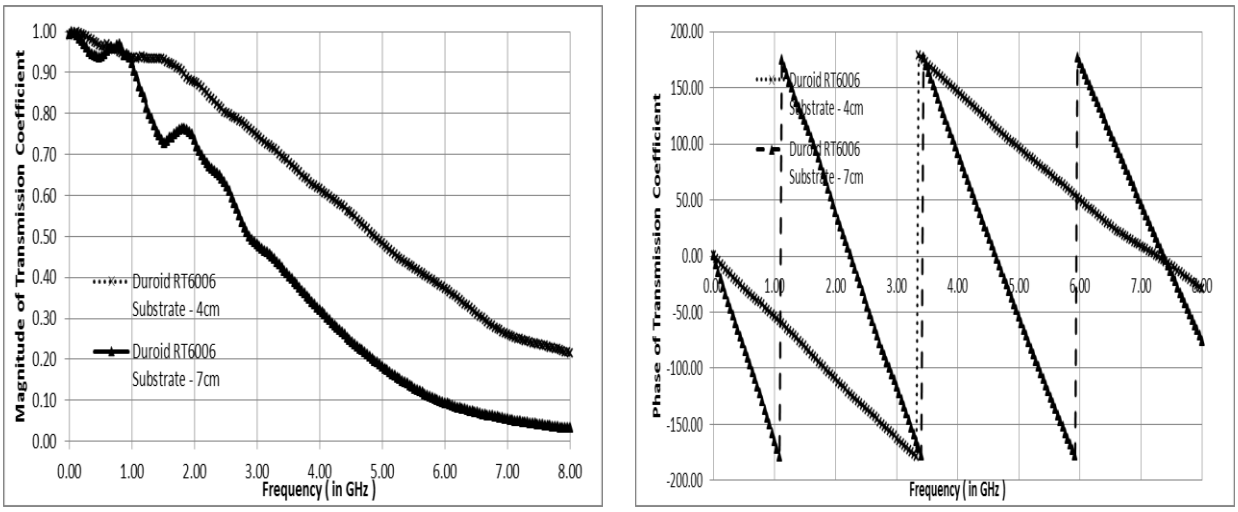

Figure 4.3.6 a) Reflection Coefficient & b) Transmission Coefficient for sample Water against frequency

4.4 Comparison of measured data for 50° RT Duroid 6006 substrate with the different line length

When the bending angle is done further up to about 50° at the centre of the sensor, the scale of difference of the magnitude response for transmission coefficient is small between the different line lengths for all the samples used. It is also can be seen that the magnitude response for reflection coefficient where the rate of recurrence is increasing as the transmission line length is increasing.

a)

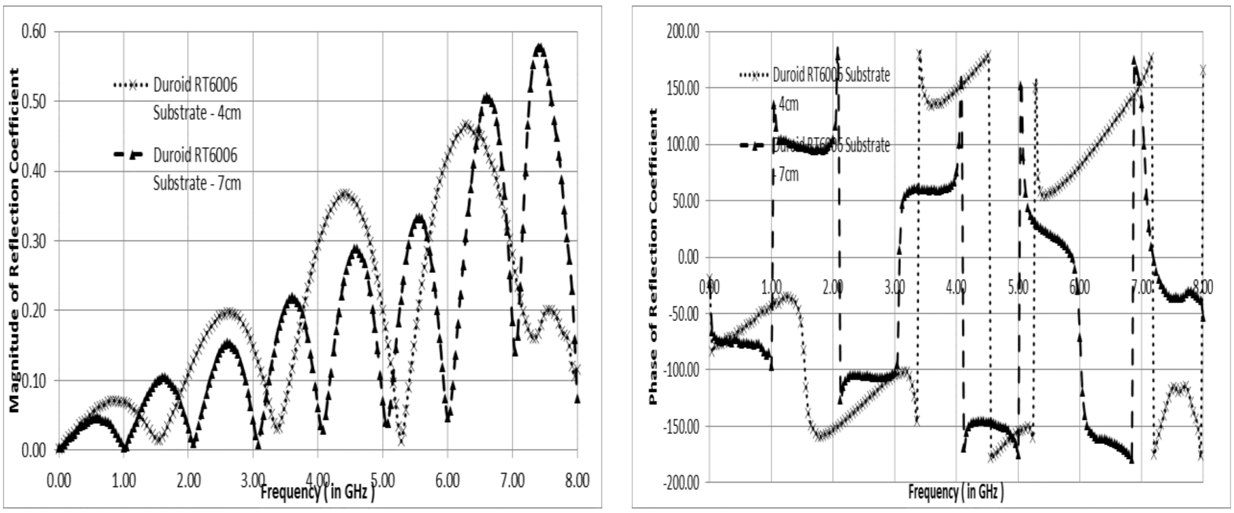

b)

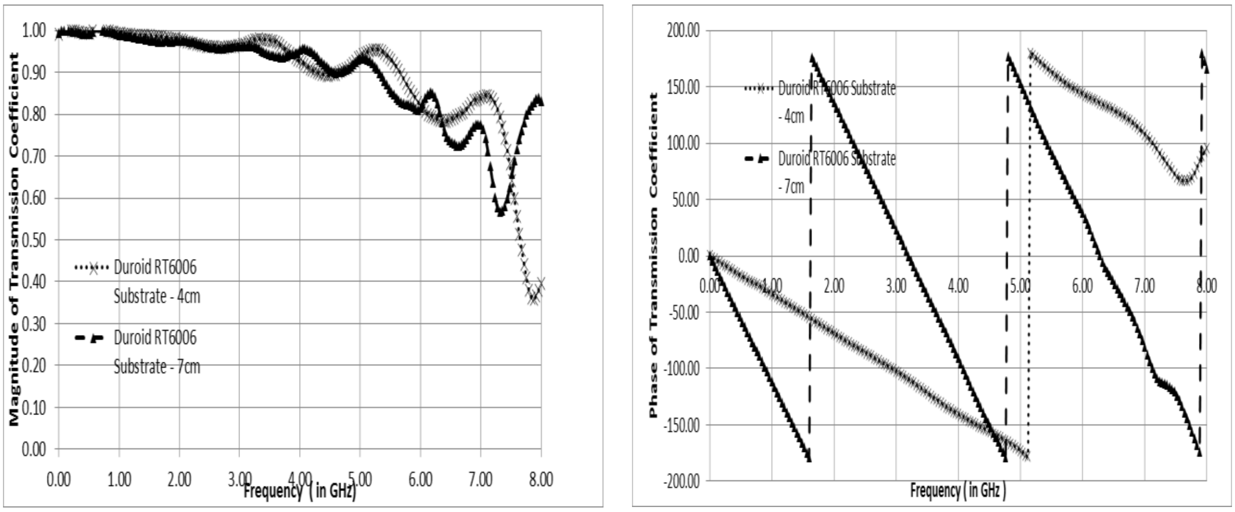

Figure 4.4.1 a) Reflection Coefficient & b) Transmission Coefficient for sample Air against frequency

a)

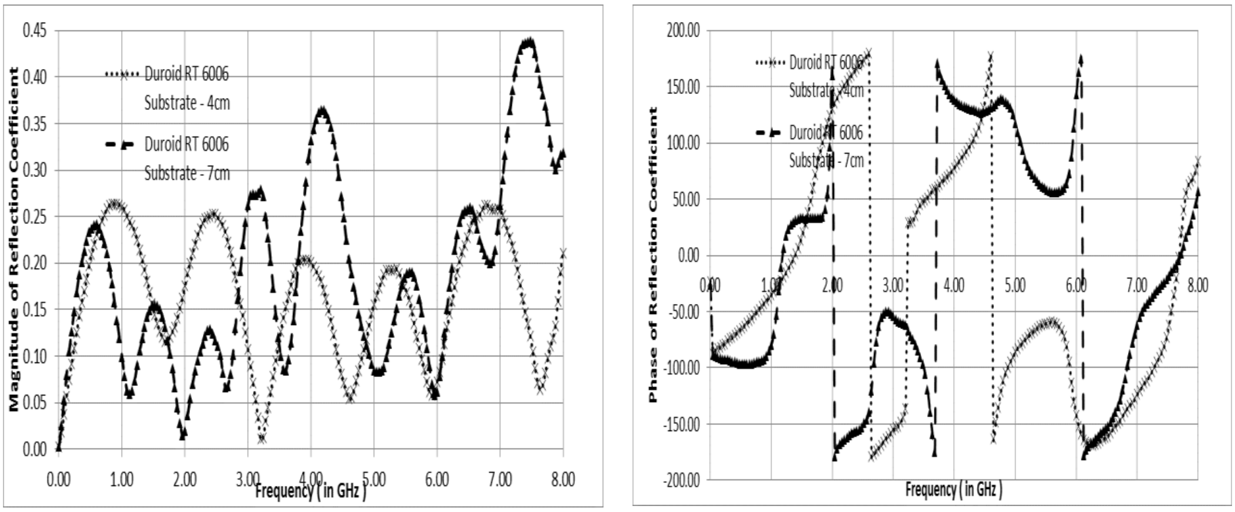

b)

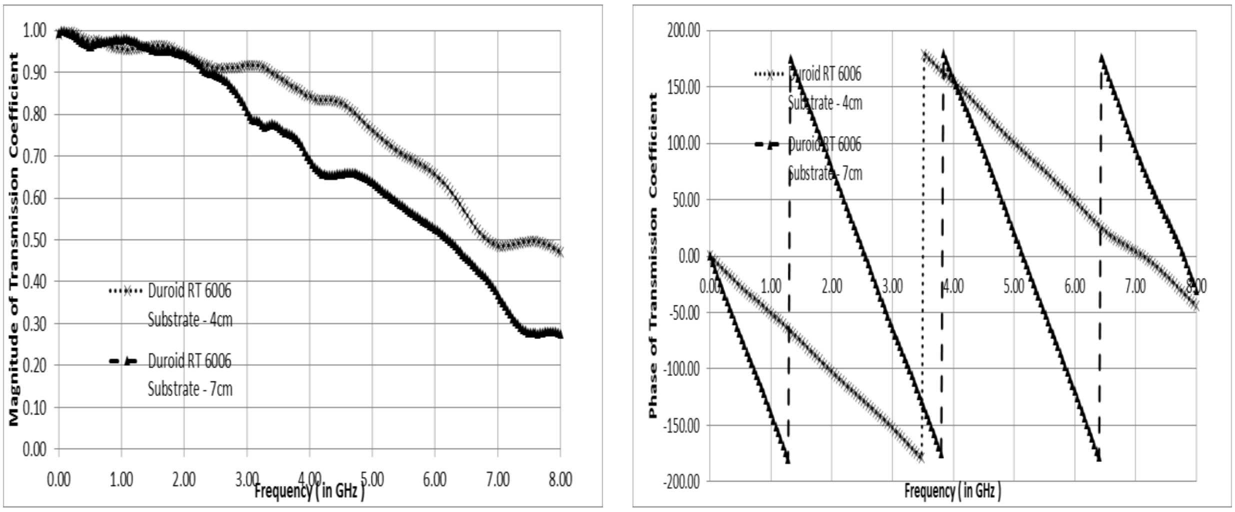

Figure 4.4.2 a) Reflection Coefficient & b) Transmission Coefficient for sample Acetone against frequency

a)

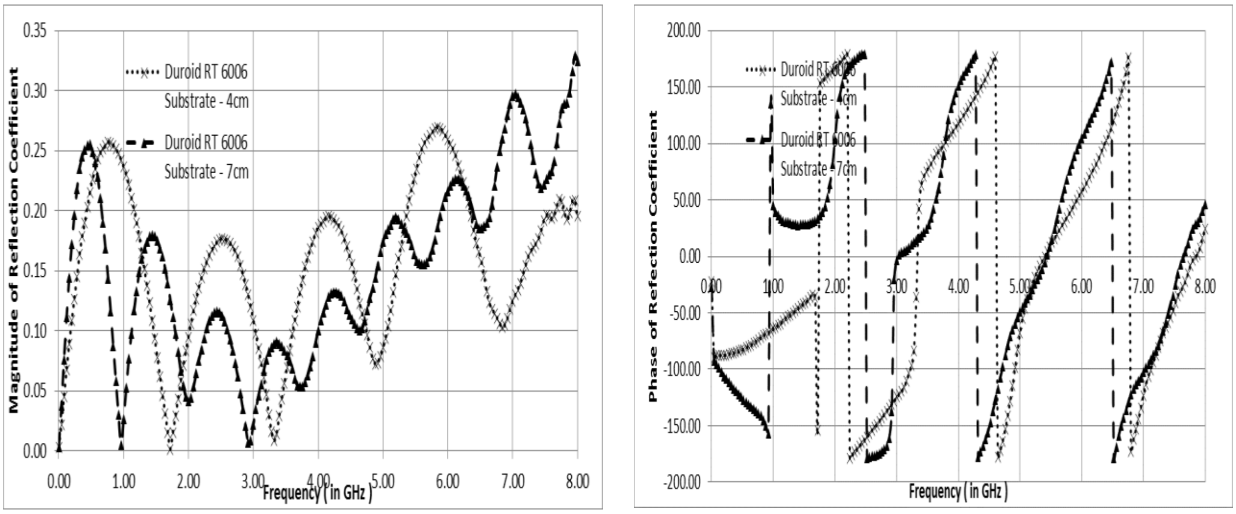

b)

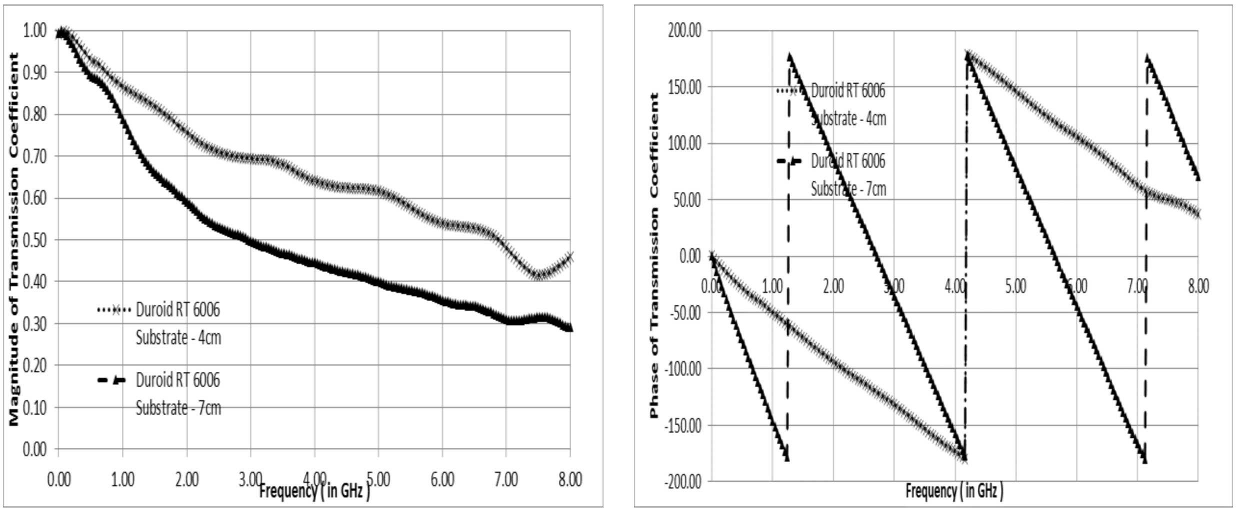

Figure 4.4.3 a) Reflection Coefficient & b) Transmission Coefficient for sample Ethanol against frequency

a)

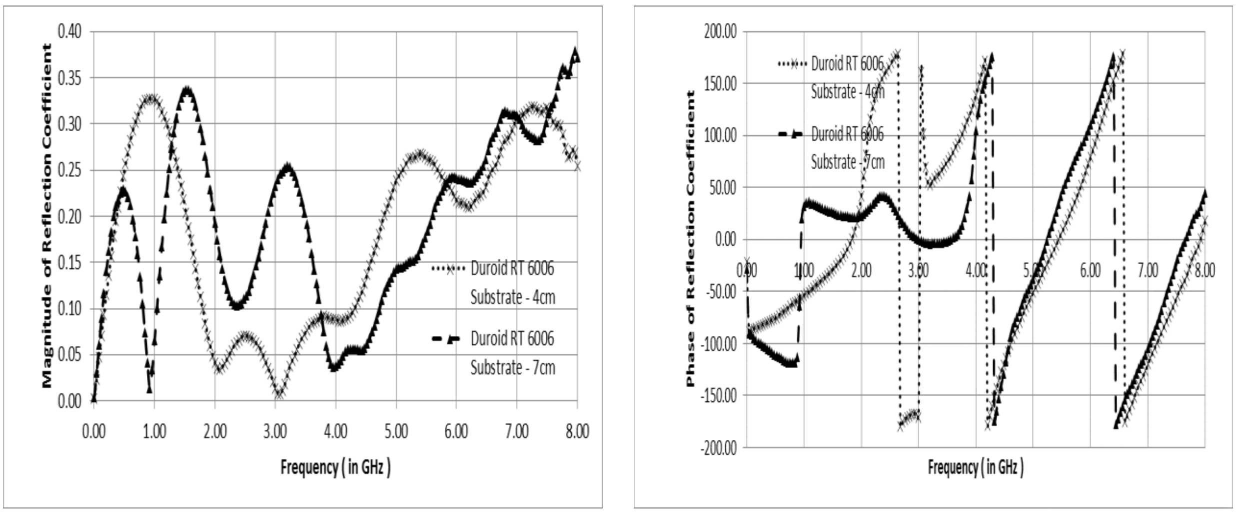

b)

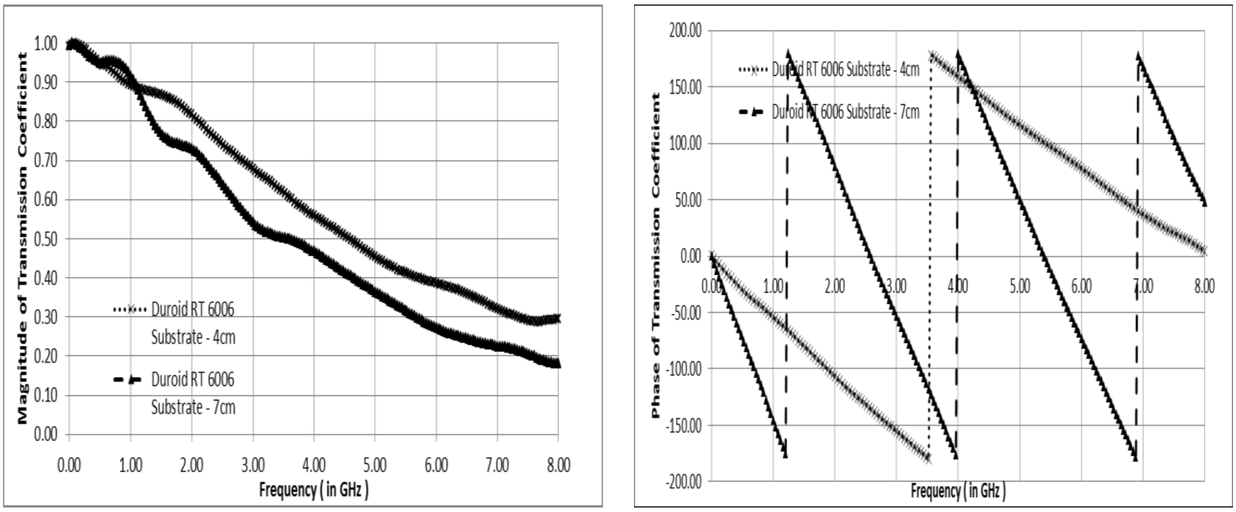

Figure 4.4.4 a) Reflection Coefficient & b) Transmission Coefficient for sample Methanol against frequency

a)

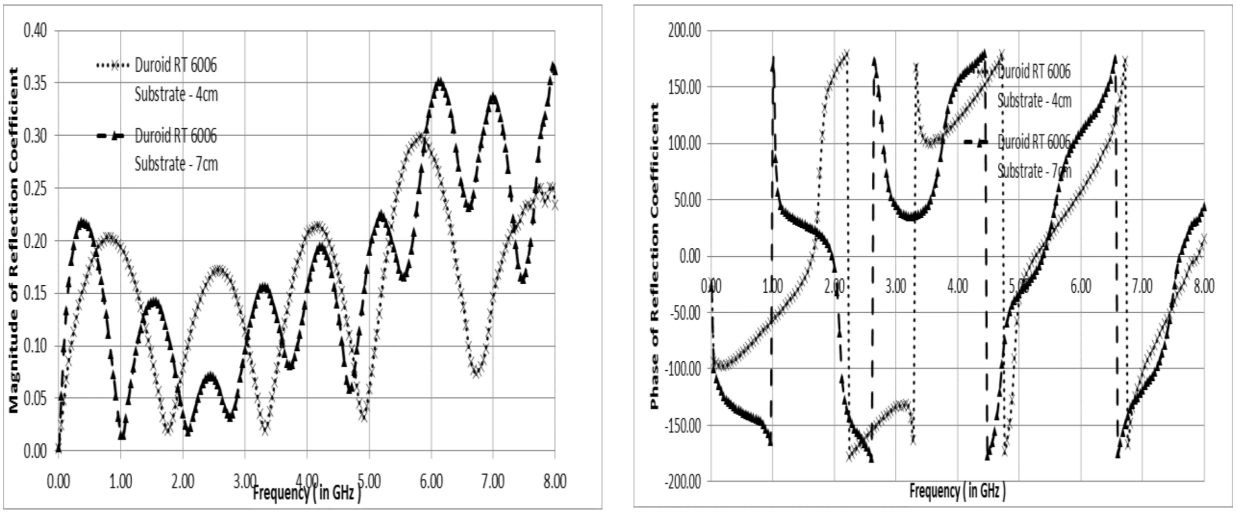

b)

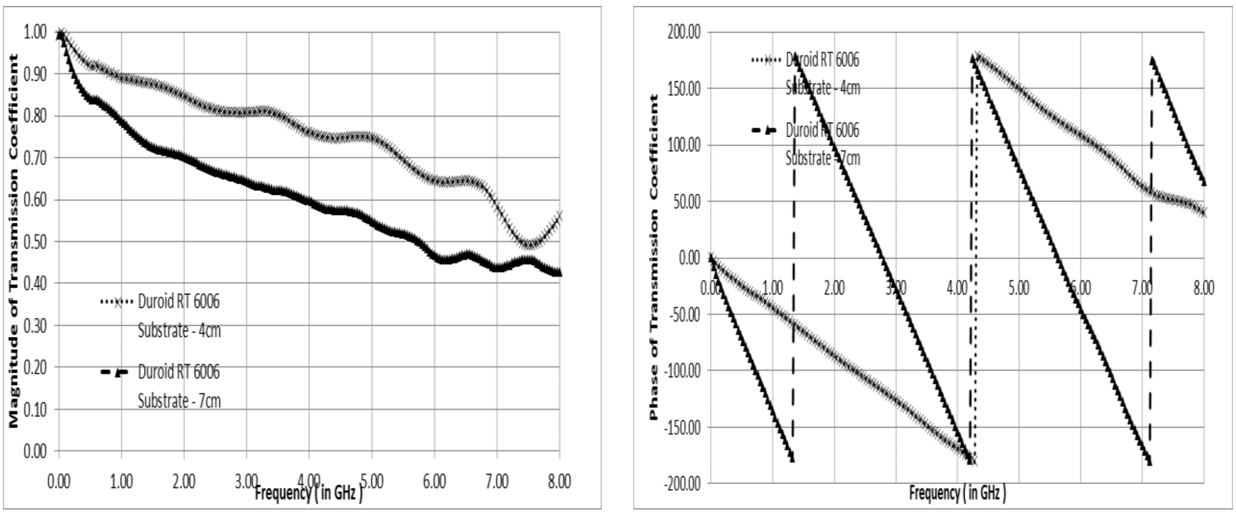

Figure 4.4.5 a) Reflection Coefficient & b) Transmission Coefficient for sample Glycerol against frequency

a)

b)

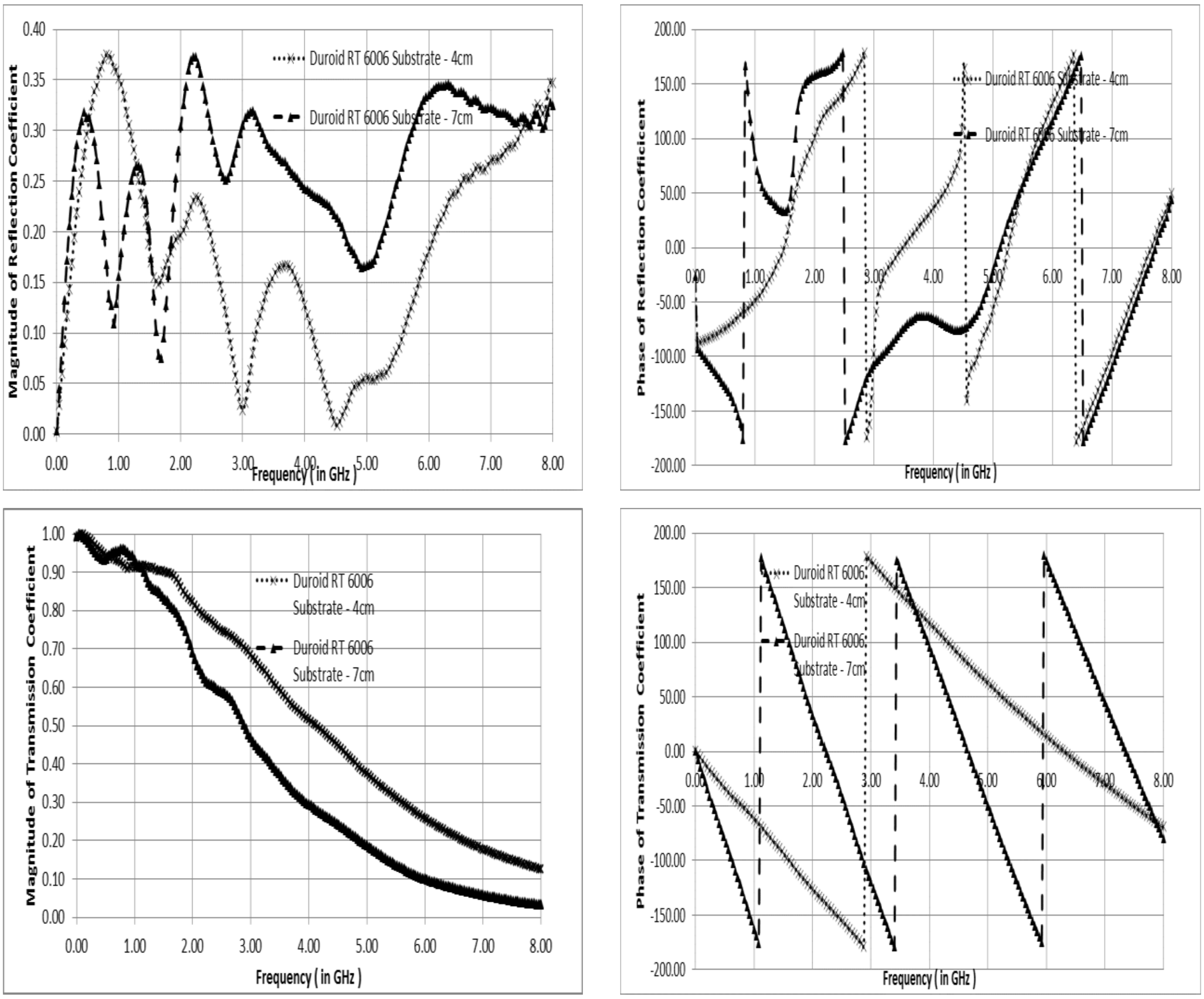

Figure 4.4.6 a) Reflection Coefficient & b) Transmission Coefficient for sample Water against frequency

4.5 Comparison of measured data and simulated data for flat RT Duroid 6006 substrate – 4cm

With the collection all the measured data for each sample, the next is the comparison between the simulated data from AWR Design Environment software and measured data from the VNA network analyzer is done and arranged in accordance to the liquid samples. When the permittivity of sample increases, the range of difference between measured data and simulated data rises. Almost for all the liquid samples, the range of difference is high from the frequency range of 3 GHz in refers to the magnitude response for the reflection coefficient. From the graphs for all the samples, in the certain range of the frequency the measured data is higher than the simulated data and vice versa. This is due to the presence of loss factor when the EM wave passing through the respective sample placed on the sensor.

a)

b)

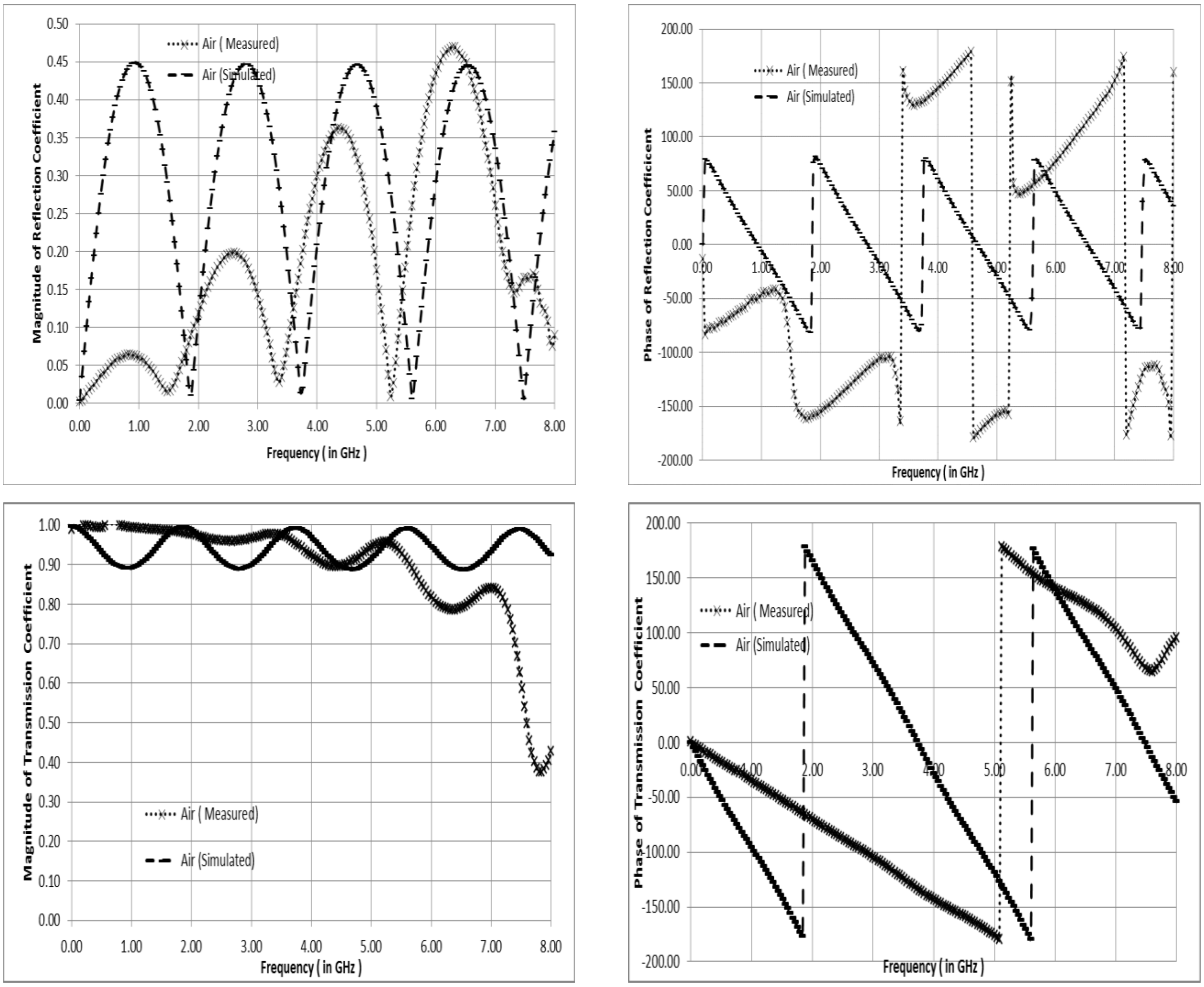

Figure 4.5.1 a) Reflection Coefficient & b) Transmission Coefficient for sample Air against frequency

a)

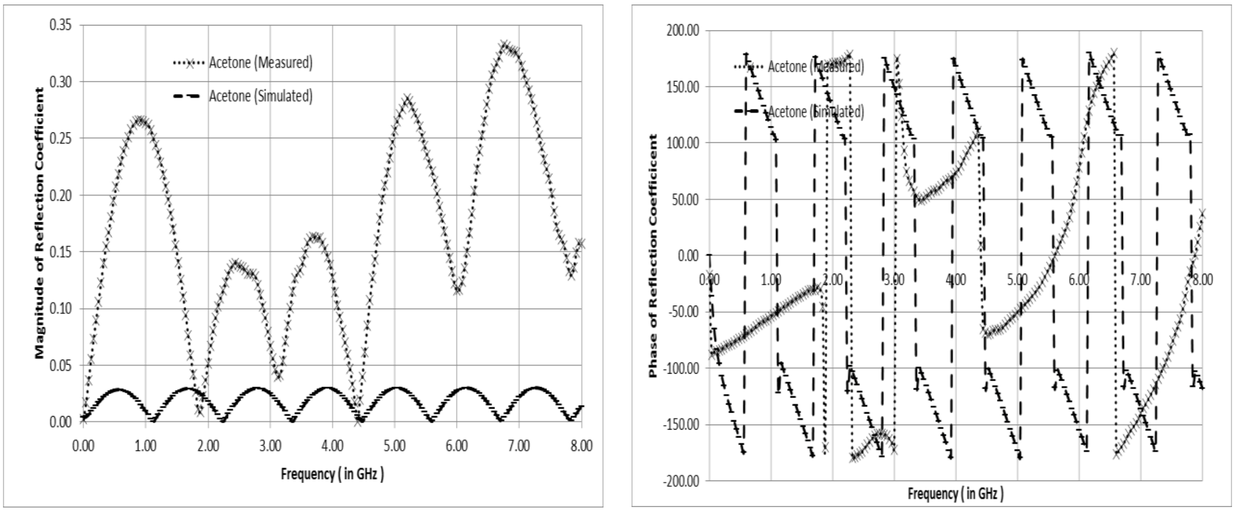

b)

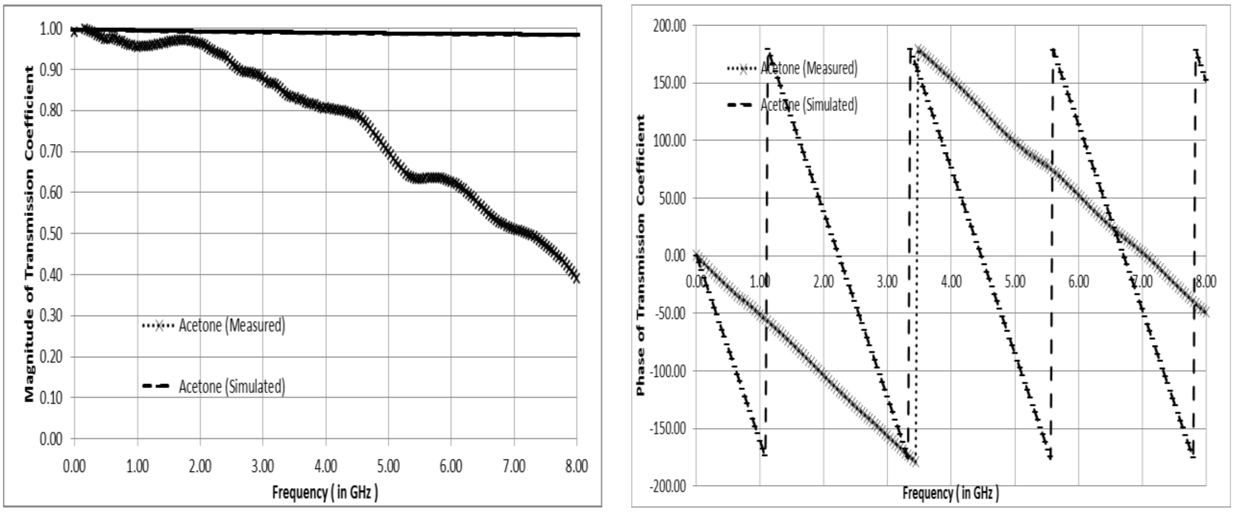

Figure 4.5.2 a) Reflection Coefficient & b) Transmission Coefficient for sample Acetone against frequency

a)

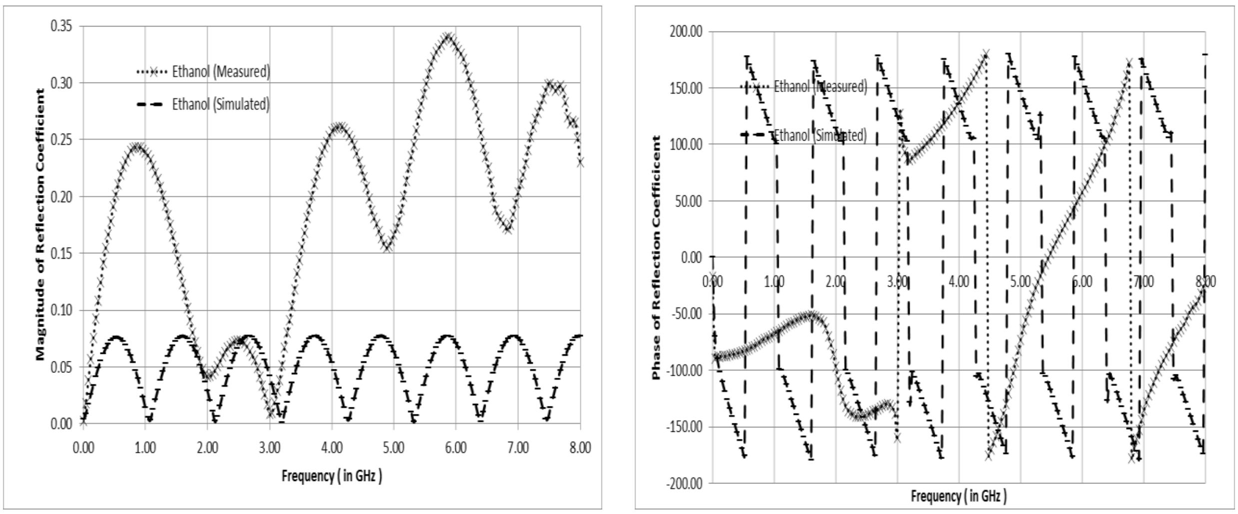

b)

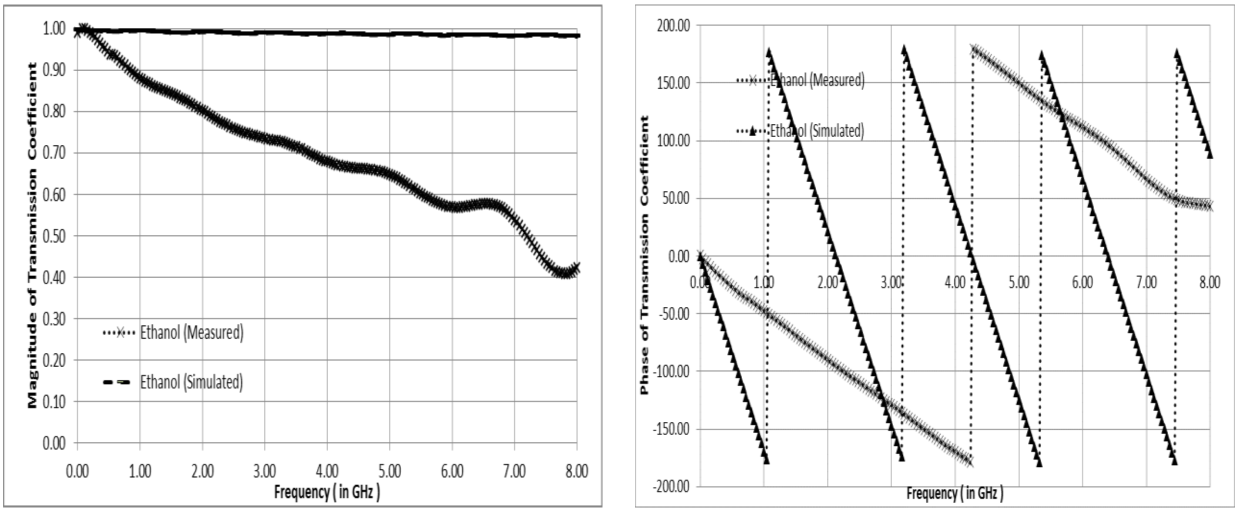

Figure 4.5.3 a) Reflection Coefficient & b) Transmission Coefficient for sample Ethanol against frequency

a)

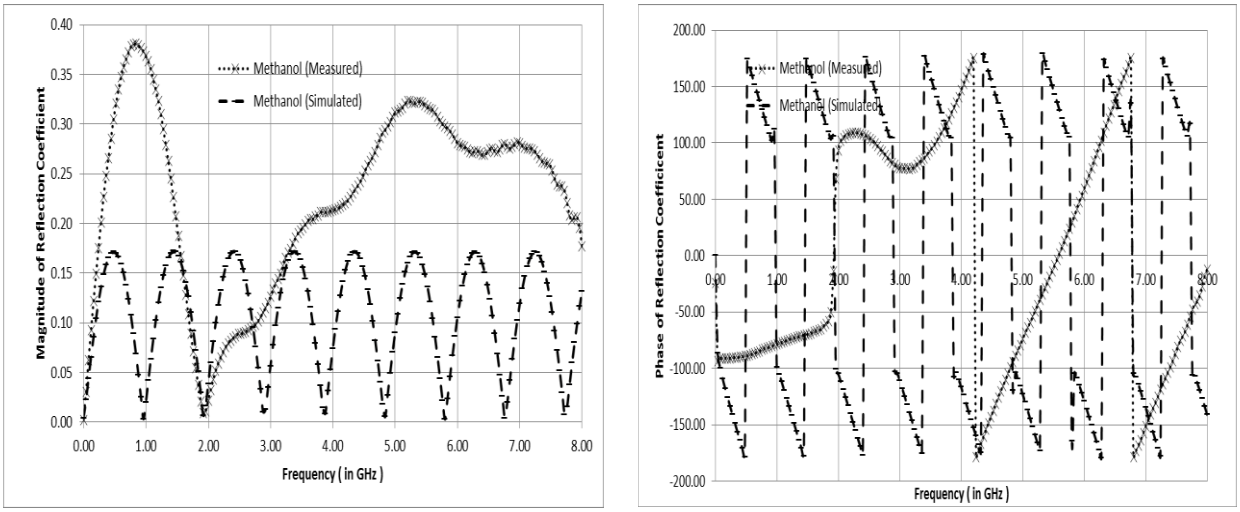

b)

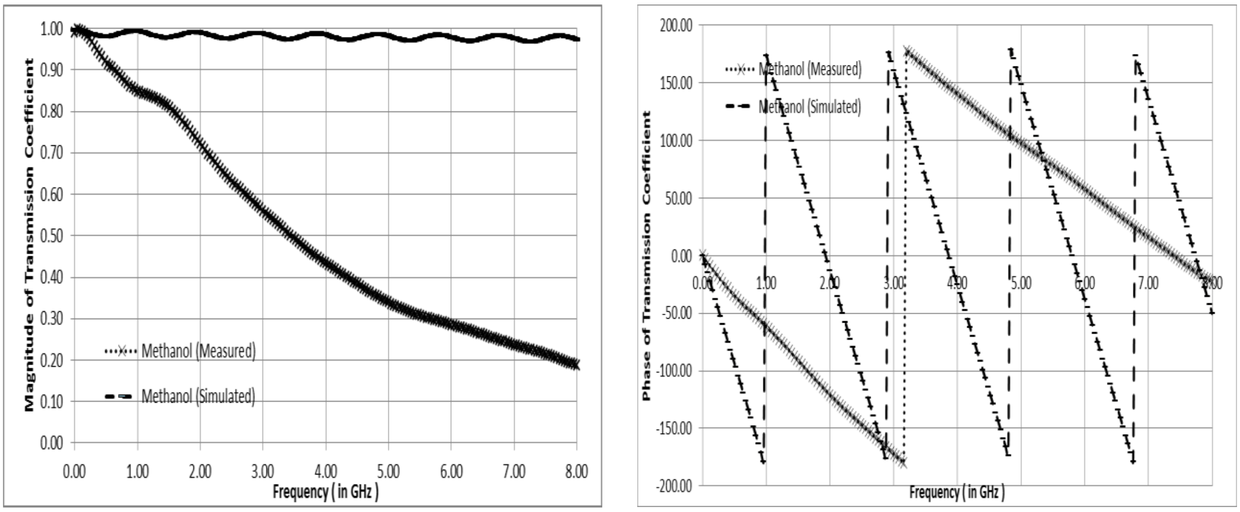

Figure 4.5.4 a) Reflection Coefficient & b) Transmission Coefficient for sample Methanol against frequency

a)

b)

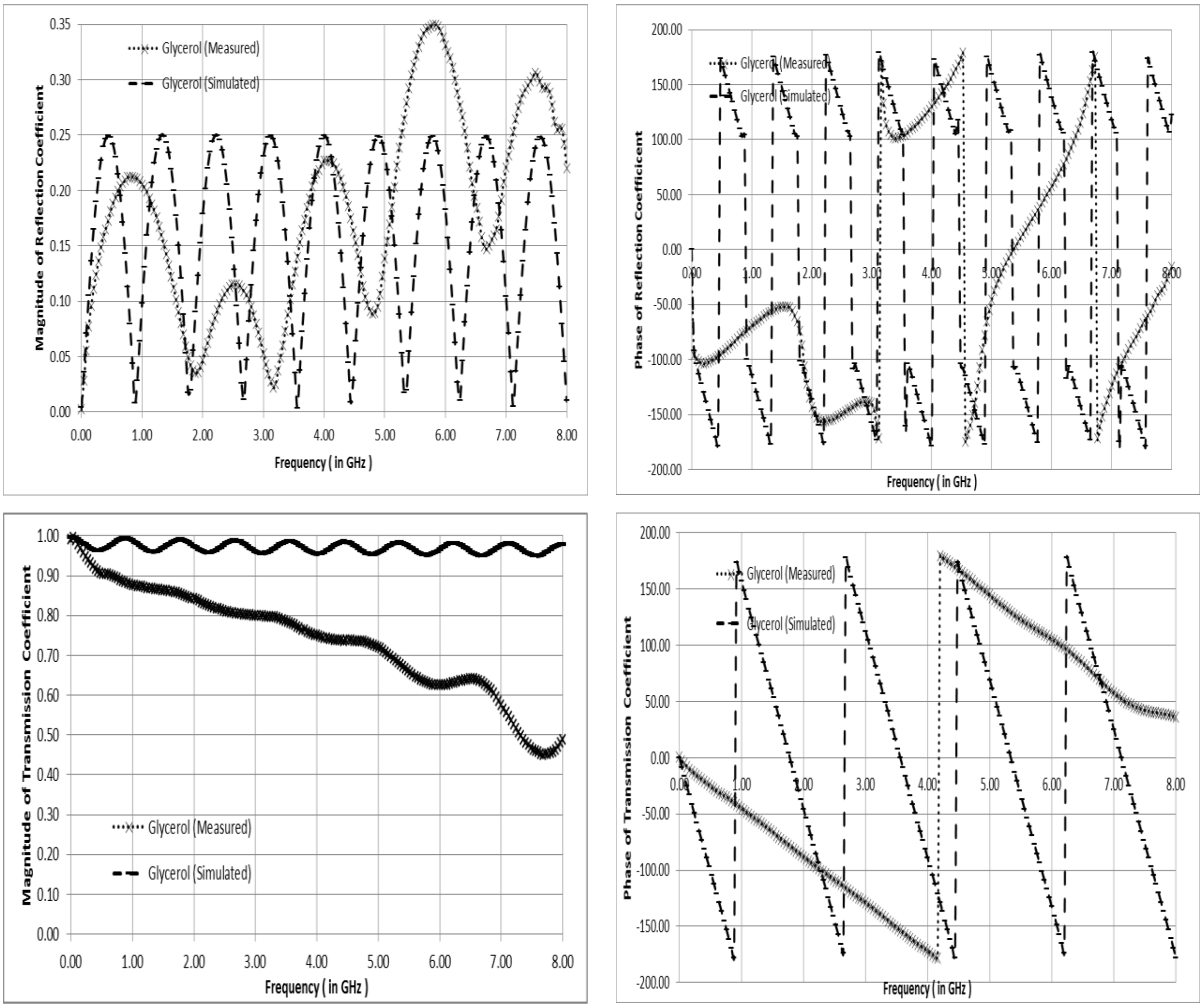

Figure 4.5.5 a) Reflection Coefficient & b) Transmission Coefficient for sample Glycerol against frequency

a)

b)

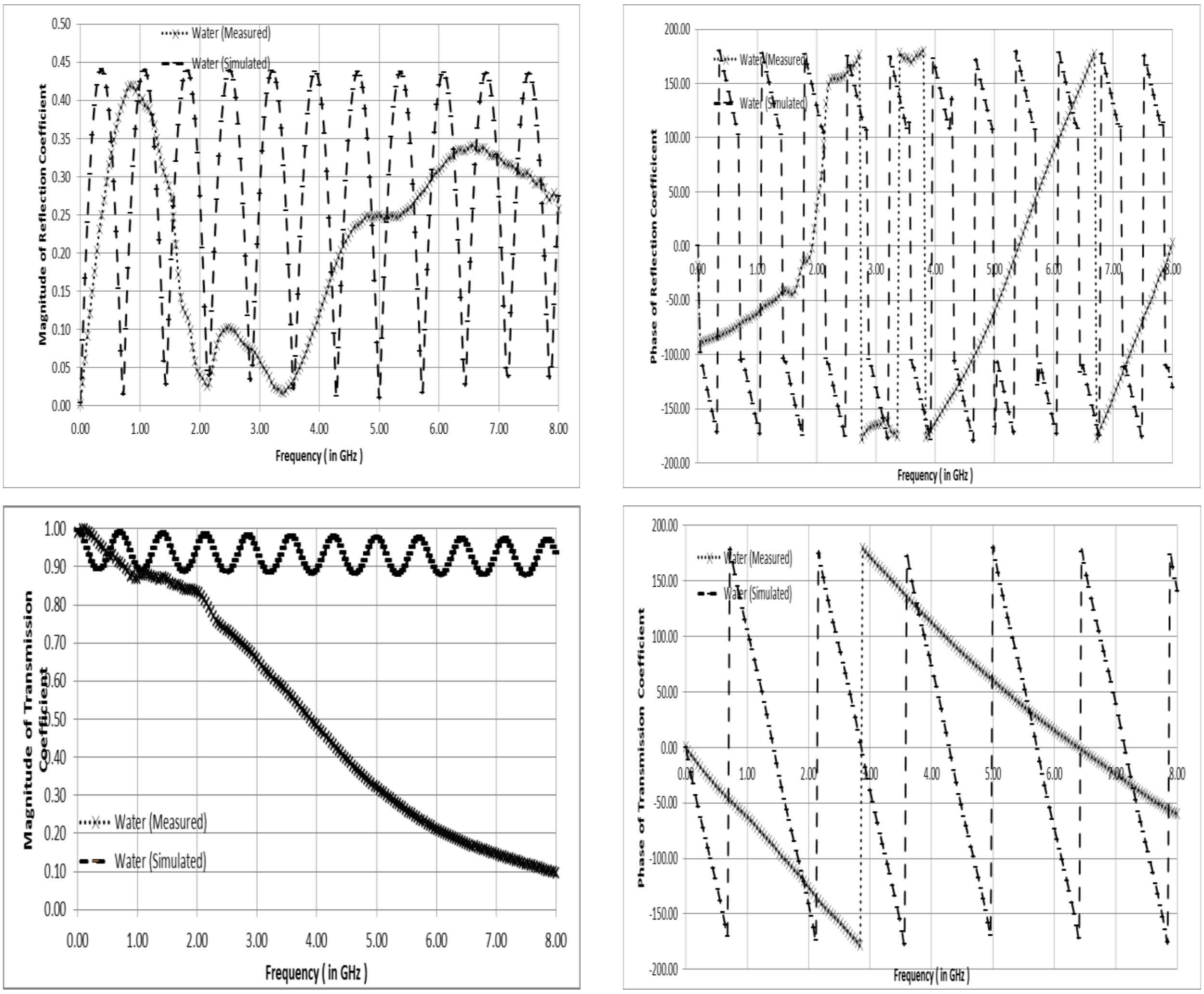

Figure 4.5.6 a) Reflection Coefficient & b) Transmission Coefficient for sample Water against frequency

4.6 Comparison of measured data and simulated data for flat RT Duroid 6006 substrate – 7cm

Similarly to the previous section but the line length of the microstrip sensor is about 7cm. In regard to the reflection coefficient, the scale of difference between the measured data and simulated data started to varies approximately at about 1.6 GHz of frequency as due to the selective of part of the EM wave being transmitted over the microstrip line.

a)

b)

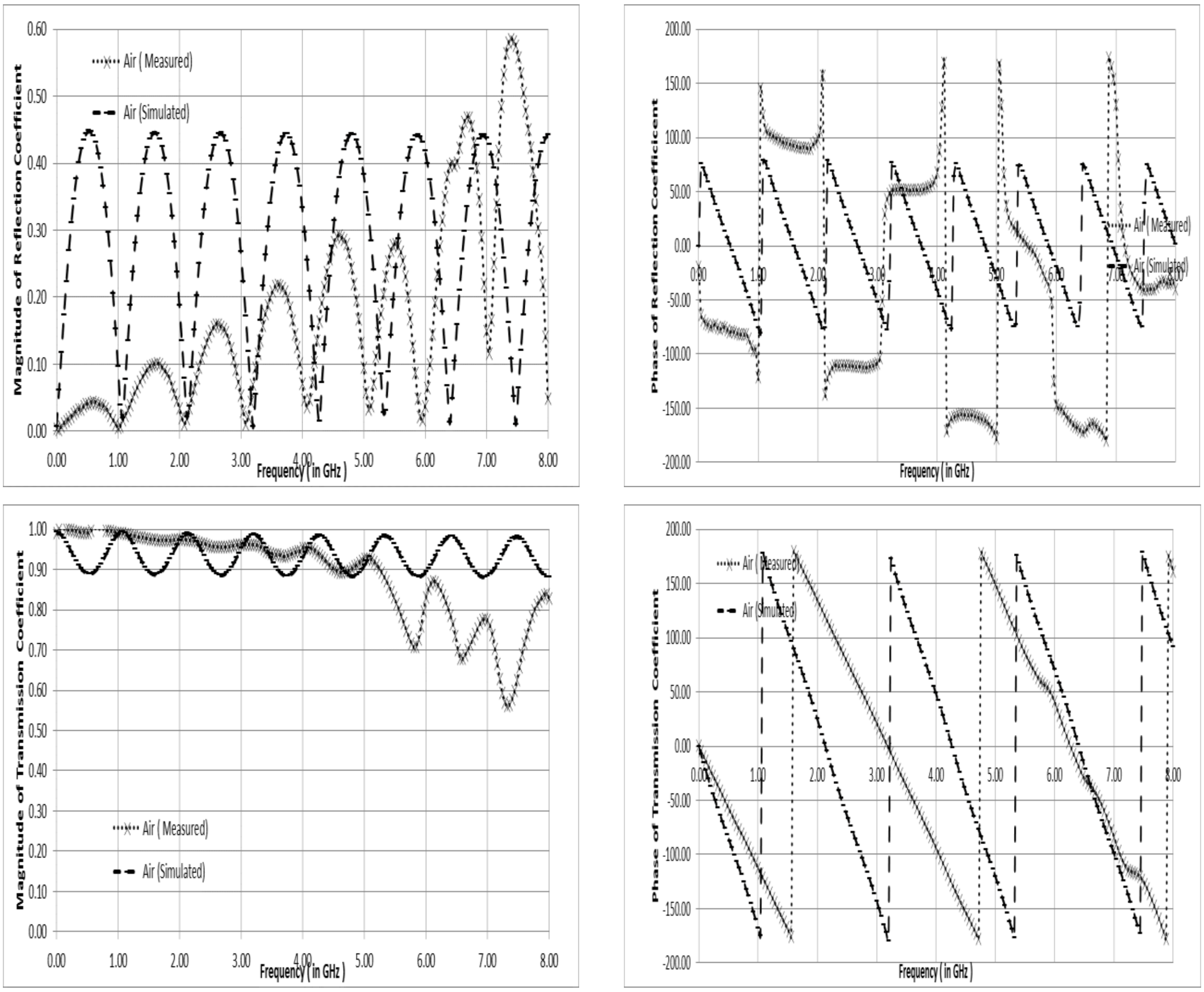

Figure 4.6.1 a) Reflection Coefficient & b) Transmission Coefficient for sample Air against frequency

a)

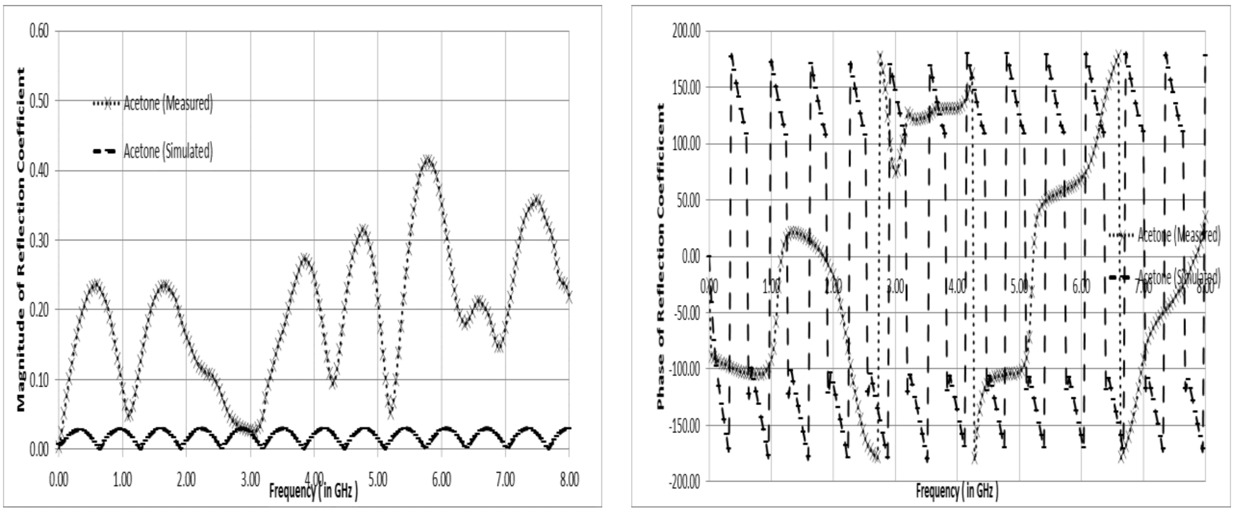

b)

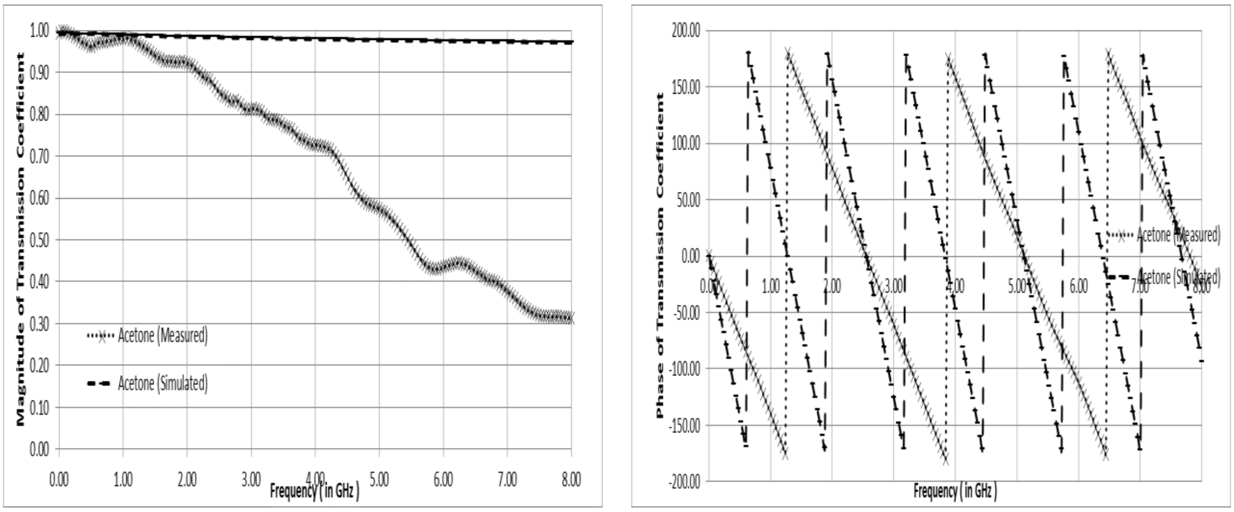

Figure 4.6.2 a) Reflection Coefficient & b) Transmission Coefficient for sample Acetone against frequency

a)

b)

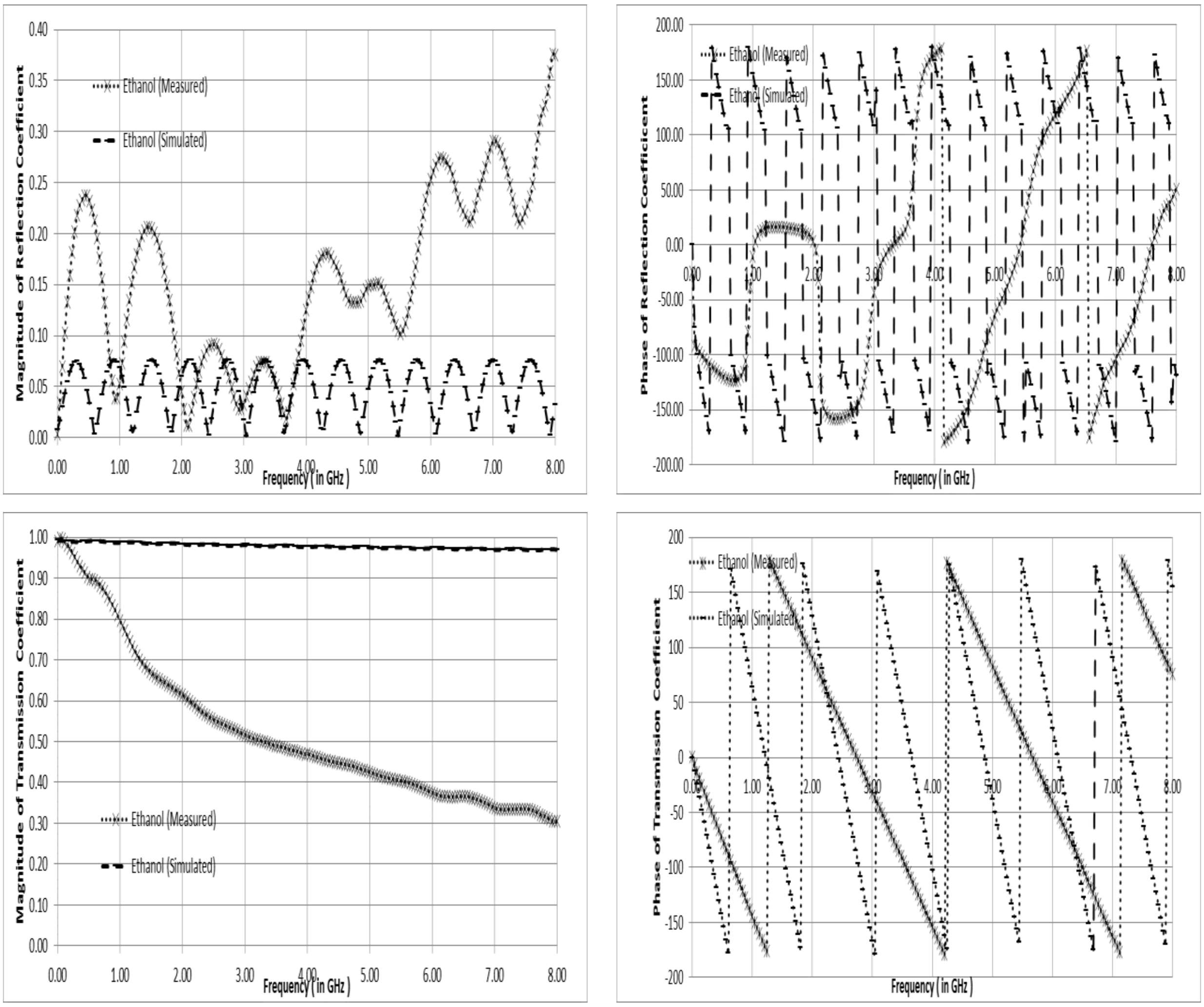

Figure 4.6.3 a) Reflection Coefficient & b) Transmission Coefficient for sample Ethanol against frequency

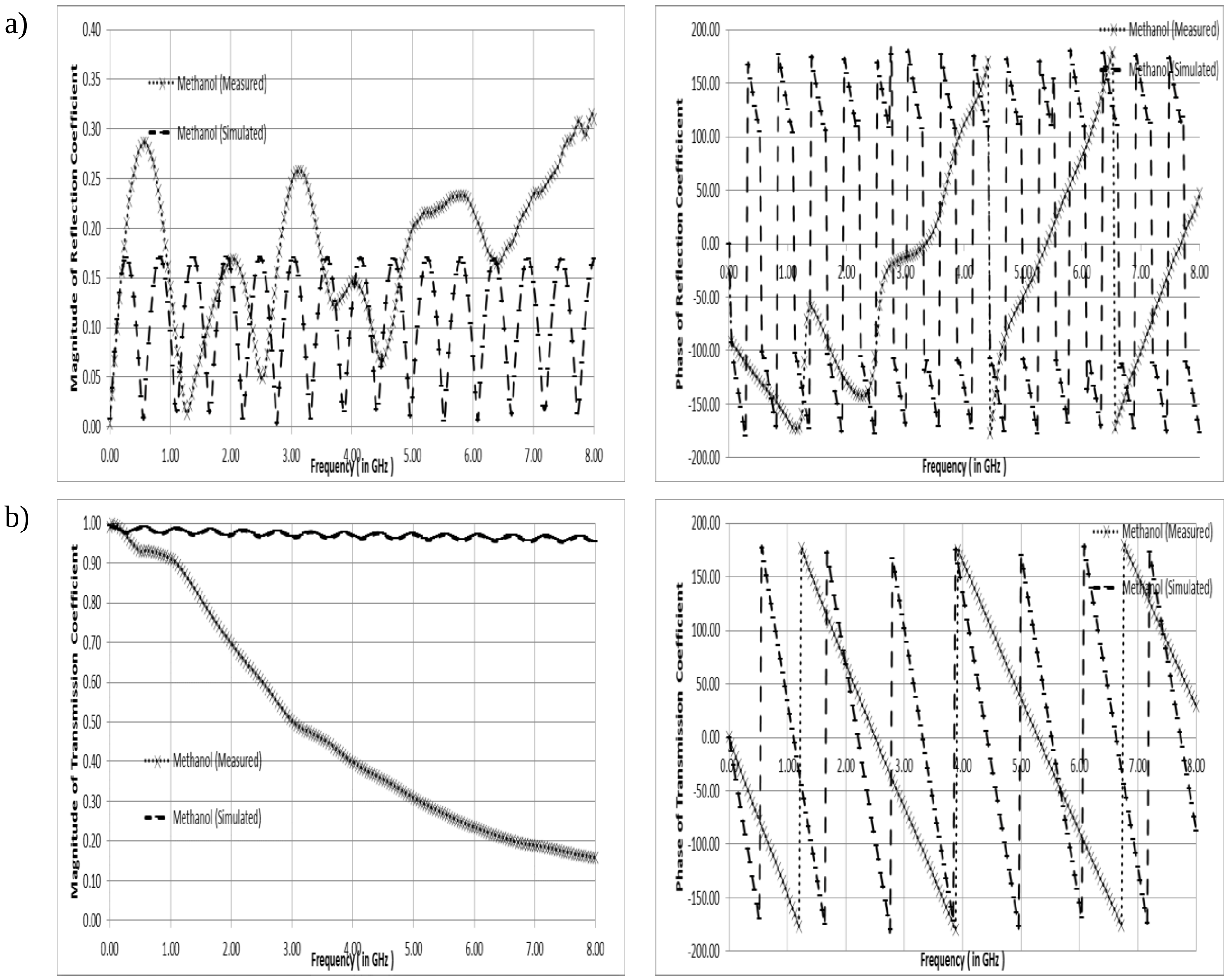

Figure 4.6.4 a) Reflection Coefficient & b) Transmission Coefficient for sample Methanol against frequency

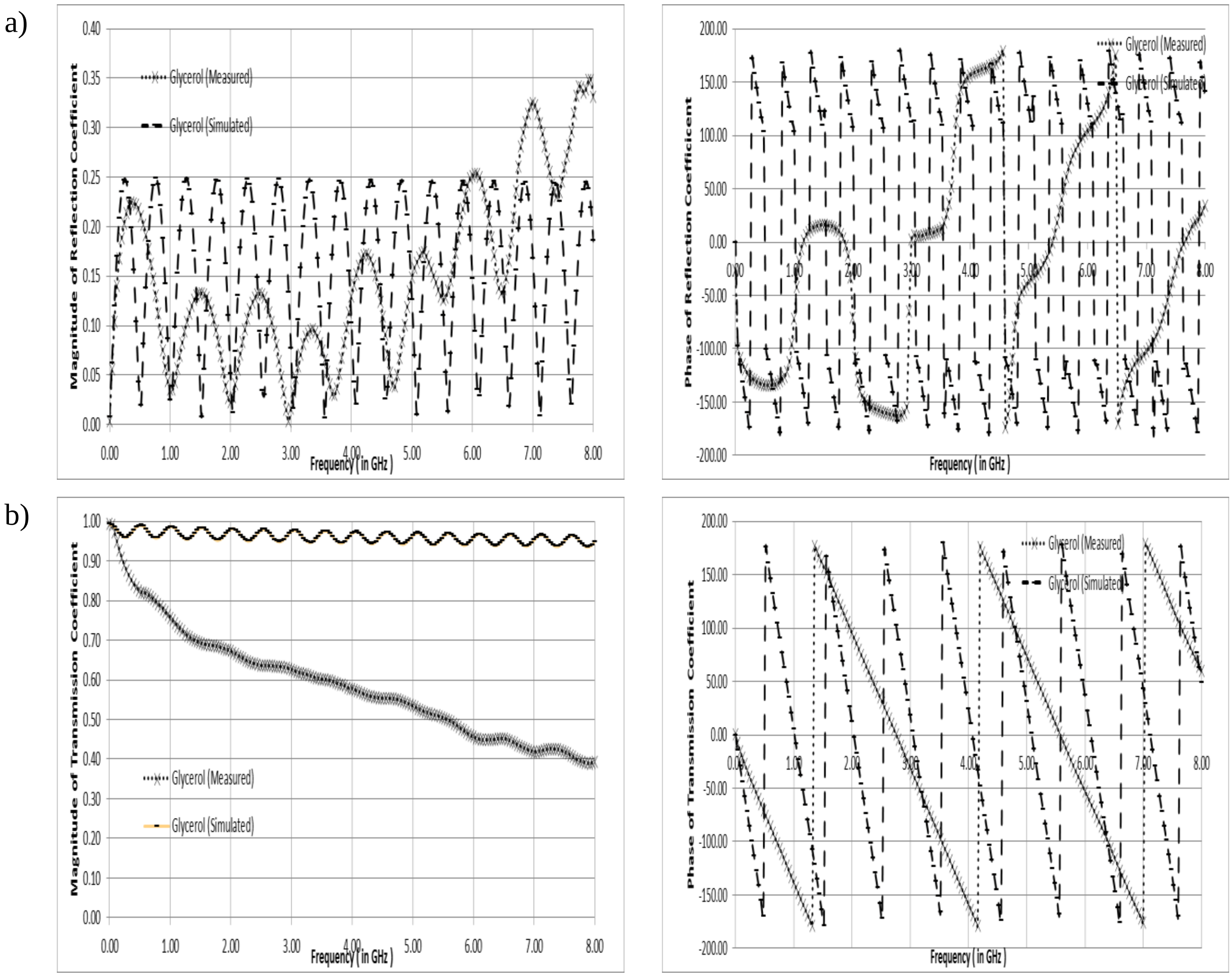

Figure 4.6.5 a) Reflection Coefficient & b) Transmission Coefficient for sample Glycerol against frequency

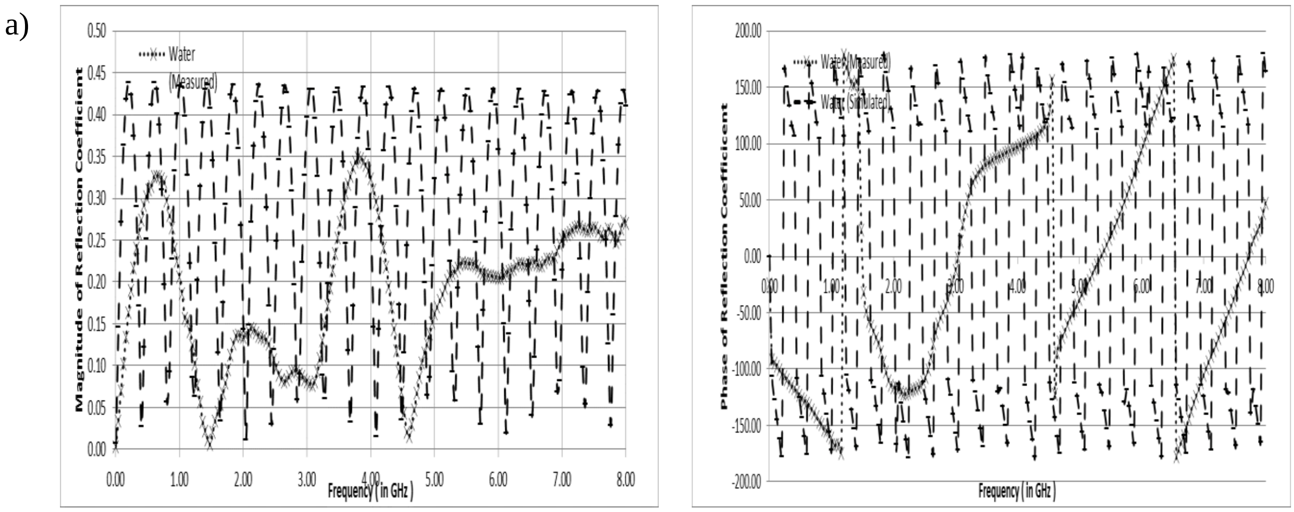

b)

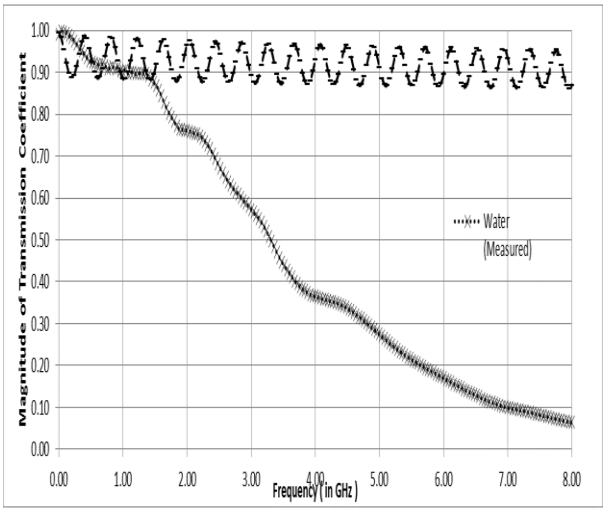

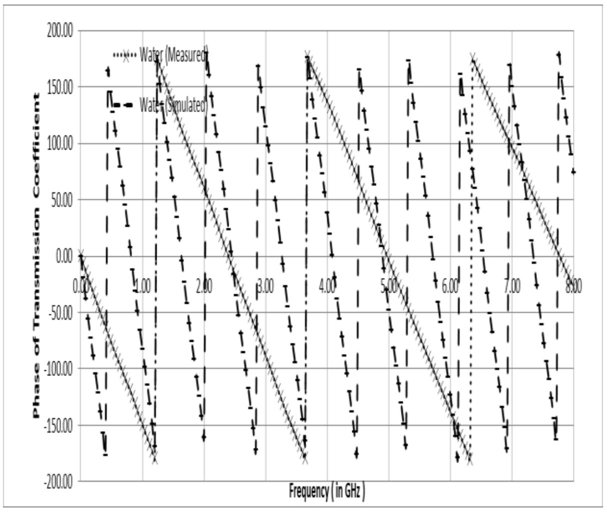

Figure 4.6.6 a) Reflection Coefficient & b) Transmission Coefficient for sample Water against frequency

4.7 Comparison of measured data for RT Duroid 6006 substrate based on from flat to different bending angle – 4cm

Coming to this section is the comparison of the RT Duroid 6006 substrate of 40mm length of the line and on the next section is for about 70 mm line length from flat surface to the next two bending angles of 20° and 50° of the sensor. It is noticed that for sample air, there is no difference in the both magnitude and phase responses in transmission coefficient and reflection coefficient. In regarding to transmission coefficient in both magnitude response and phase response, the samples of acetone, ethanol and glycerol are close to fall under same range but this applies to 4 cm line length. As for the 7 cm line length, samples of acetone, ethanol and methanol having the slightest difference labelled under the transmission coefficient. There difference in both magnitude and phase responses between from flat to different bending area does not occurs in the sequential form.

a)

b)

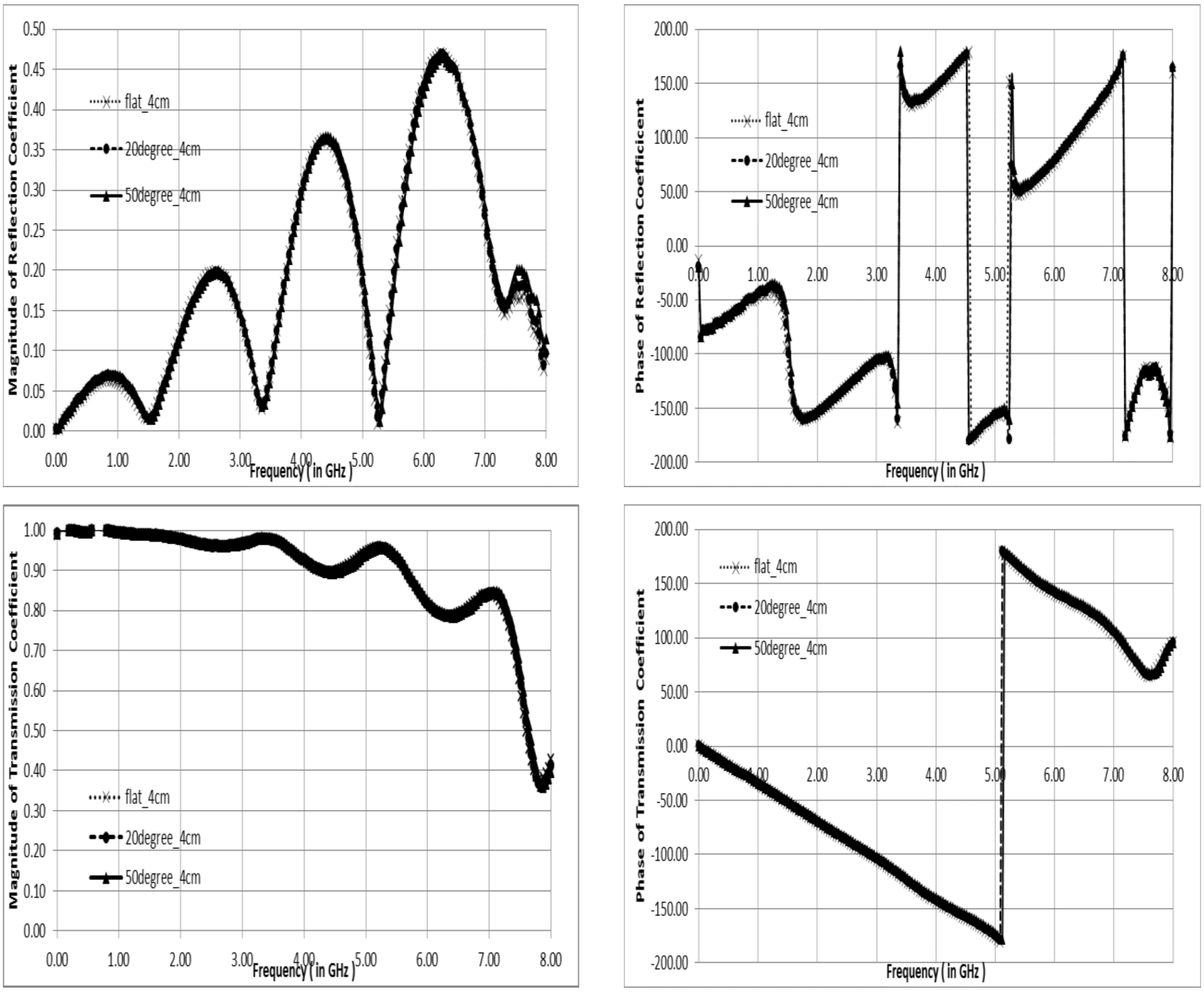

Figure 4.7.1 a) Reflection Coefficient & b) Transmission Coefficient for sample Air against frequency

a)

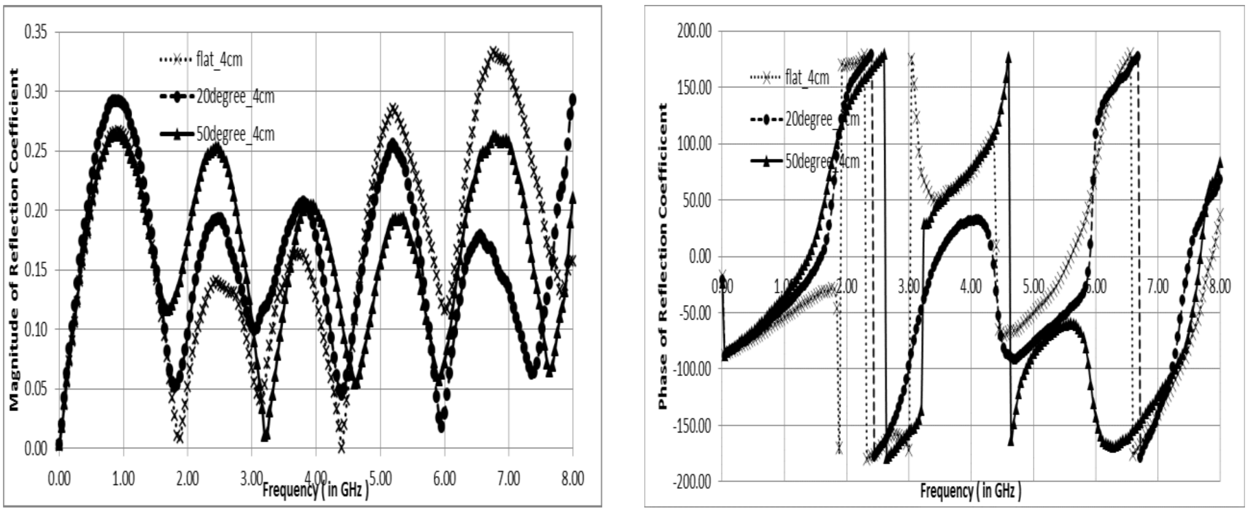

b)

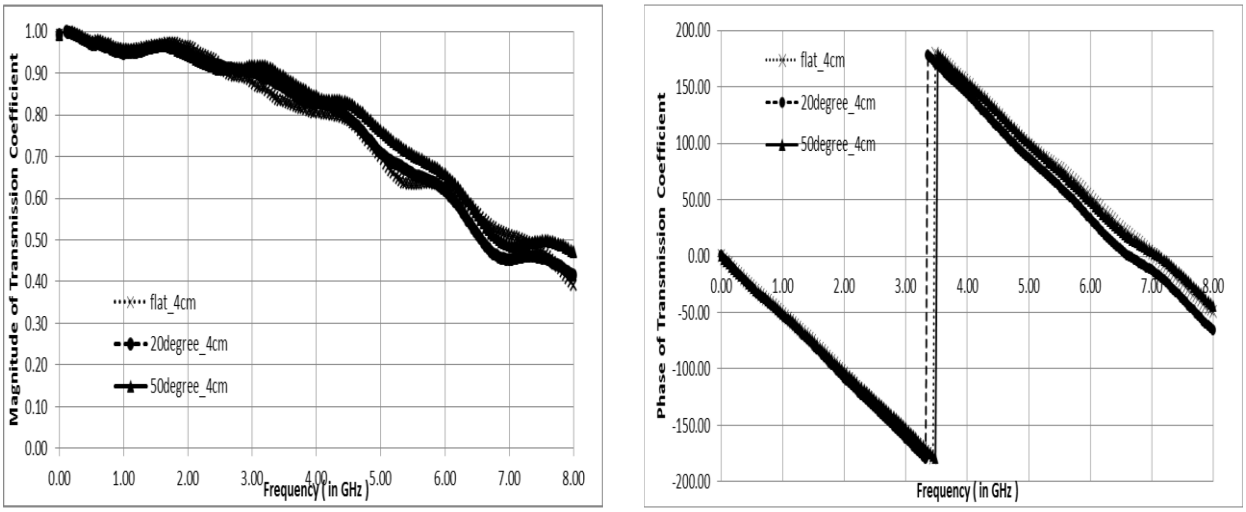

Figure 4.7.2 a) Reflection Coefficient & b) Transmission Coefficient for sample Acetone against frequency

a)

b)

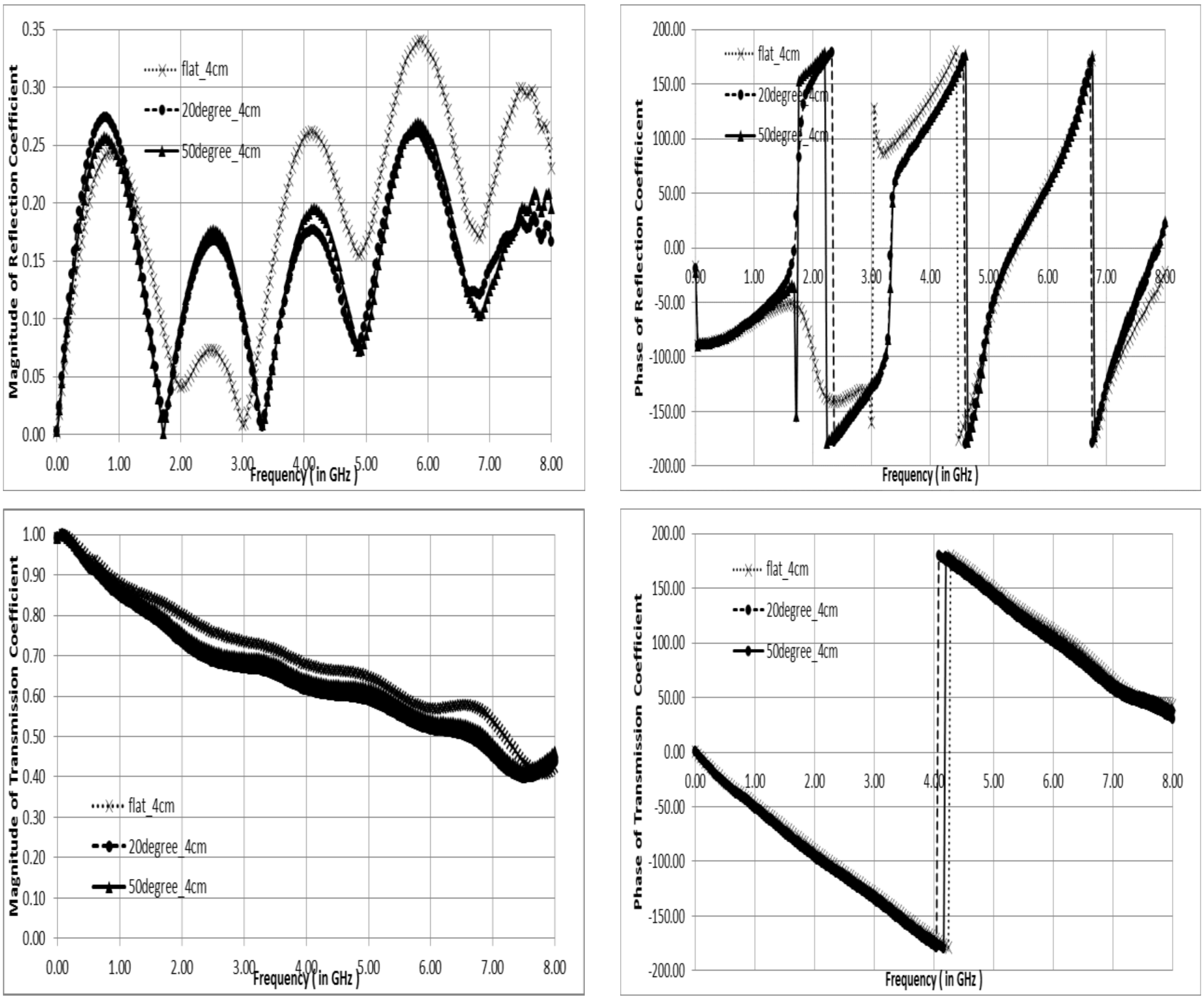

Figure 4.7.3 a) Reflection Coefficient & b) Transmission Coefficient for sample Ethanol against frequency

a)

b)

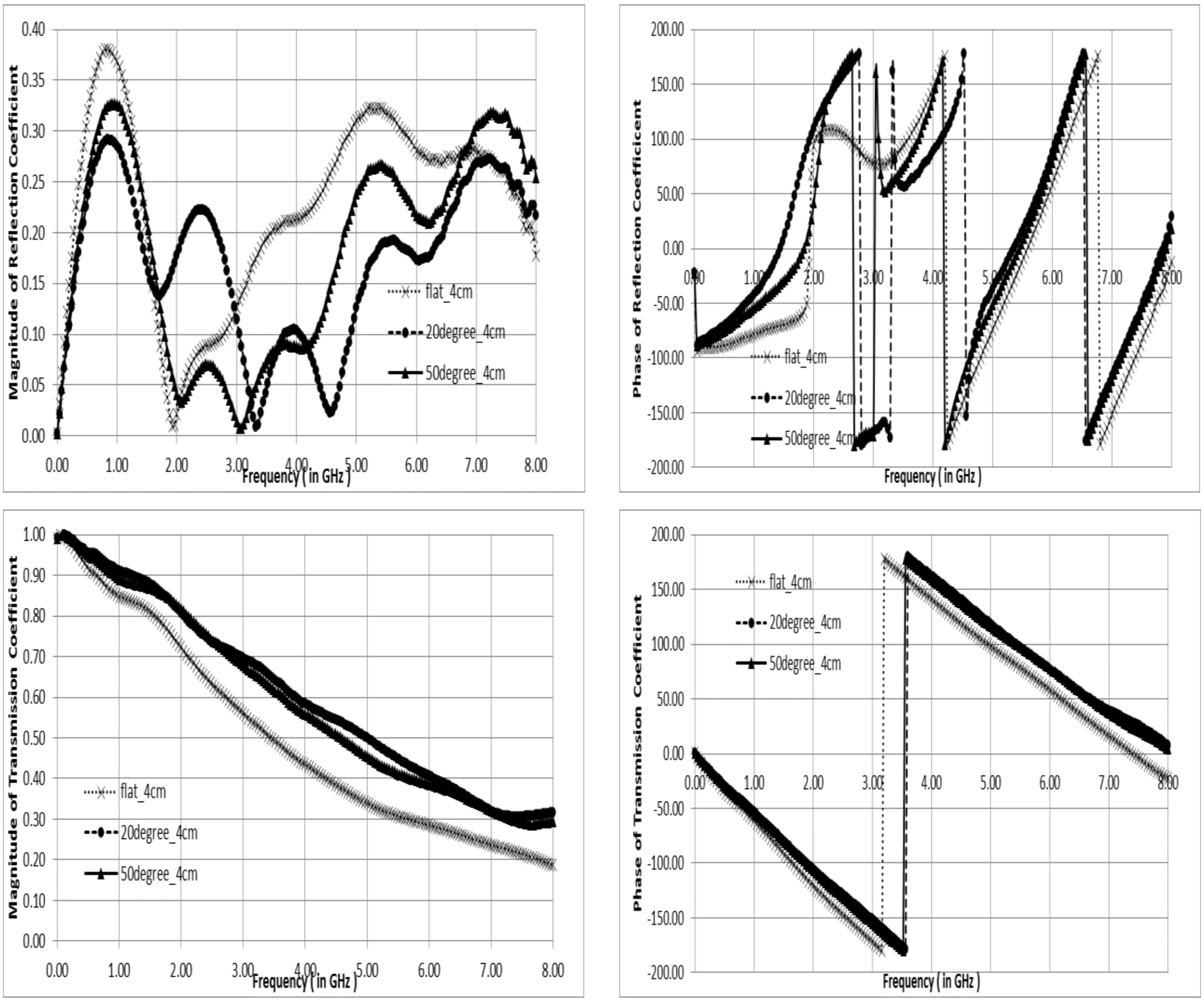

Figure 4.7.4 a) Reflection Coefficient & b) Transmission Coefficient for sample Methanol against frequency

a)

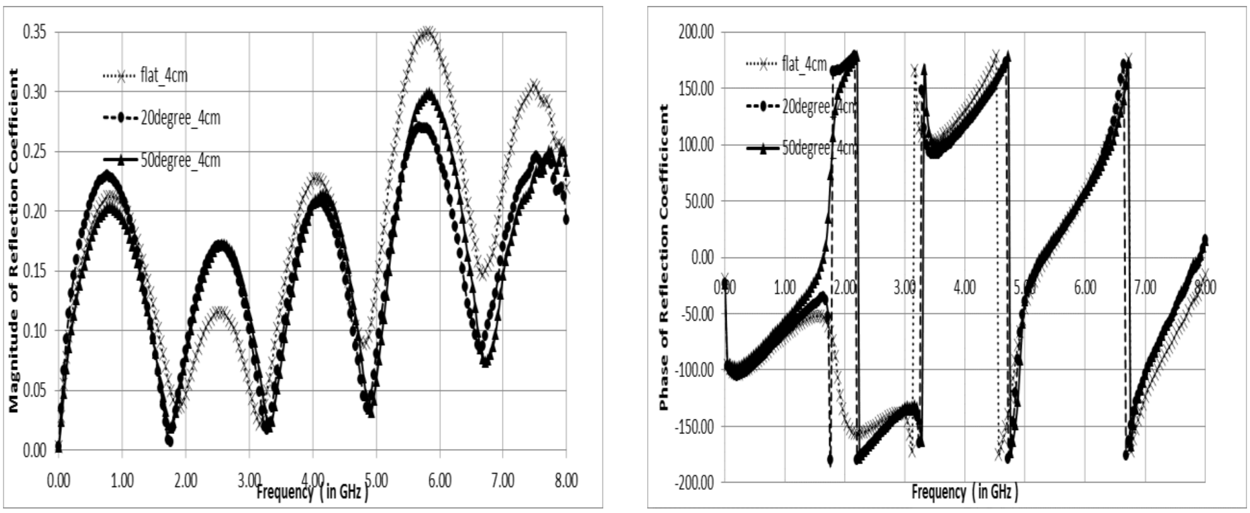

b)

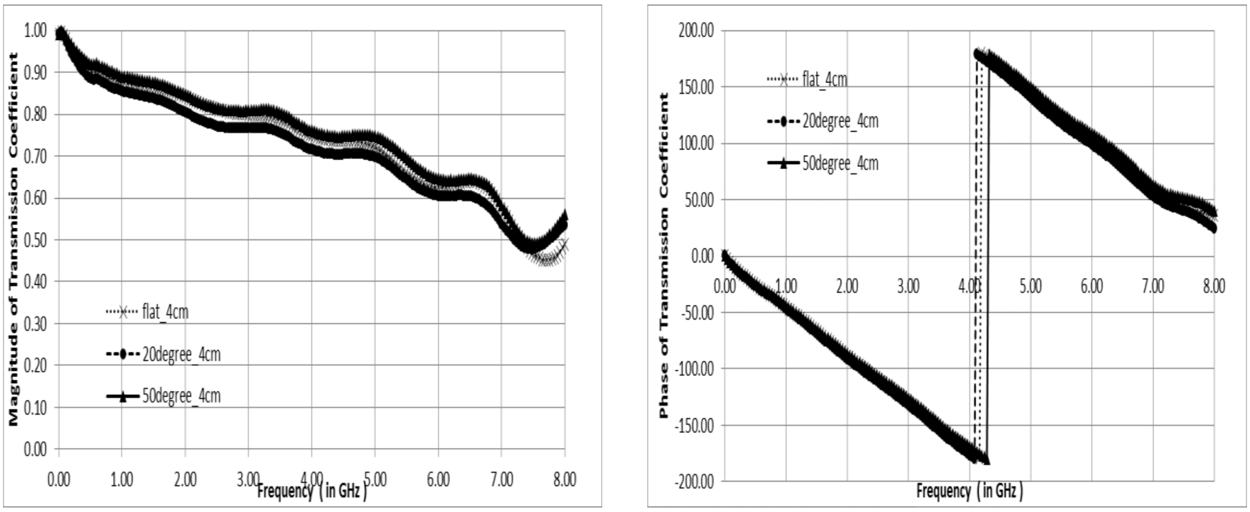

Figure 4.7.5 a) Reflection Coefficient & b) Transmission Coefficient for sample Glycerol against frequency

a)

b)

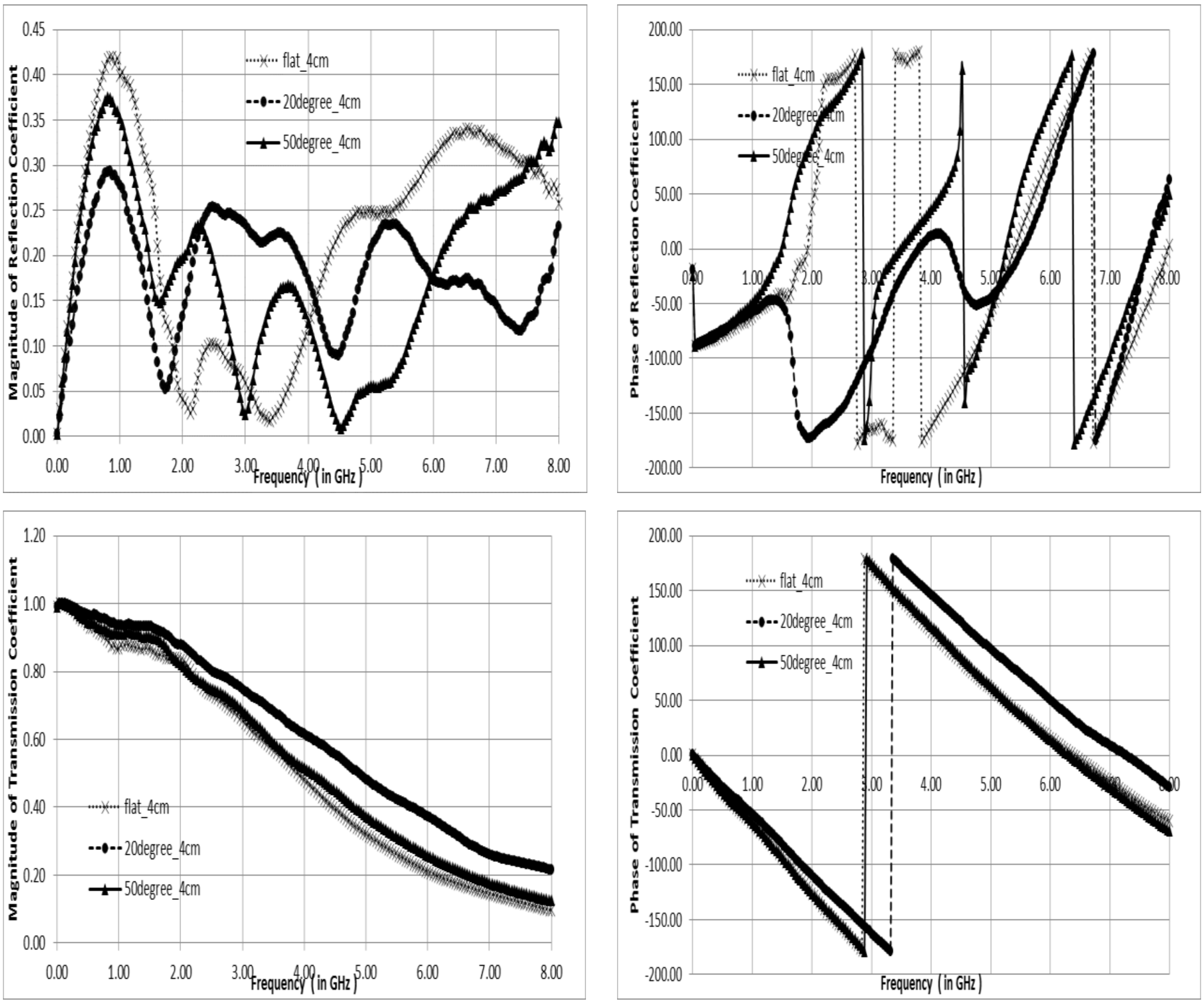

Figure 4.7.6 a) Reflection Coefficient & b) Transmission Coefficient for sample Water against frequency

4.8 Comparison of measured data for RT Duroid 6006 substrate based on from flat to different bending angle – 7cm

The line length of the sensor is 7cm and the performance of the magnitude and phase responses are shown below for the relevant samples from the microstrip line being from flat surface, 20° bending angle followed by the 50° are being compared. Similar in previous section, the performance is same for air both in magnitude response and phase response. Likewise, when the permittivity of the sample is lower, the performances in the transmission coefficient and reflection coefficient have slight difference.

a)

b)

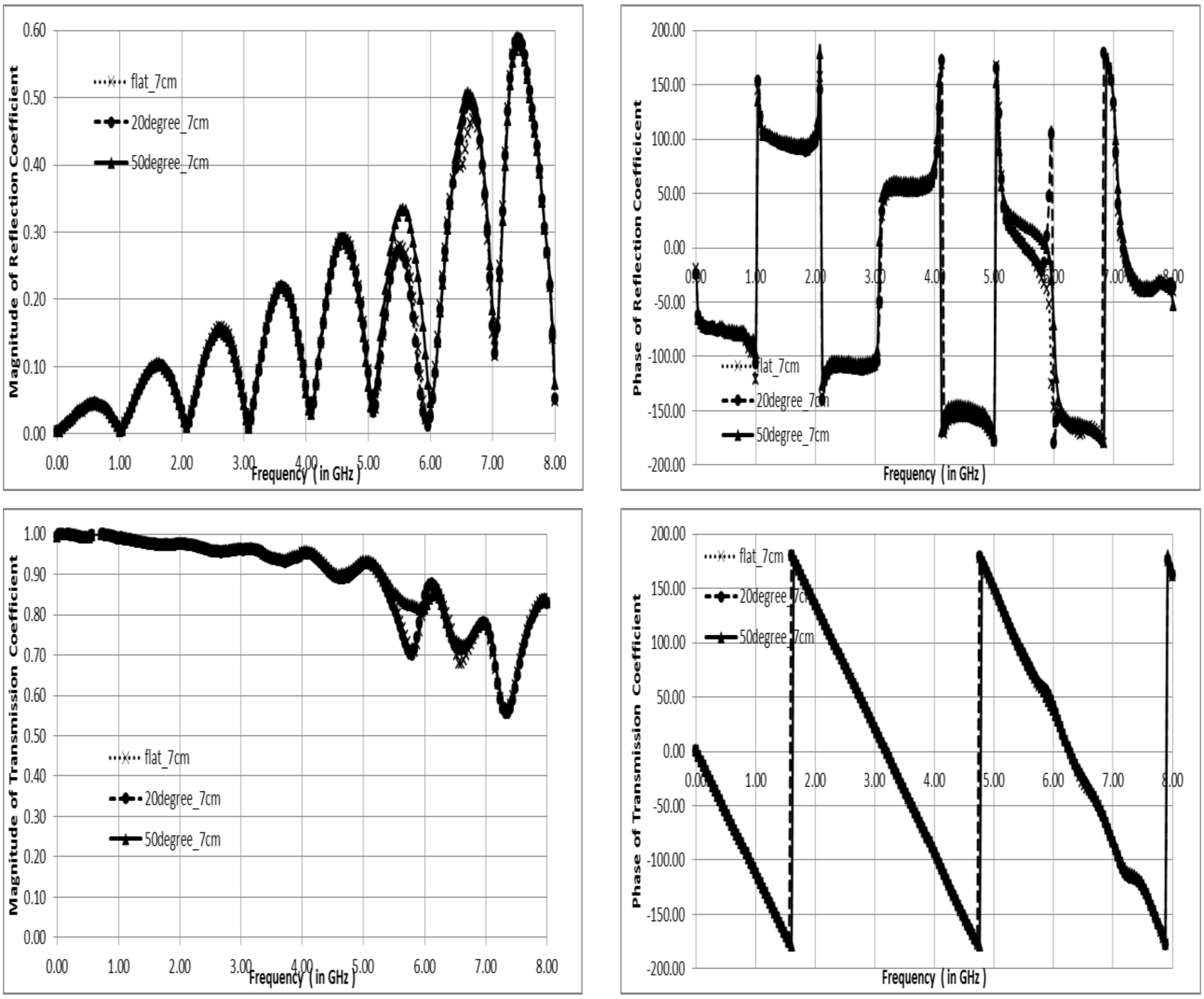

Figure 4.8.1 a) Reflection Coefficient & b) Transmission Coefficient for sample Air against frequency

a)

b)

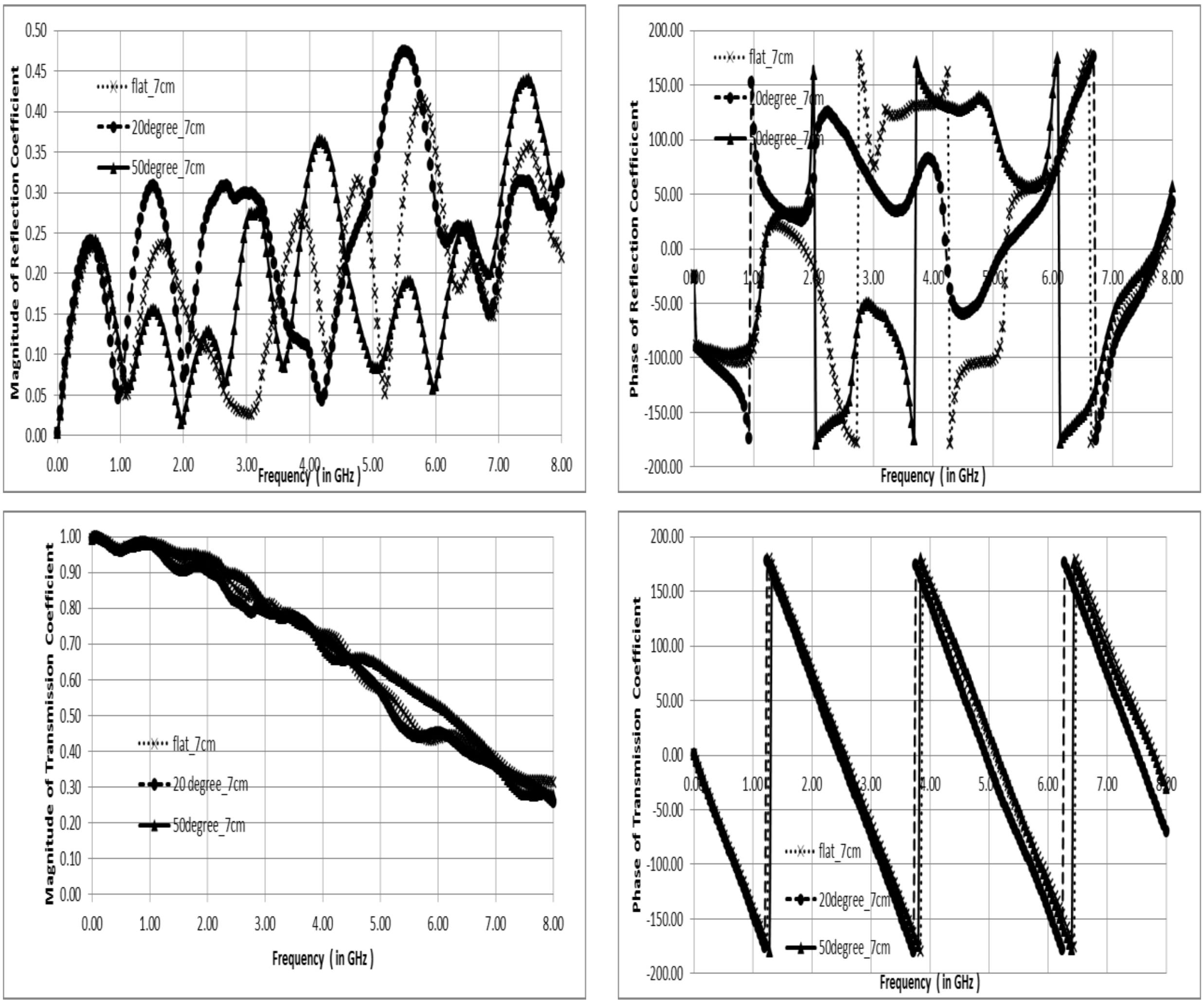

Figure 4.8.2 a) Reflection Coefficient & b) Transmission Coefficient for sample Acetone against frequency

a)

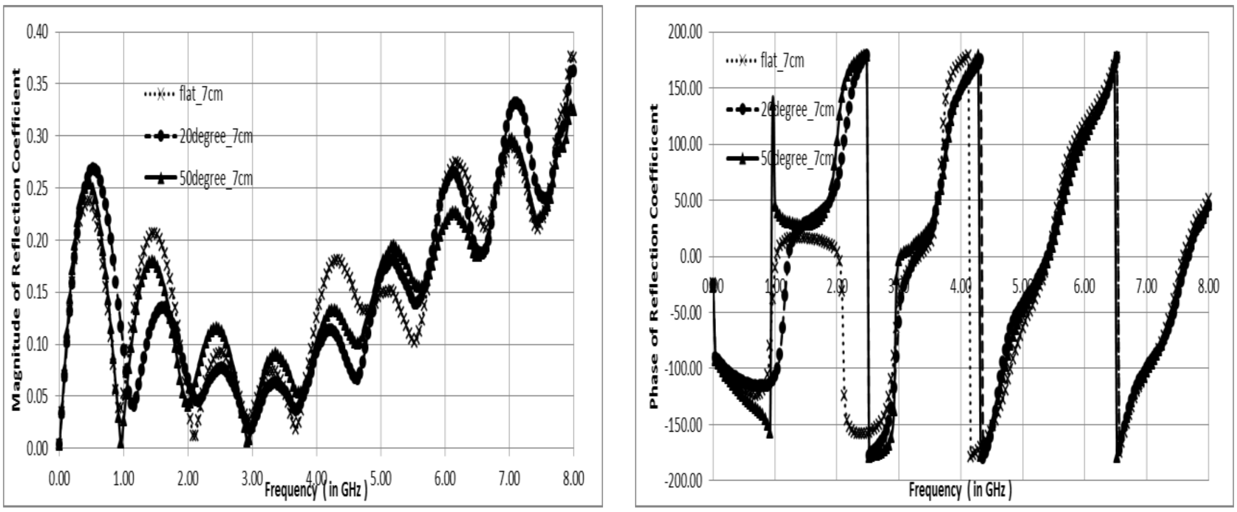

b)

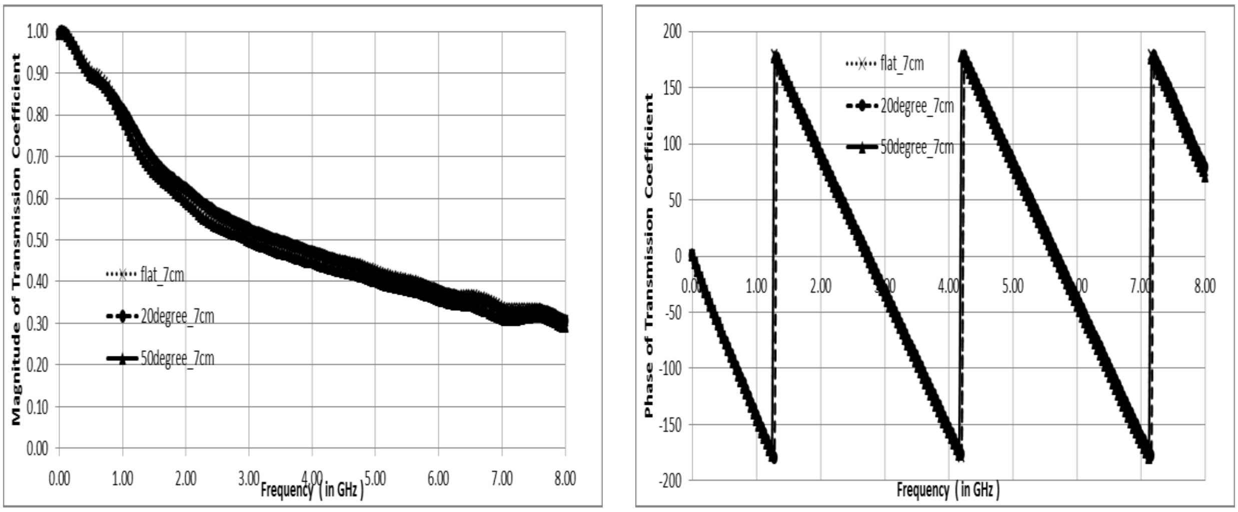

Figure 4.8.3 a) Reflection Coefficient & b) Transmission Coefficient for sample Ethanol against frequency

a)

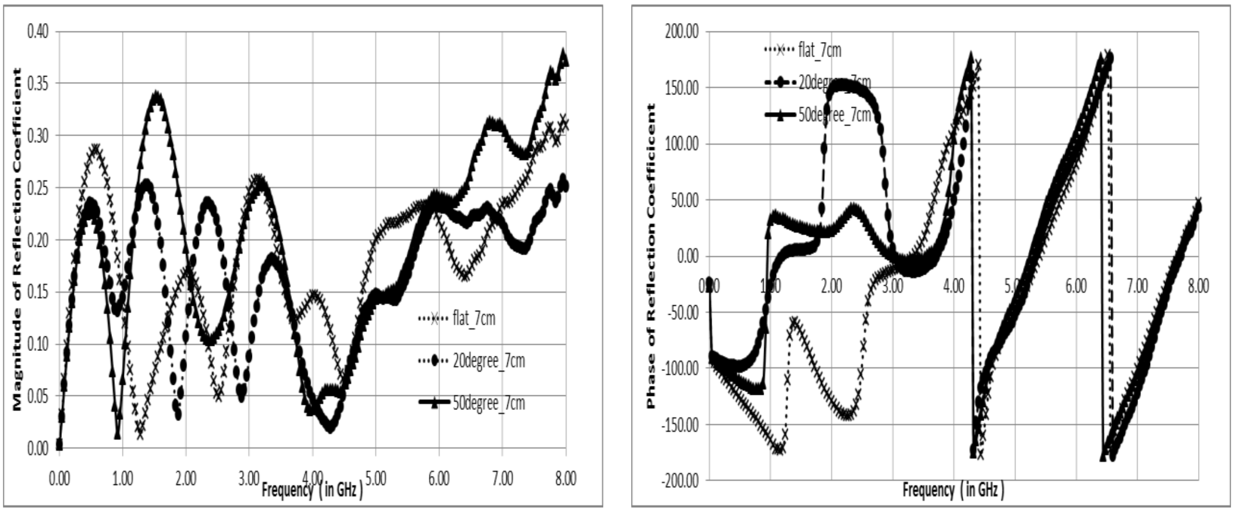

b)

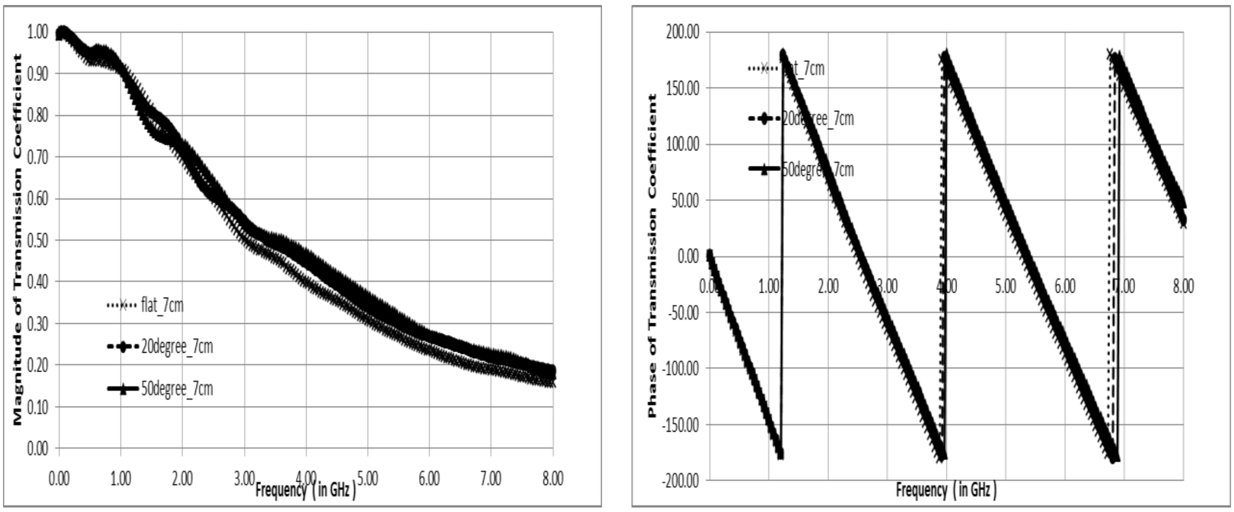

Figure 4.8.4 a) Reflection Coefficient & b) Transmission Coefficient for sample Methanol against frequency

a)

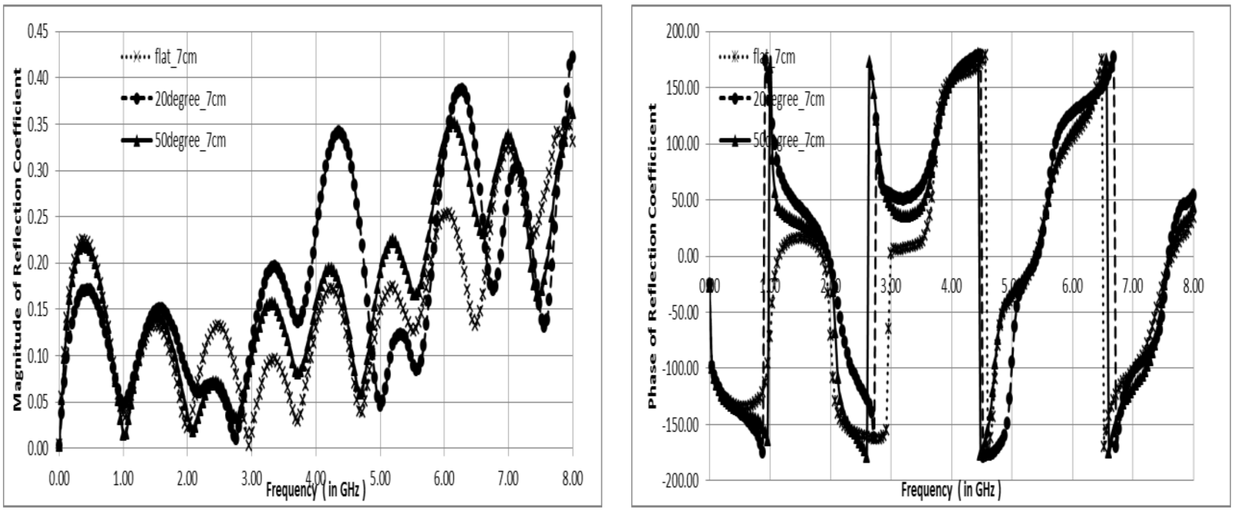

b)

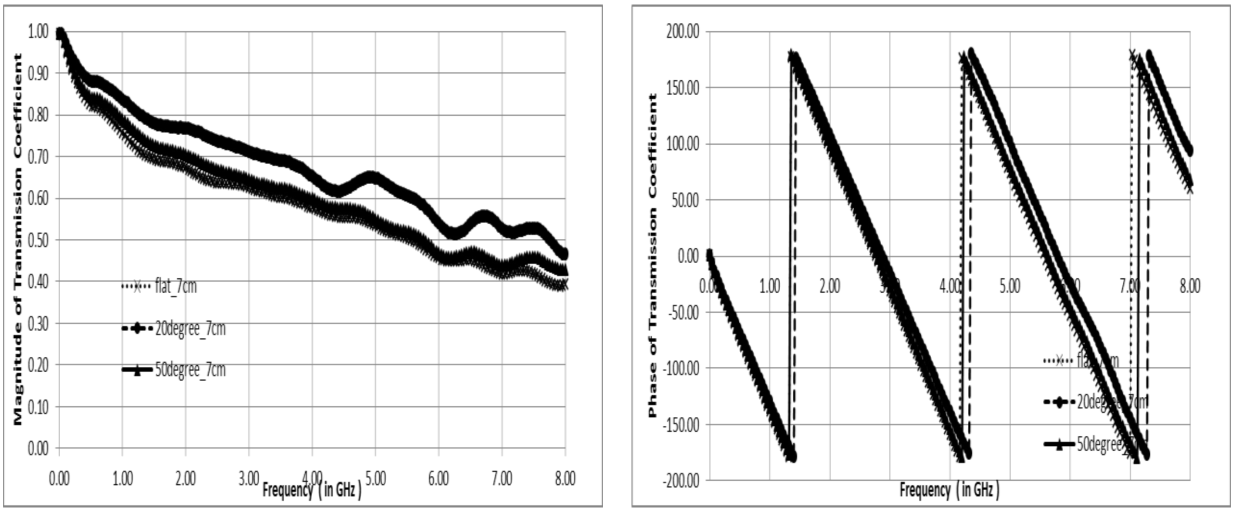

Figure 4.8.5 a) Reflection Coefficient & b) Transmission Coefficient for sample Glycerol against frequency

a)

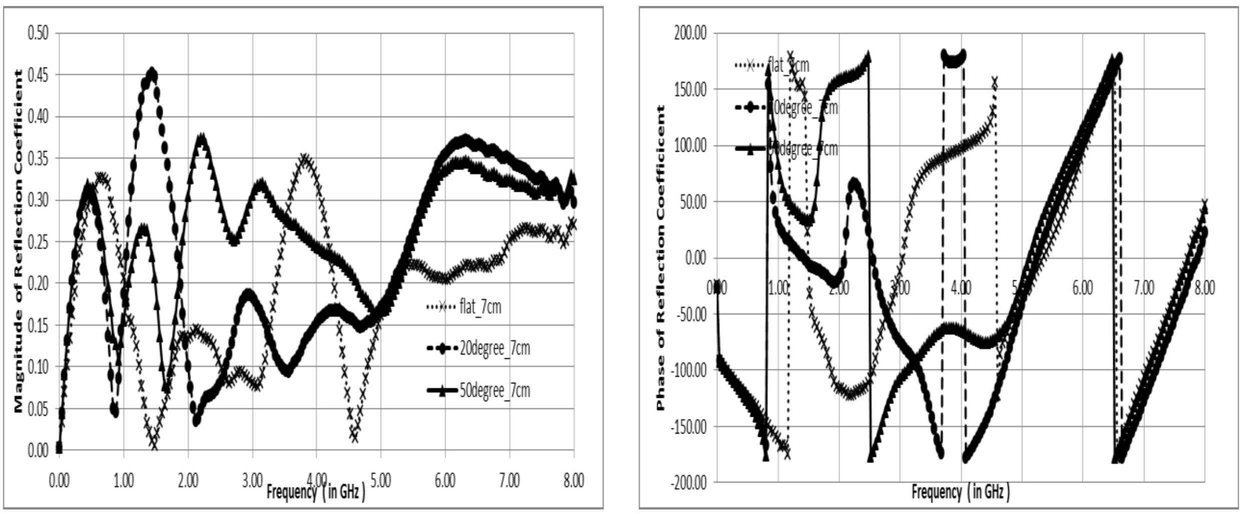

b)

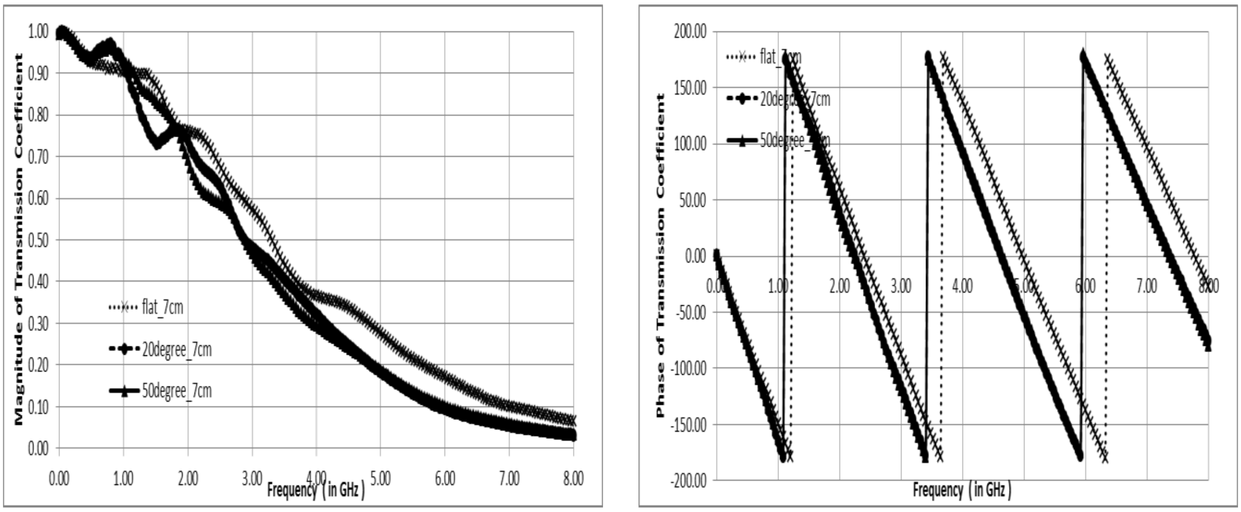

Figure 4.8.6 a) Reflection Coefficient & b) Transmission Coefficient for sample Water against frequency

4.9 Comparison of measured data for FR-4 substrate with different line length

For this section, FR - 4 substrate has been selected to test the behaviour towards different line length of the microstrip line sensor. Since, it is a low cost substrate, it is acceptable to the low permittivity of sample. From the comparison, it can be observed that the performance given when line length of 7cm is not satisfactory at the lower frequency range as there is a design of it is not accurate in terms of the placing of the launcher.

a)

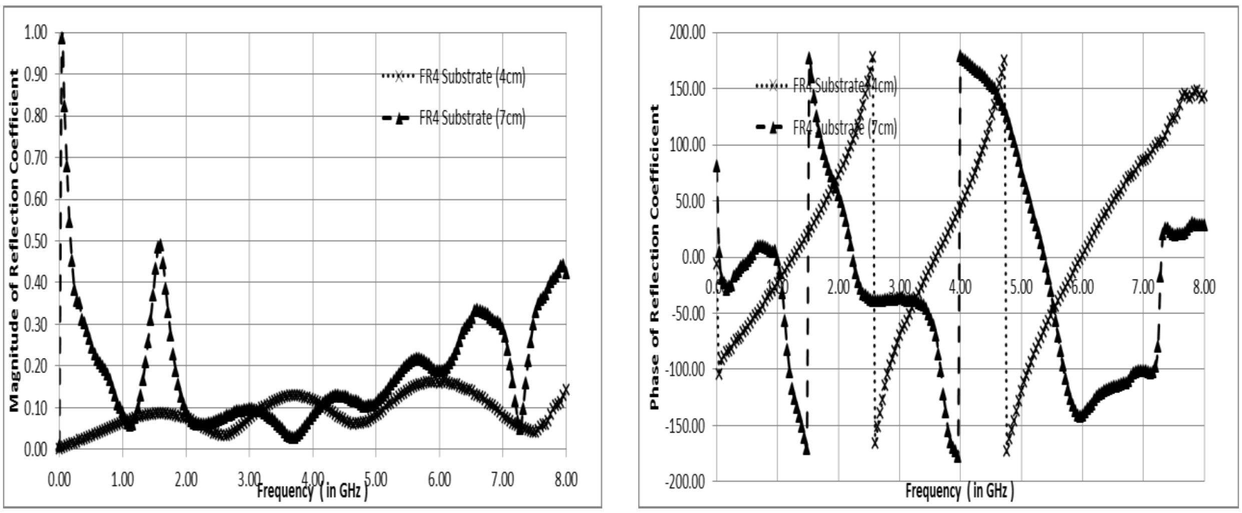

b)

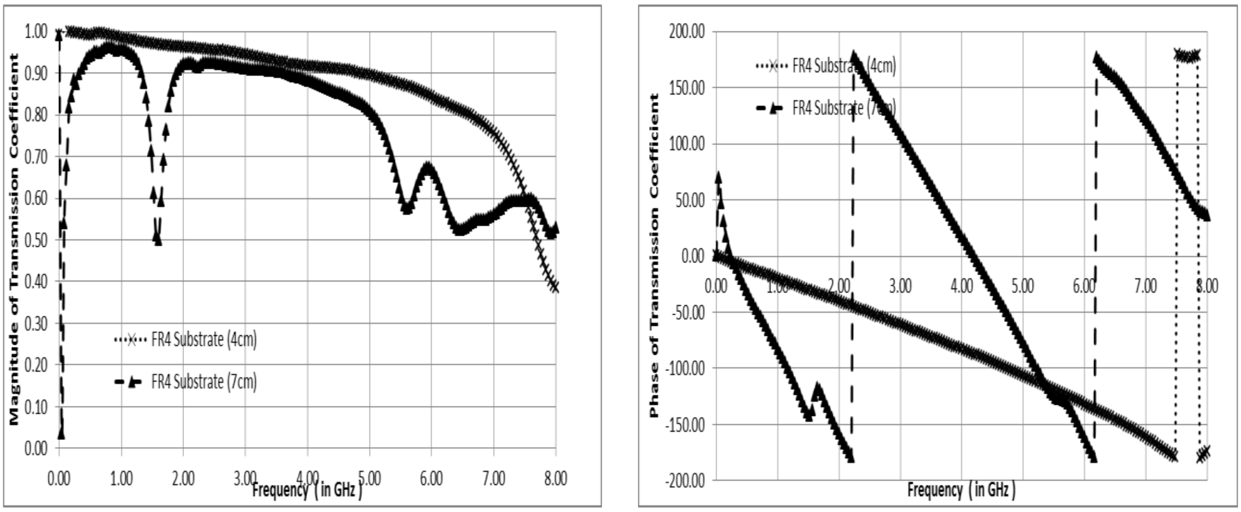

Figure 4.9.1 a) Reflection Coefficient & b) Transmission Coefficient for sample Air against frequency

a)

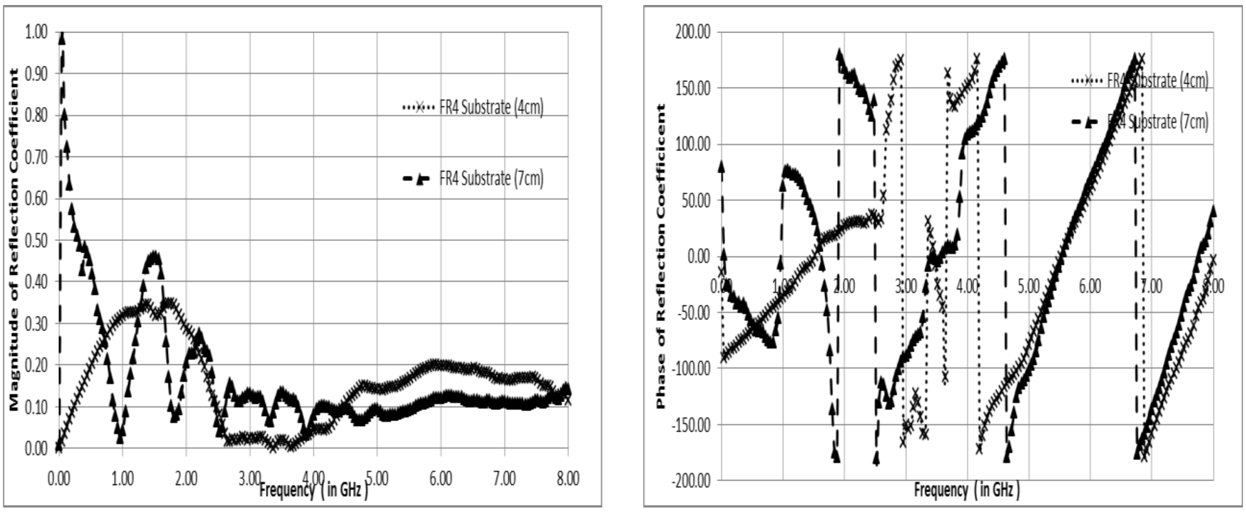

b)

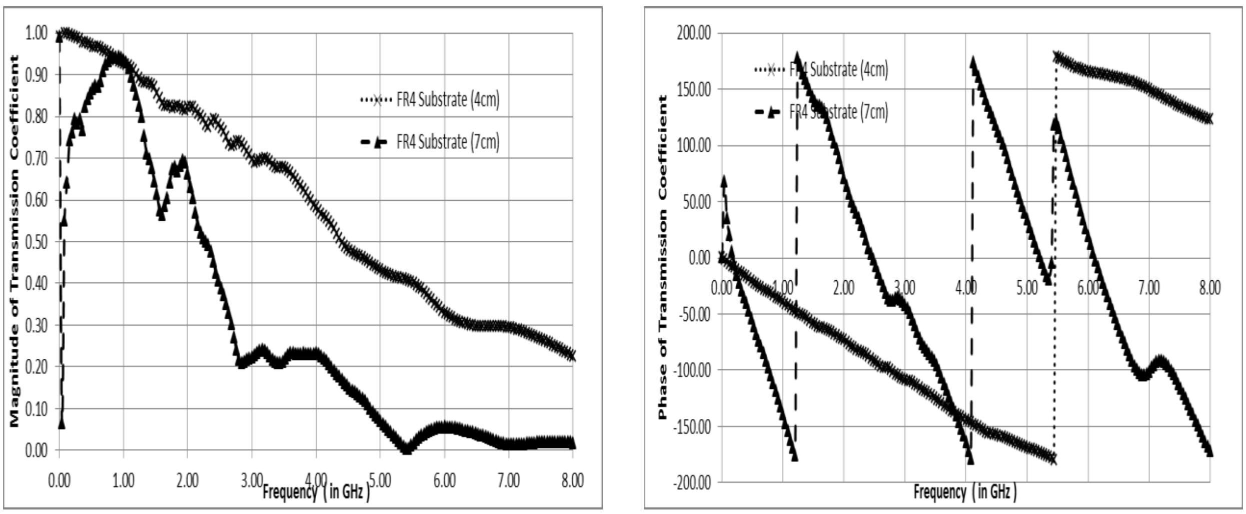

Figure 4.9.2 a) Reflection Coefficient & b) Transmission Coefficient for sample Acetone against frequency

a)

b)

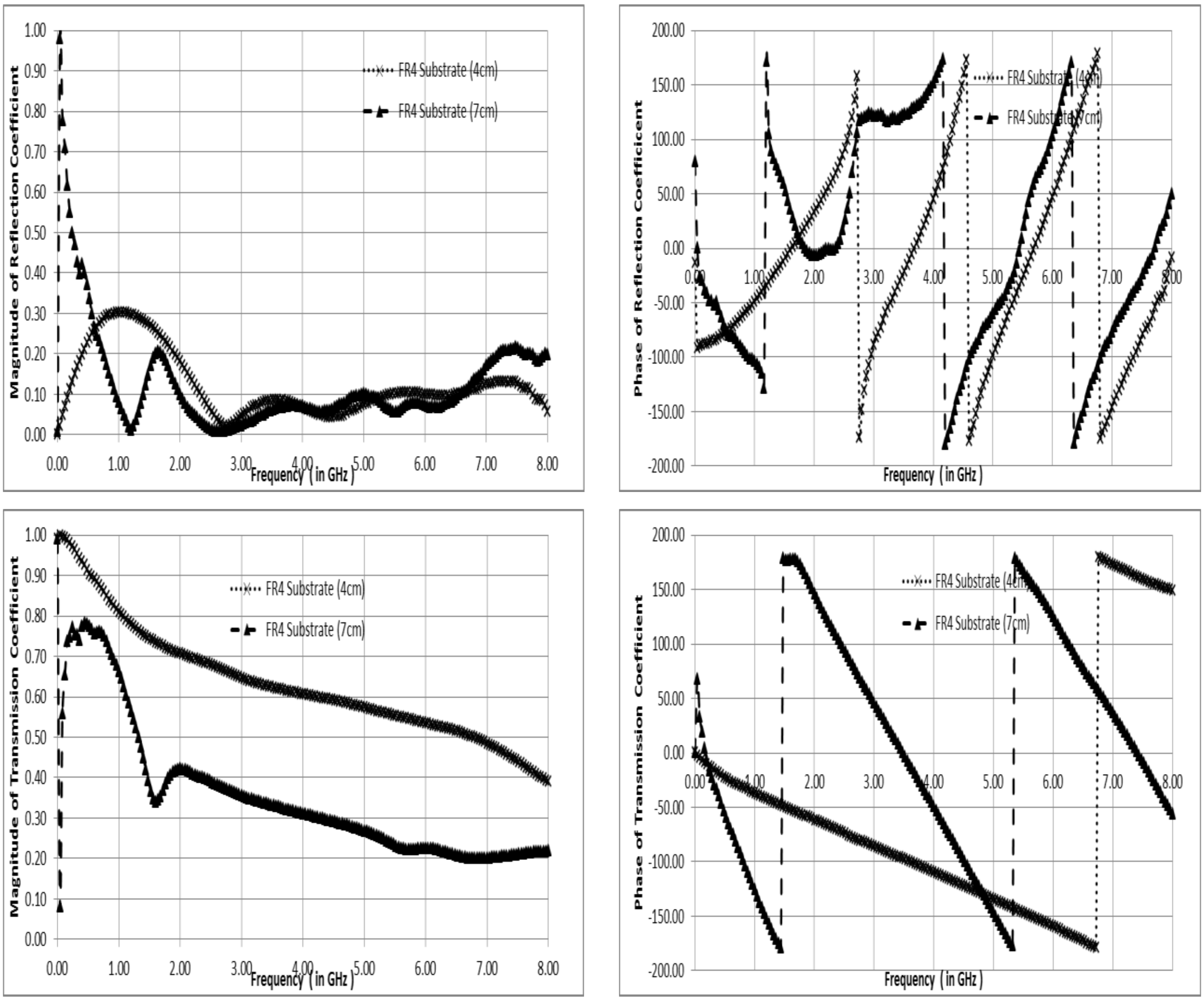

Figure 4.9.3 a) Reflection Coefficient & b) Transmission Coefficient for sample Ethanol against frequency

a)

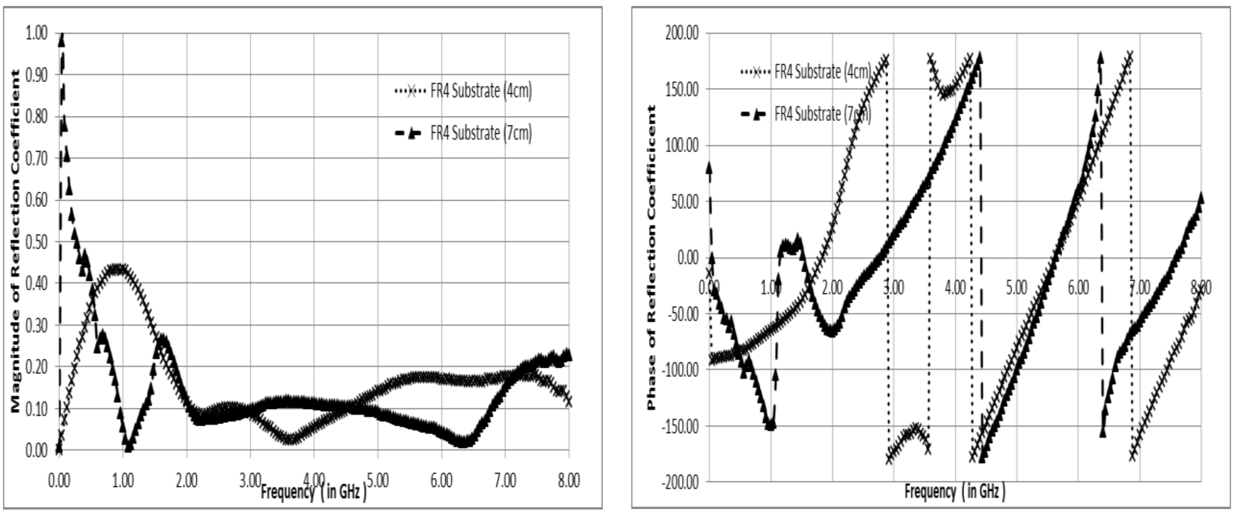

b)

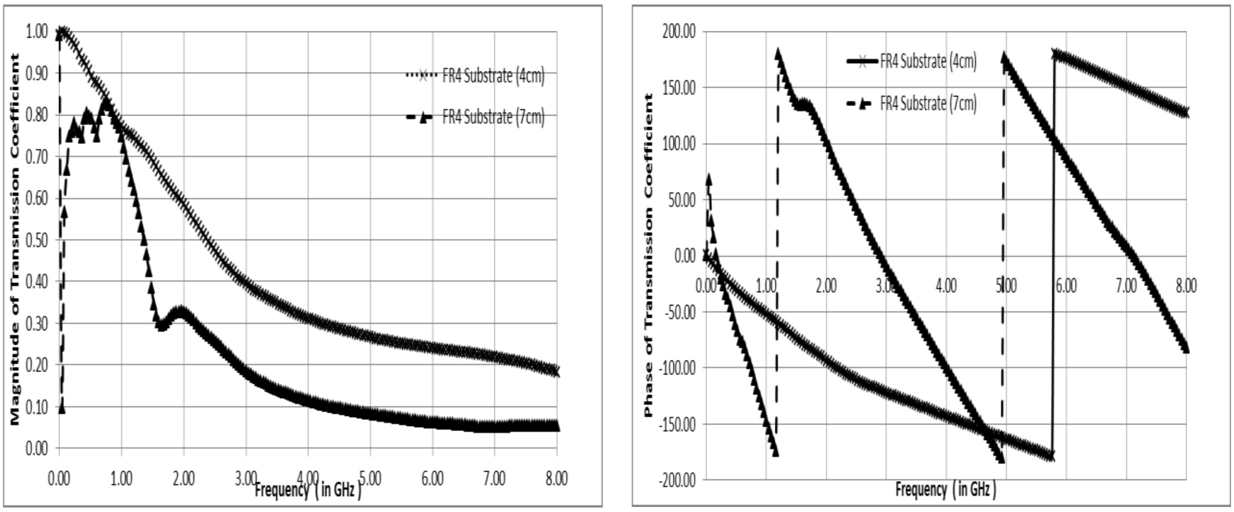

Figure 4.9.4 a) Reflection Coefficient & b) Transmission Coefficient for sample Methanol against frequency

a)

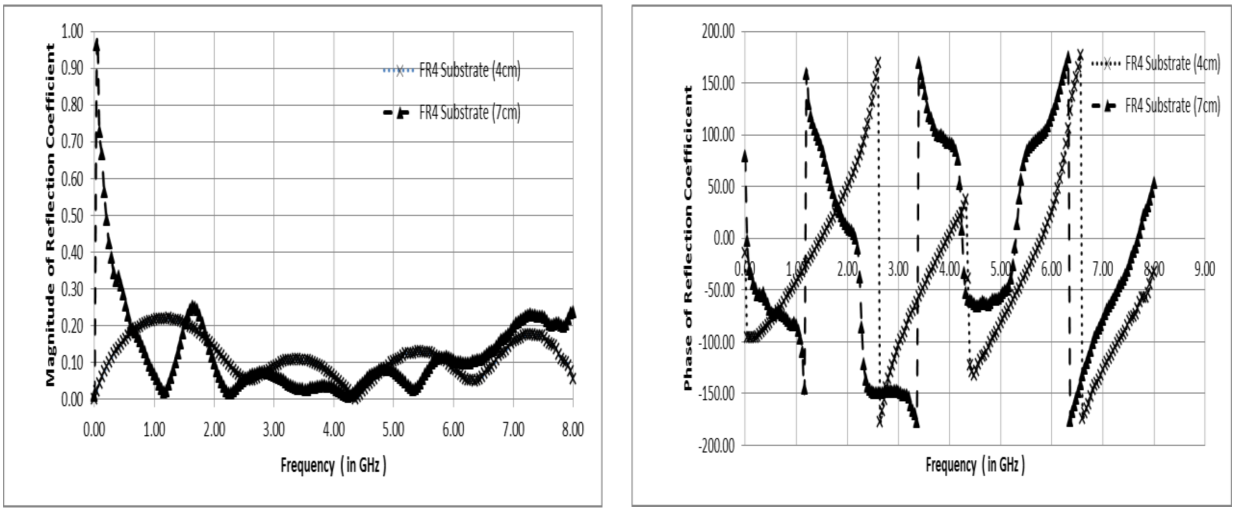

b)

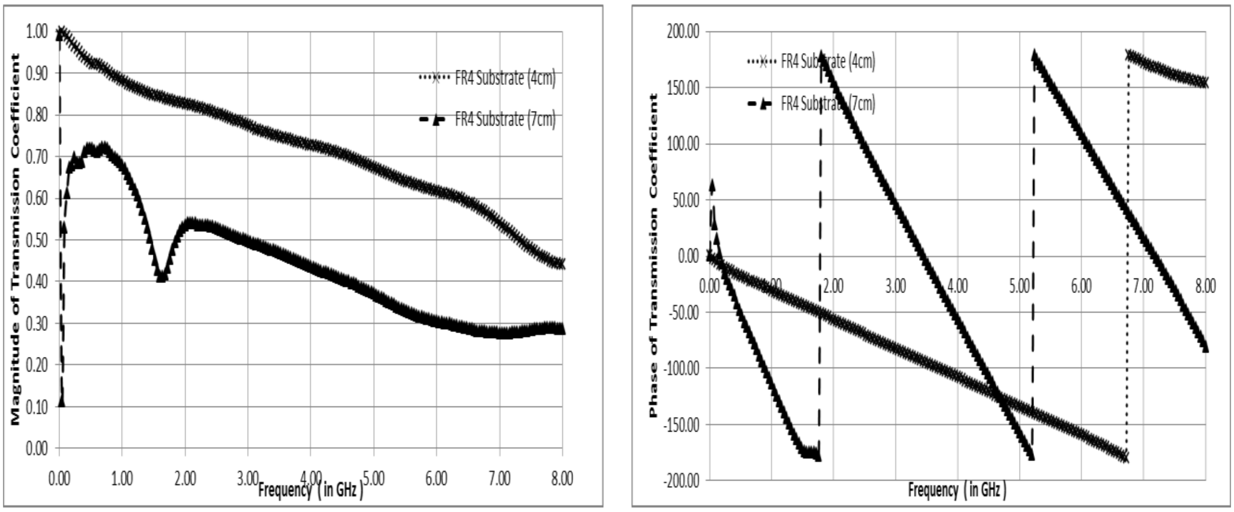

Figure 4.9.5 a) Reflection Coefficient & b) Transmission Coefficient for sample Glycerol against frequency

a)

b)

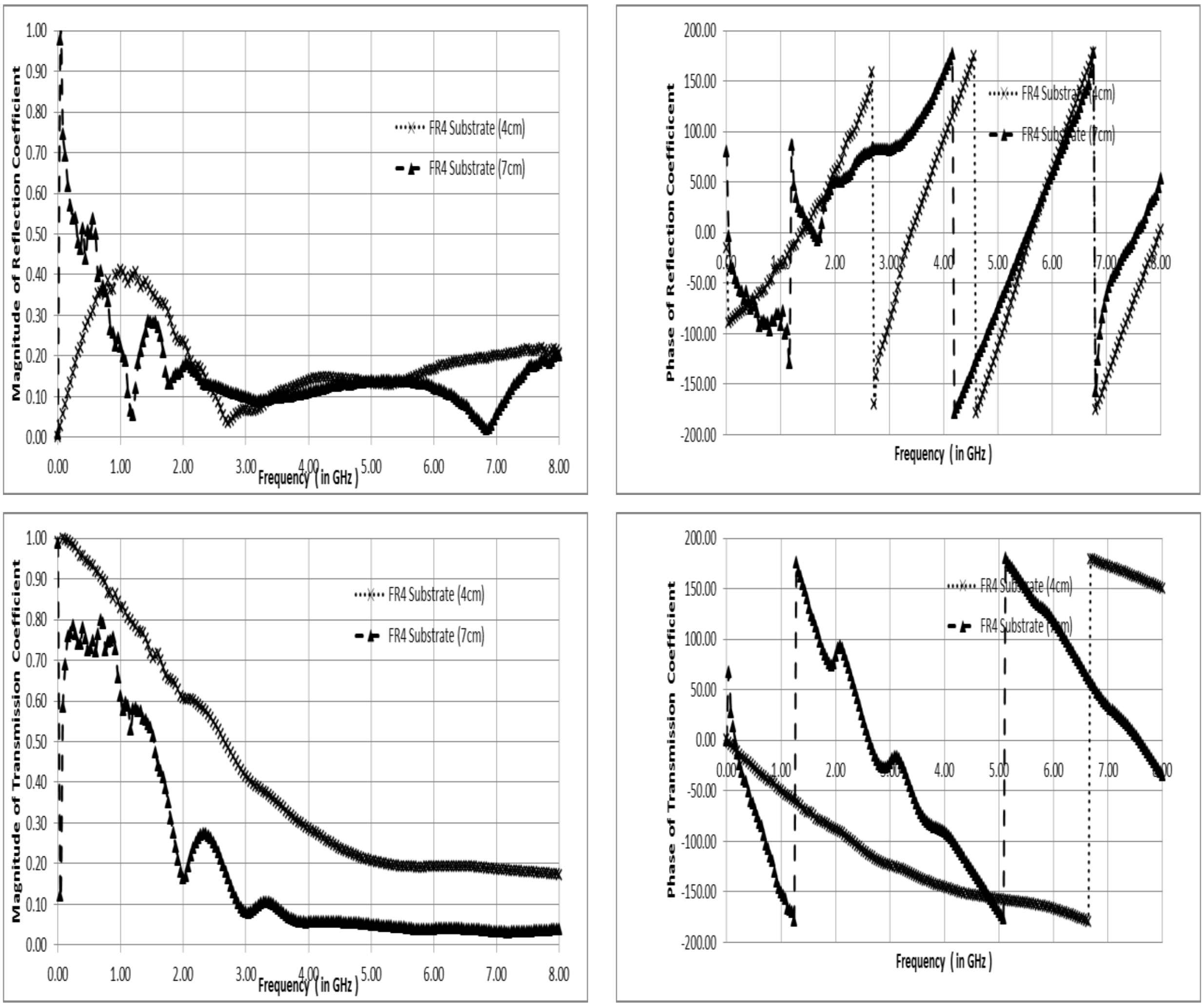

Figure 4.9.6 a) Reflection Coefficient & b) Transmission Coefficient for sample Water against frequency

4.10 Comparison of measured data for FR- 4 & RT Duroid 6006 substrate with 4 cm length

As for the 4 cm length of the microstrip line, the performance shown for the both the substrates used are different for each sample used. For instance, in the air medium, by using the RT Duroid 6006 substrate, the magnitude of reflection coefficient increases exponentially along an increase in the frequency of the EM wave. This shows that with a better copper substrate used, the performance of the wave transmitting is far more better. For the case of methanol and water samples, in both the substrates, the magnitude of transmission coefficient decreases when the frequency increases. This behaviour occurs due to the occurrence of the extent interaction between the field and the induced dipole of molecule.

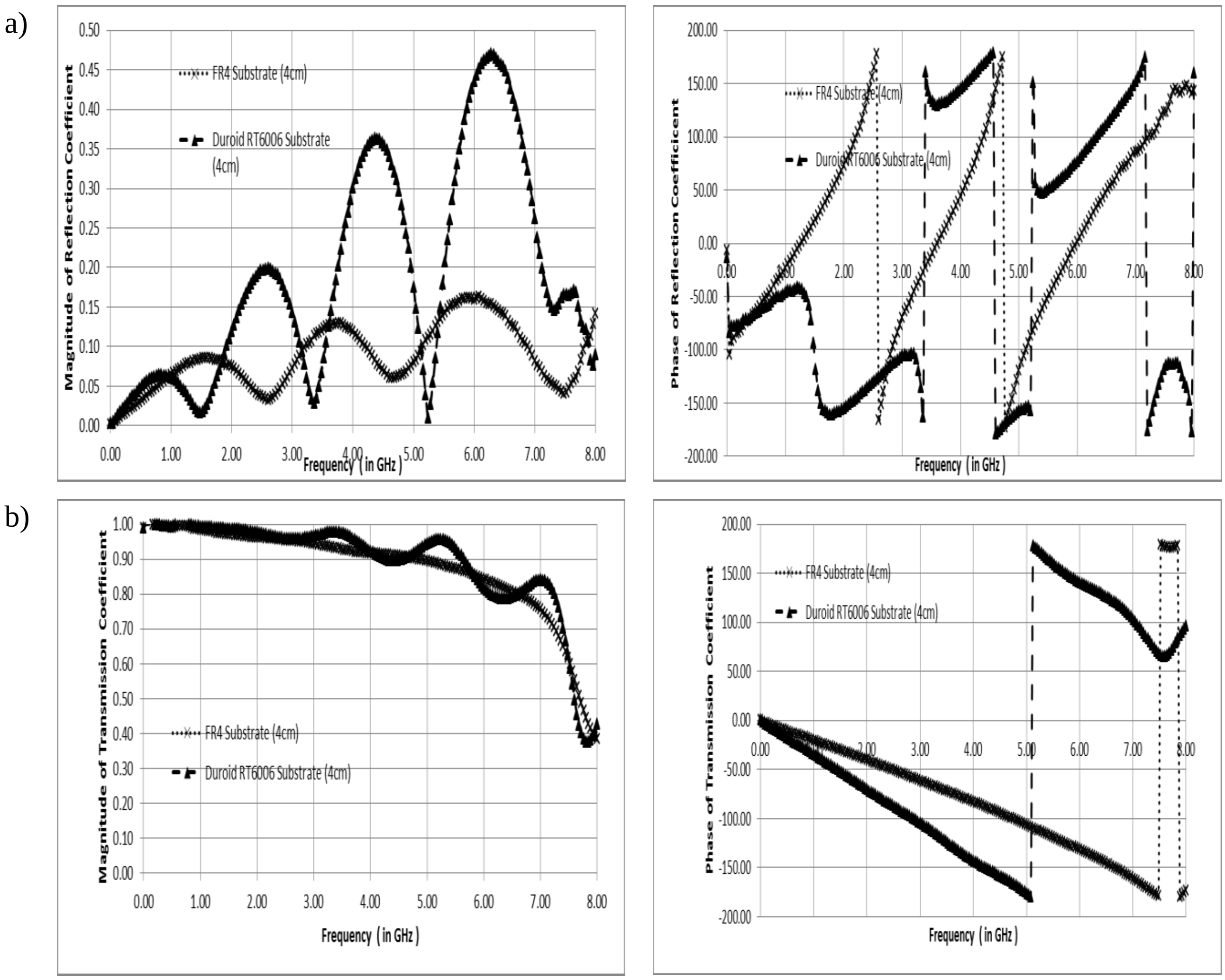

Figure 4.10.1 a) Reflection Coefficient & b) Transmission Coefficient for sample Air against frequency

a)

b)

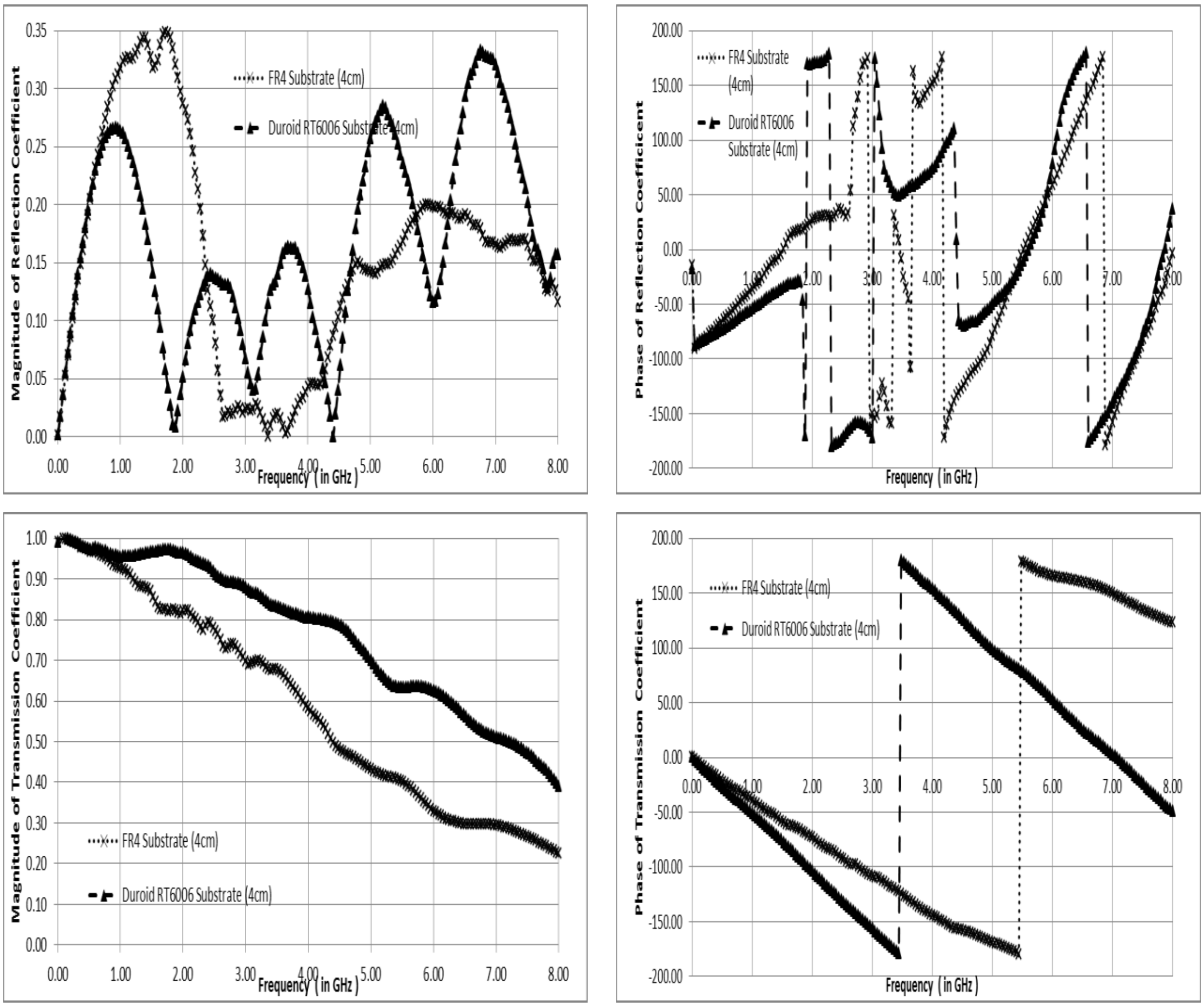

Figure 4.10.2 a) Reflection Coefficient & b) Transmission Coefficient for sample Acetone against frequency

a)

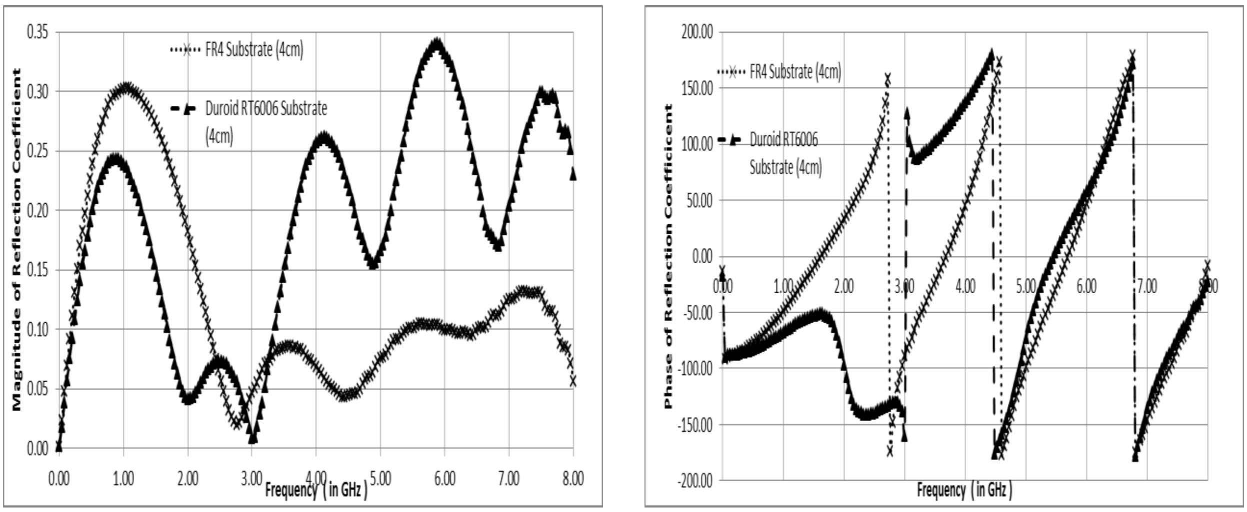

b)

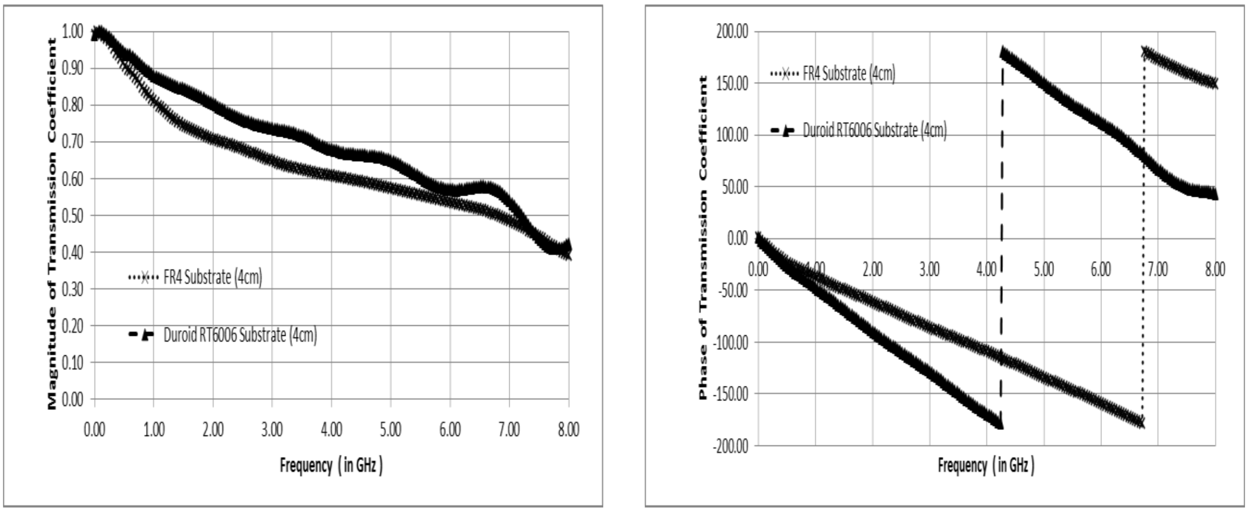

Figure 4.10.3 a) Reflection Coefficient & b) Transmission Coefficient for sample Ethanol against frequency

a)

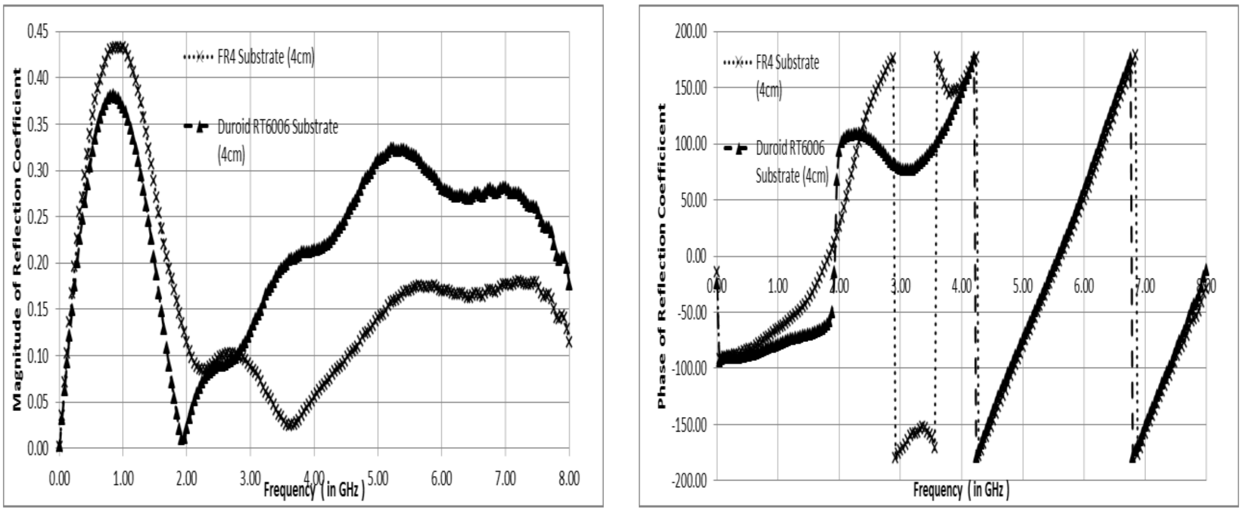

b)

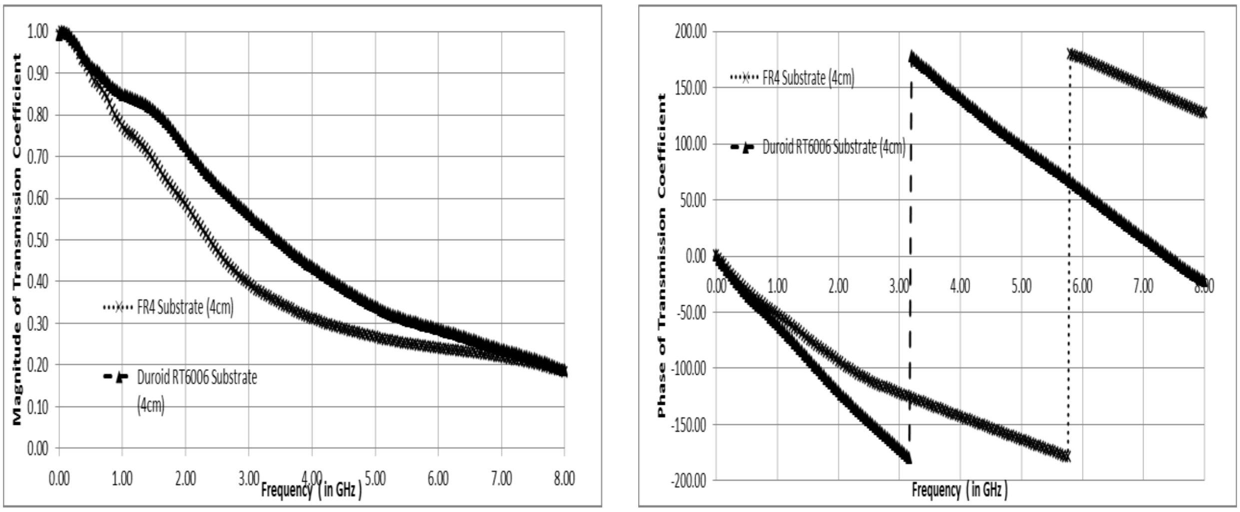

Figure 4.10.4 a) Reflection Coefficient & b) Transmission Coefficient for sample Methanol against frequency

a)

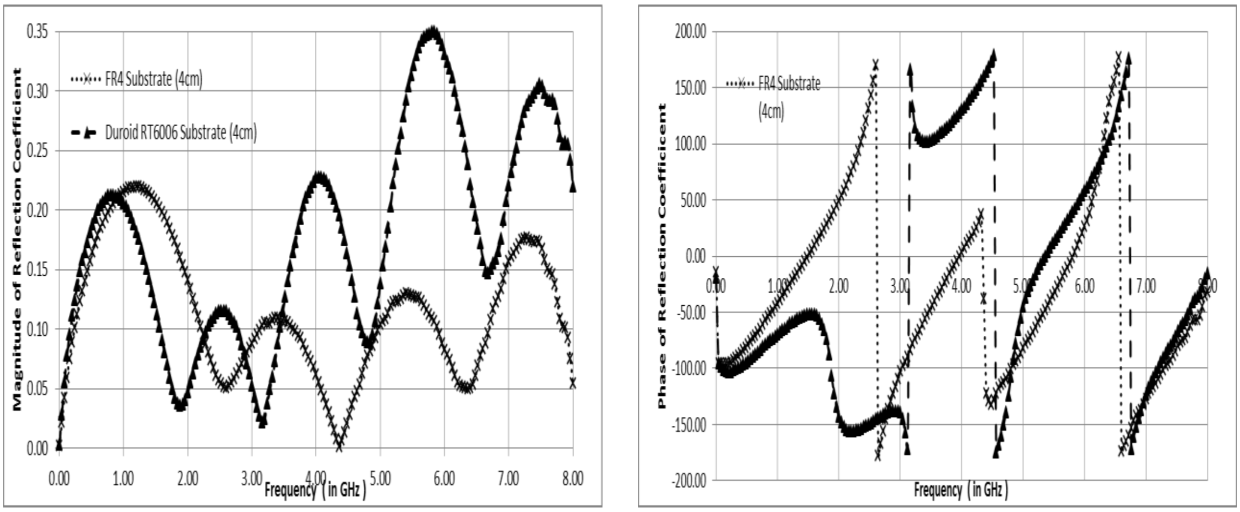

b)

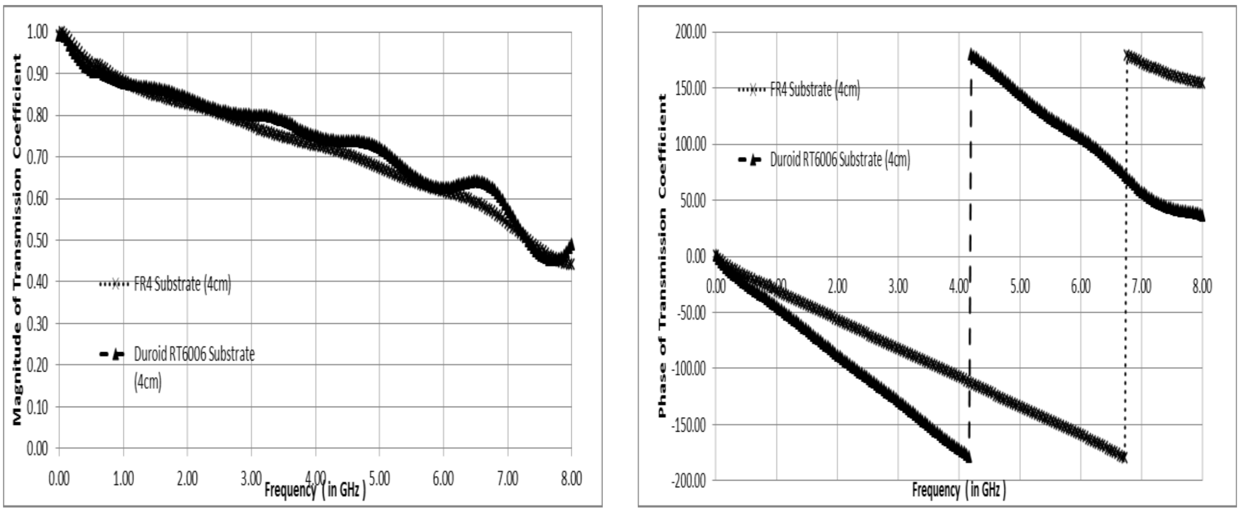

Figure 4.10.5 a) Reflection Coefficient & b) Transmission Coefficient for sample Glycerol against frequency

a)

b)

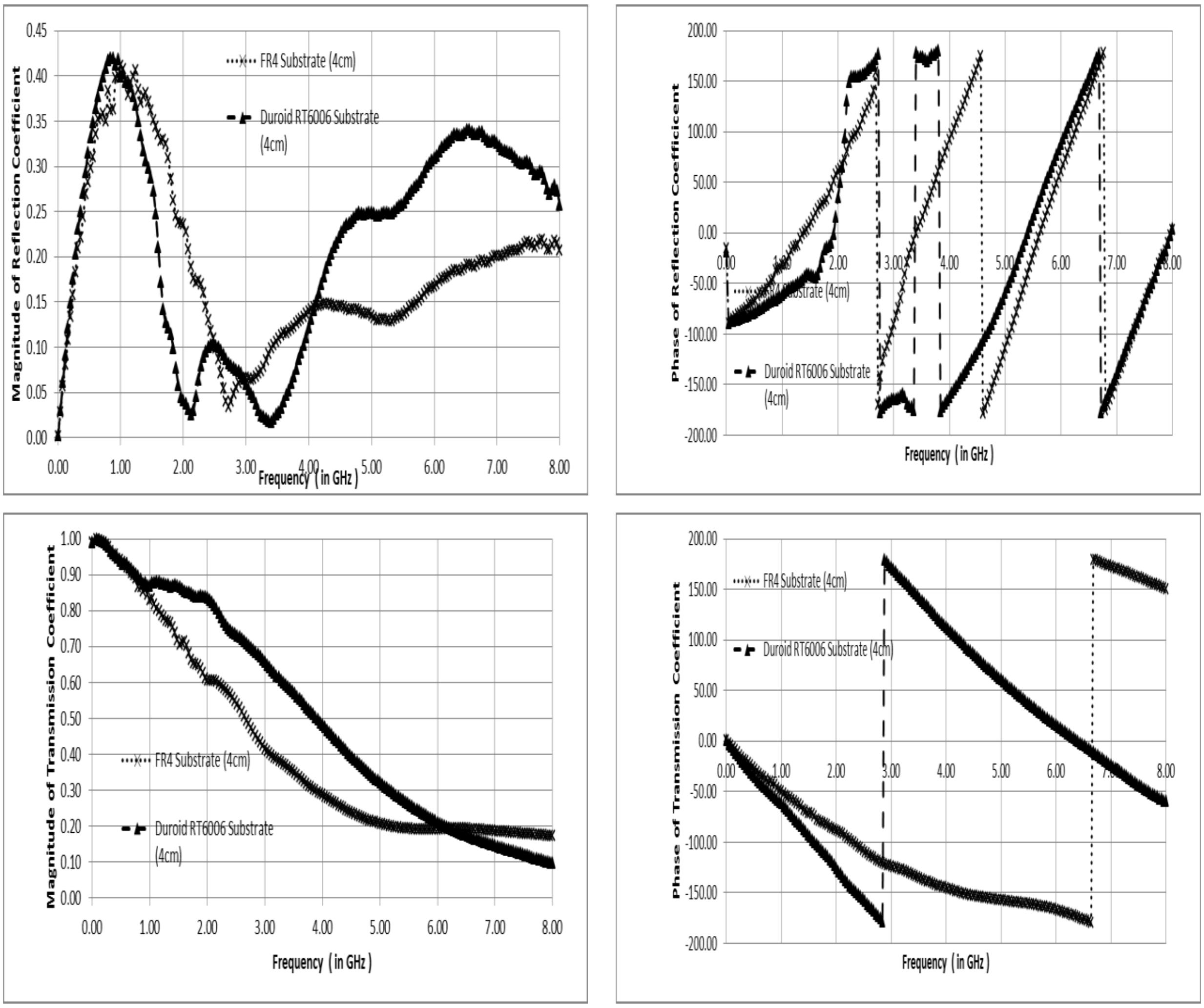

Figure 4.10.6 a) Reflection Coefficient & b) Transmission Coefficient for sample Water against frequency

4.11 Comparison of measured data for FR- 4 & RT Duroid 6006 substrate with 7 cm length

The graphs shown are on the magnitude of transmission coefficient for each sample on different substrates that have been used. Comparisons of different types of substrate towards different samples have been analysed. The flat comparison is between the FR-4 and RT Duroid 6006 substrates with the length of 7cm respectively. For all the samples given, it can be seen that the magnitude of transmission coefficient for the RT Duroid 6006 substrate is lower when compared to the FR - 4 substrate. This is due the presence of high dielectric constant for RT Duroid 6006.

a)

b)

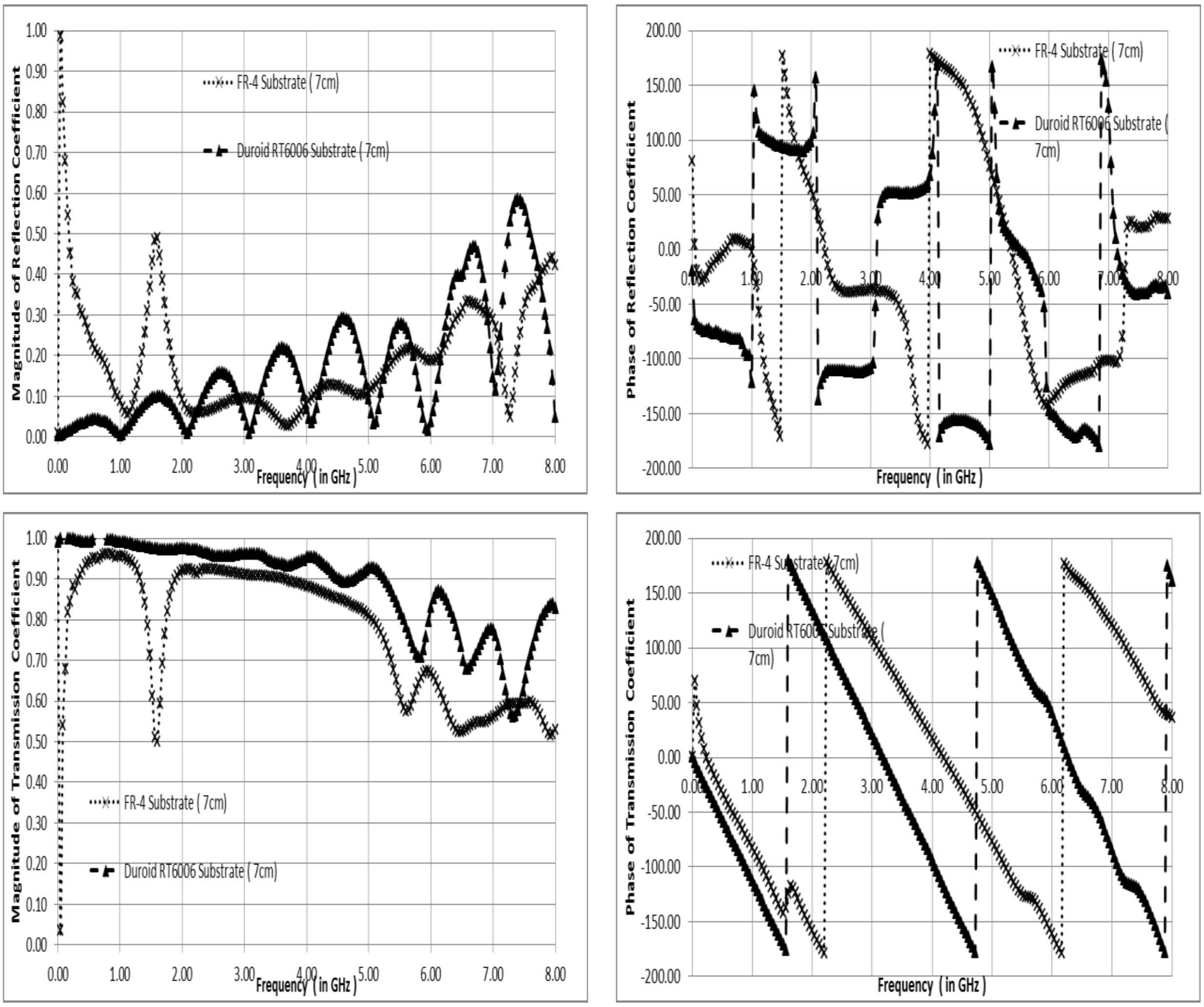

Figure 4.11.1 a) Reflection Coefficient & b) Transmission Coefficient for sample Air against frequency

a)

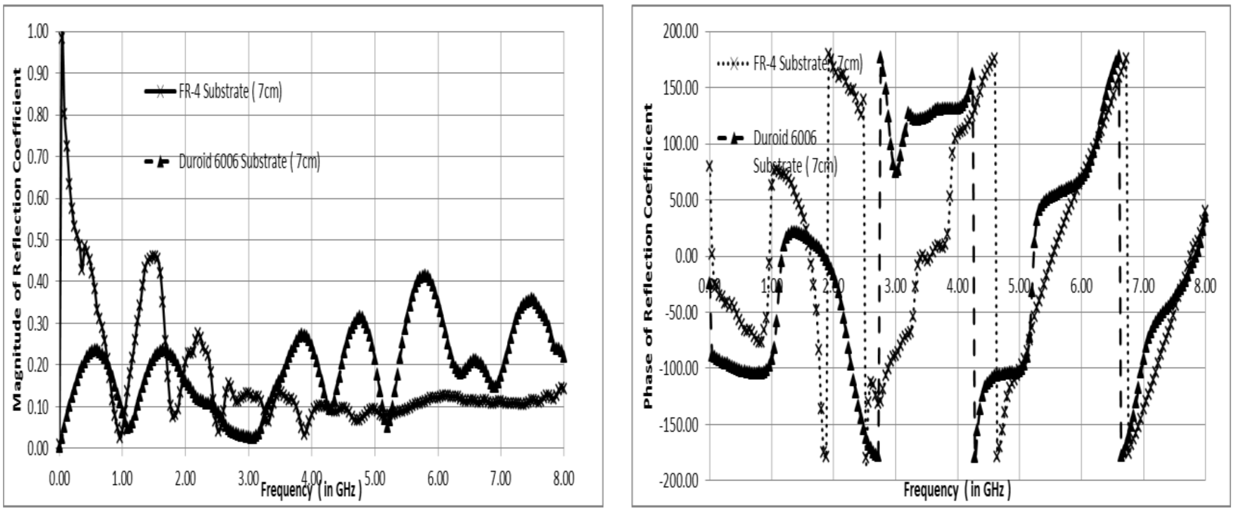

b)

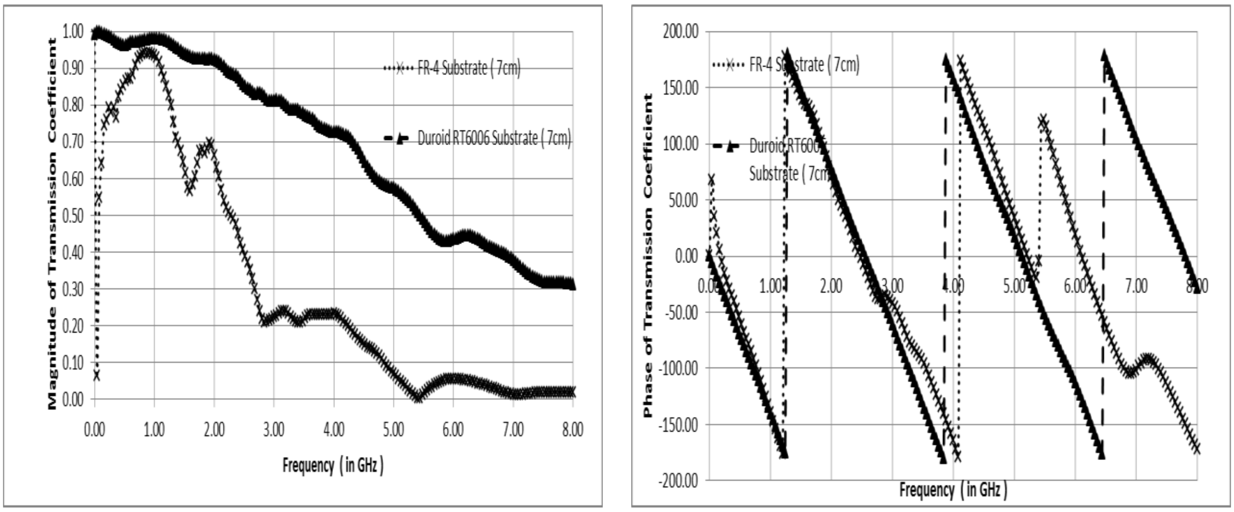

Figure 4.11.2 a) Reflection Coefficient & b) Transmission Coefficient for sample Acetone against frequency

a)

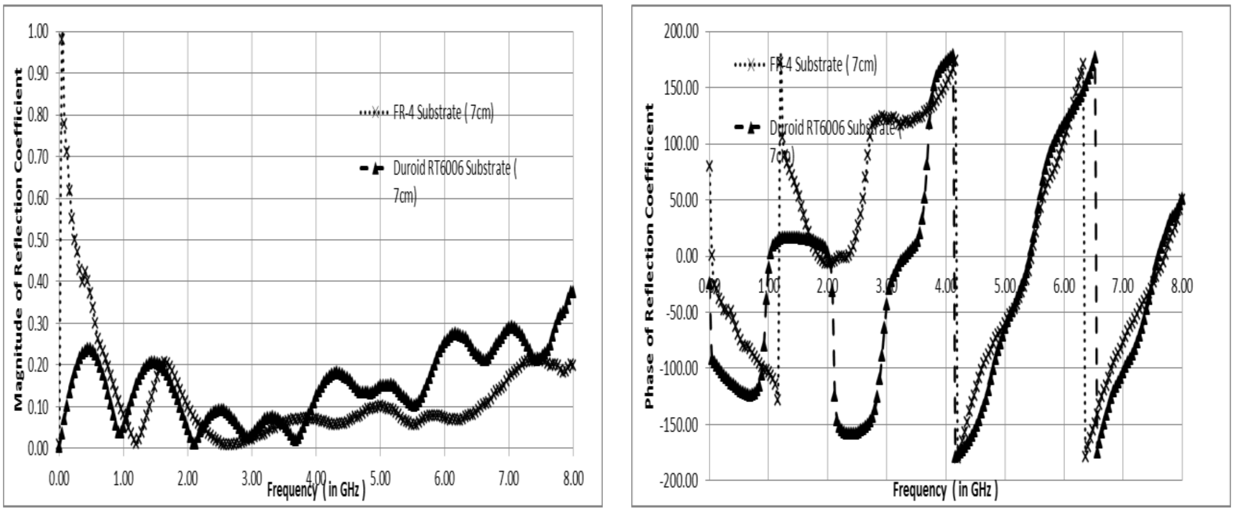

b)

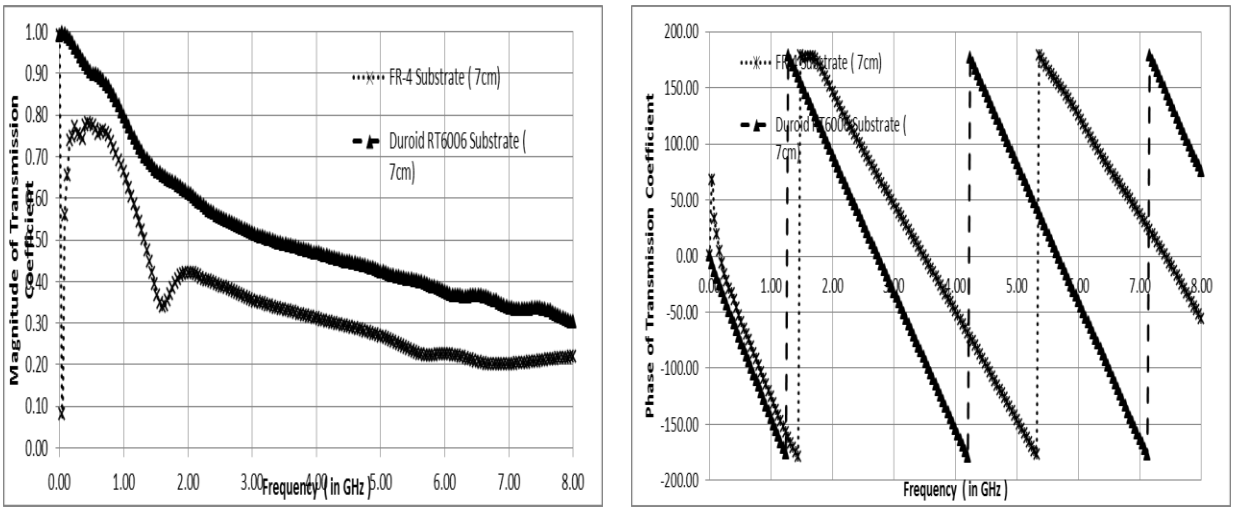

Figure 4.11.3 a) Reflection Coefficient & b) Transmission Coefficient for sample Ethanol against frequency

a)

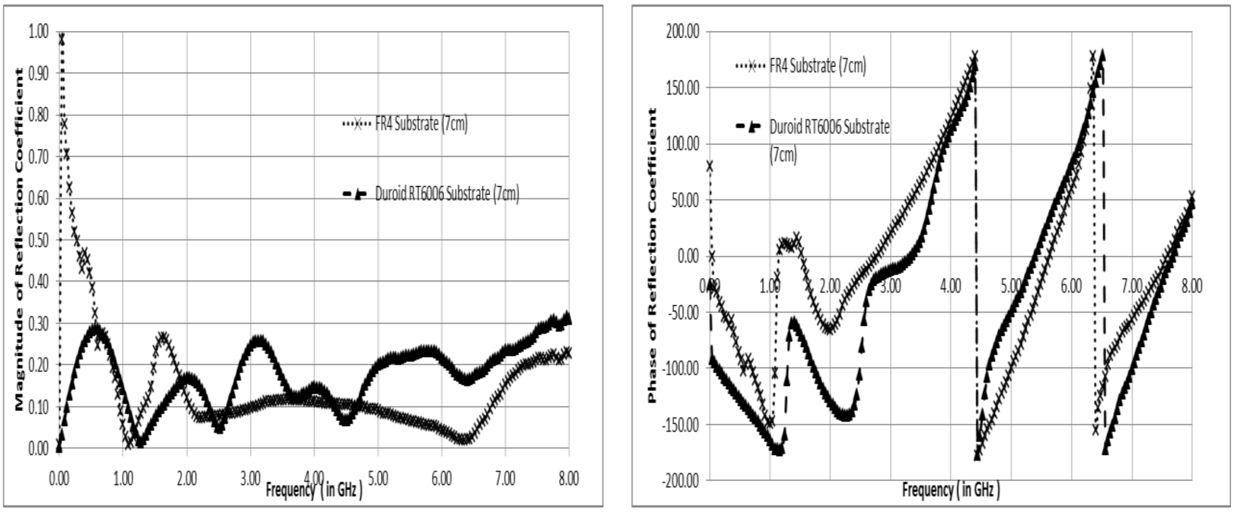

b)

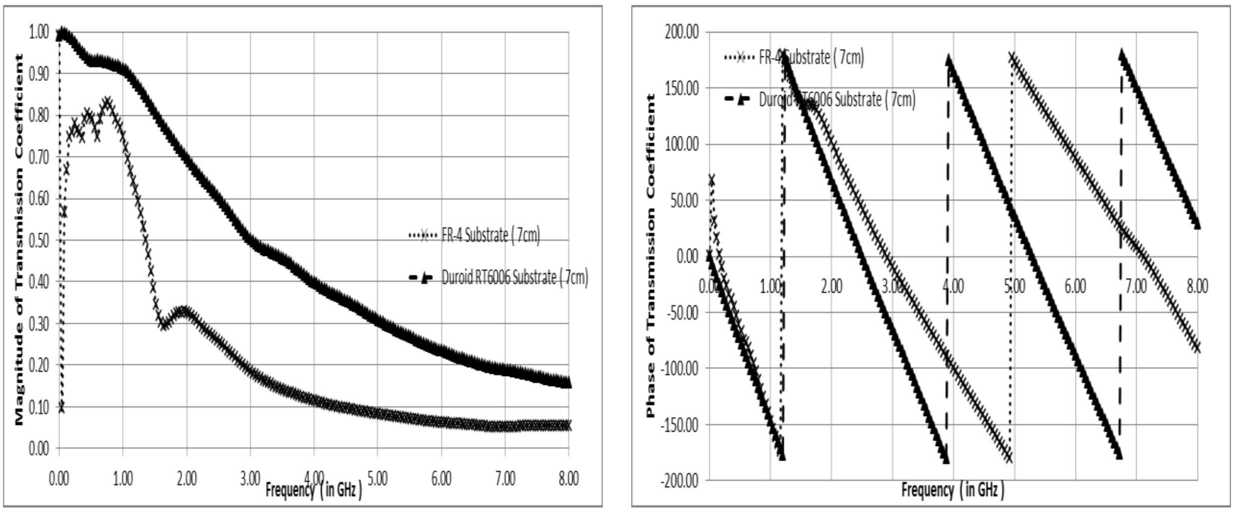

Figure 4.11.4 a) Reflection Coefficient & b) Transmission Coefficient for sample Methanol against frequency

a)

b)

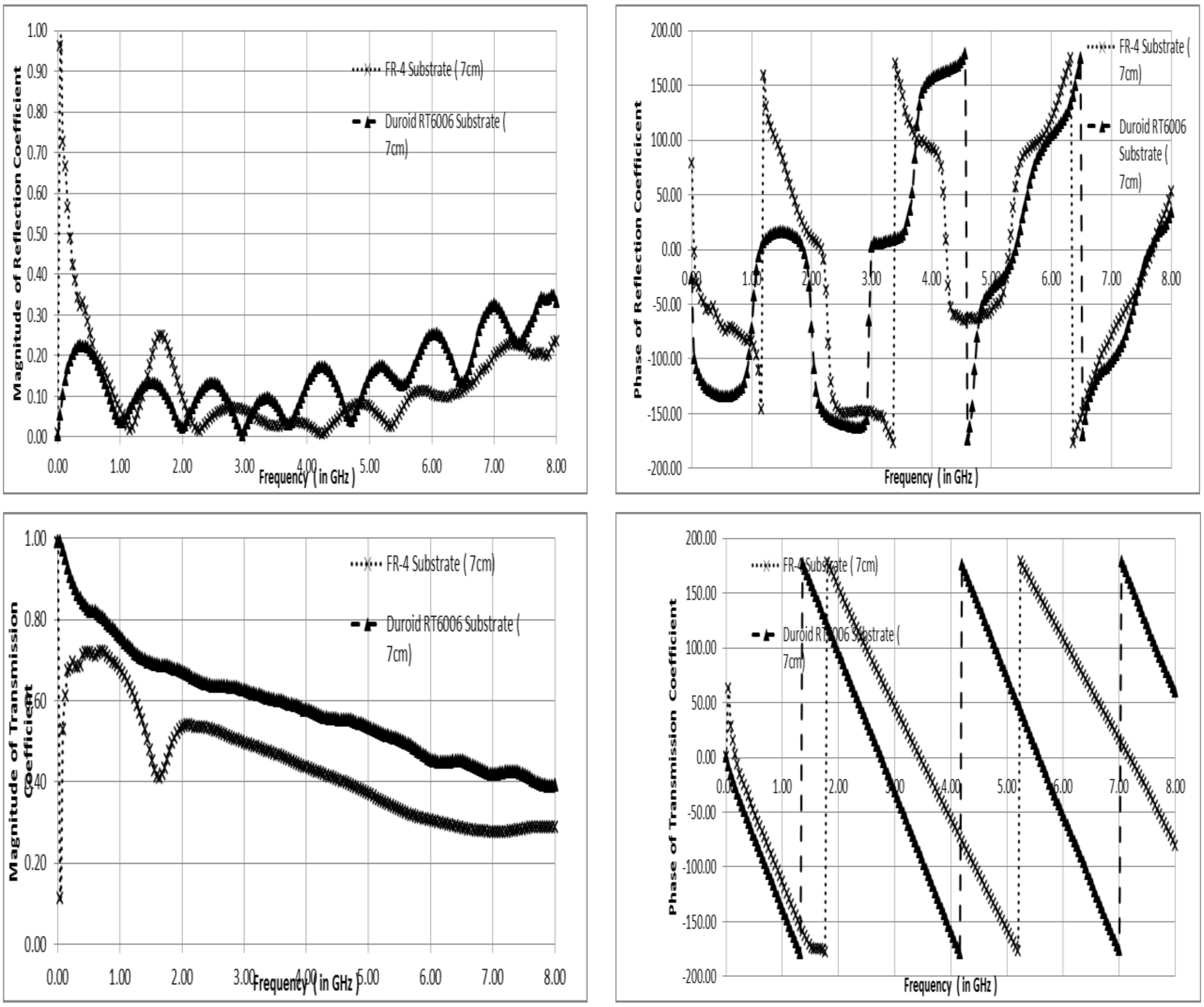

Figure 4.11.5 a) Reflection Coefficient & b) Transmission Coefficient for sample Glycerol against frequency

a)

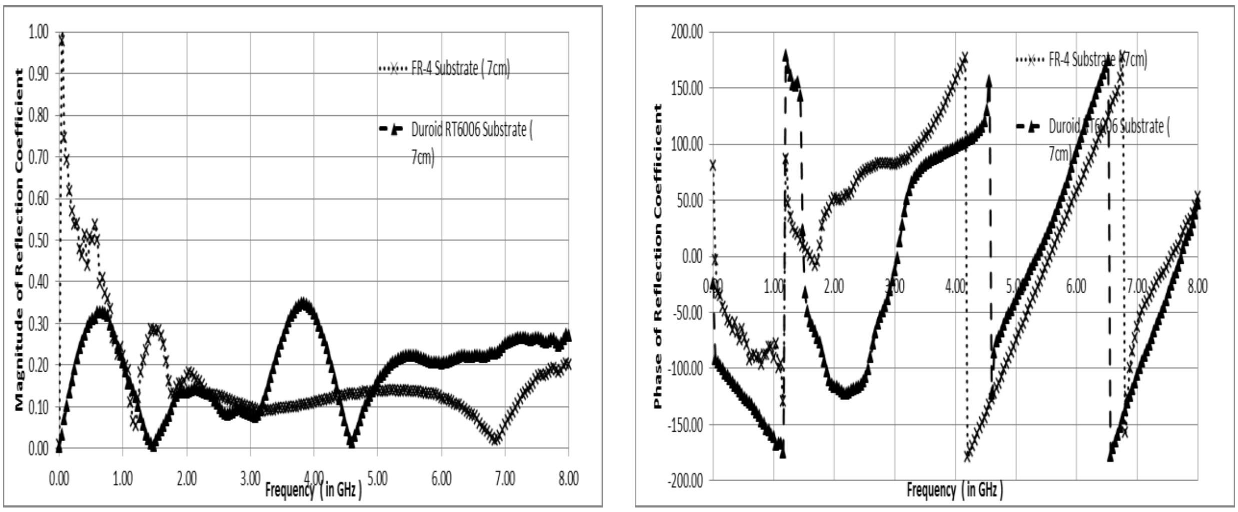

b)

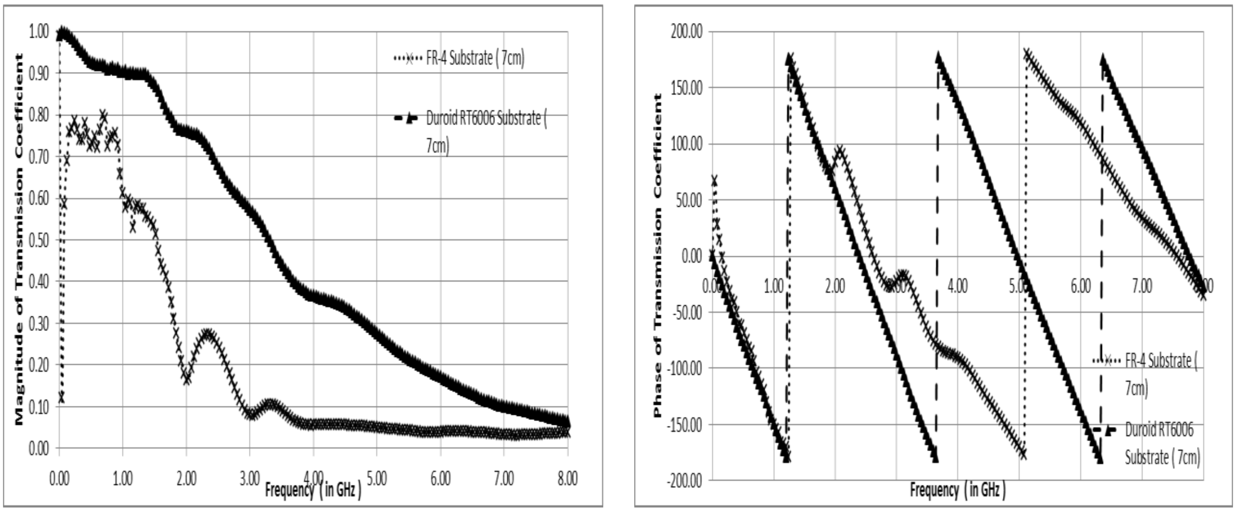

Figure 4.11.6 a) Reflection Coefficient & b) Transmission Coefficient for sample Water against frequency

4.12 Comparison of measured data and simulated data for FR - 4 substrate – 4cm

By comparing between the simulated and measured data for each sample the change in the magnitude of reflection coefficient is higher when the frequency increases especially from 3 GHz. But in the case of air sample, the magnitude increases along with the frequency of EM wave increase. This can be justifying the presence of loss factor when the EM wave passing through while in the simulation , loss of energy is not consider as the frequency increases.

a)

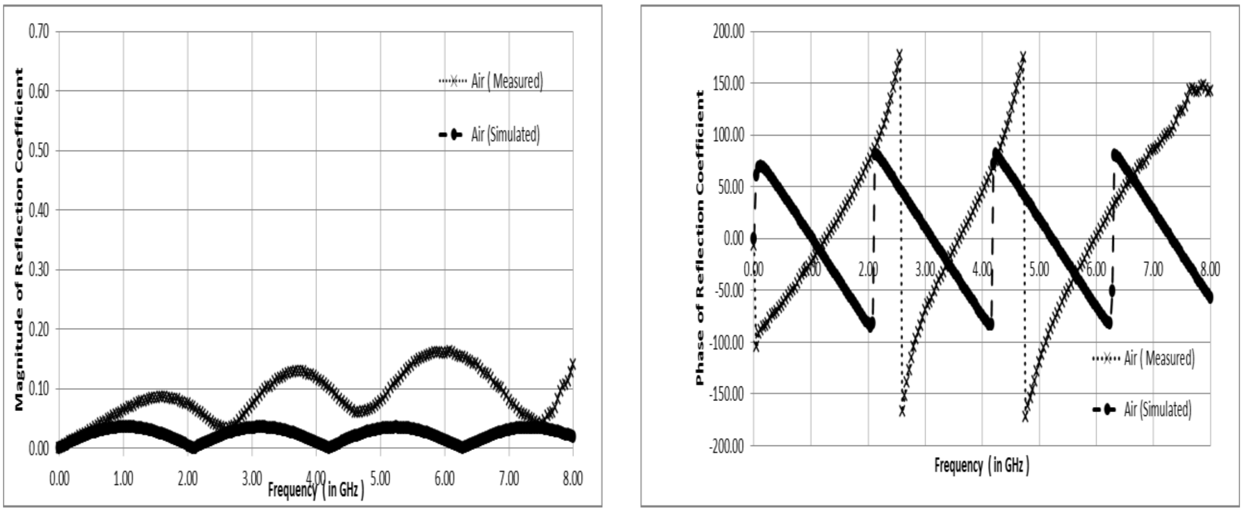

b)

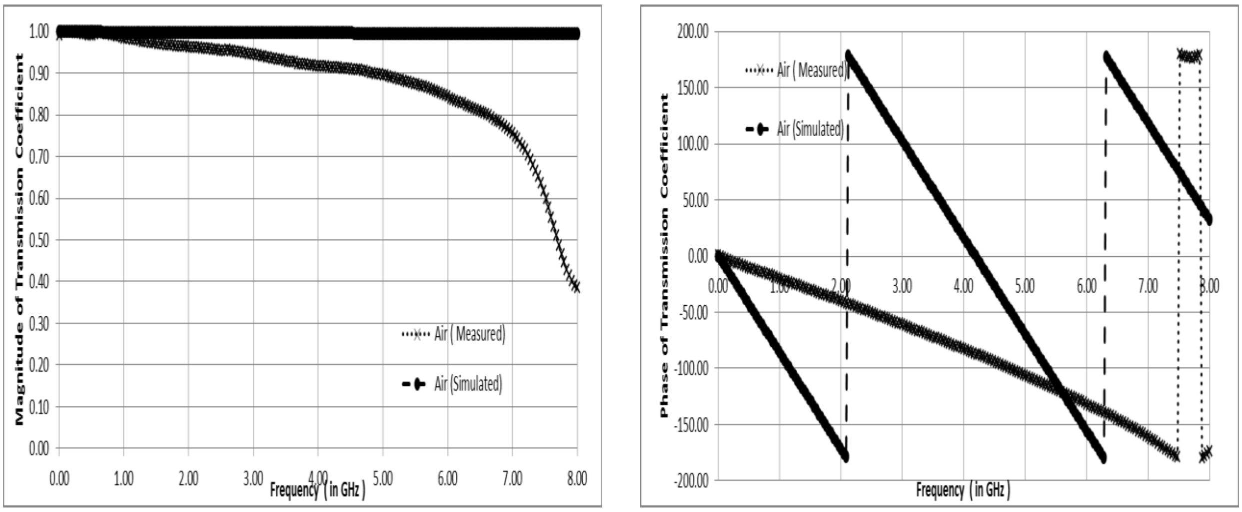

Figure 4.12.1 a) Reflection Coefficient & b) Transmission Coefficient for sample Air against frequency

a)

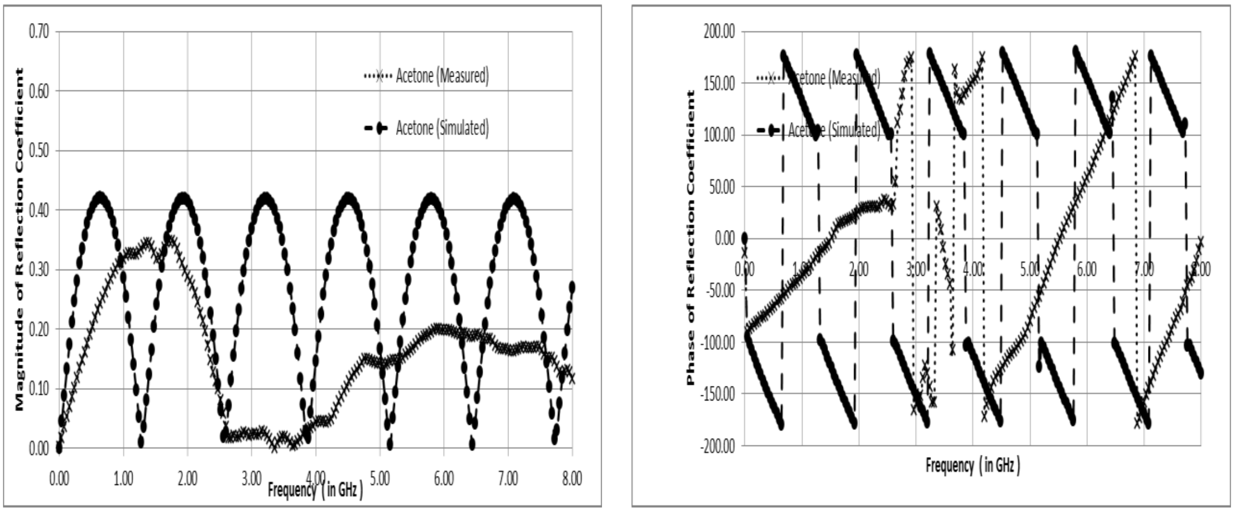

b)

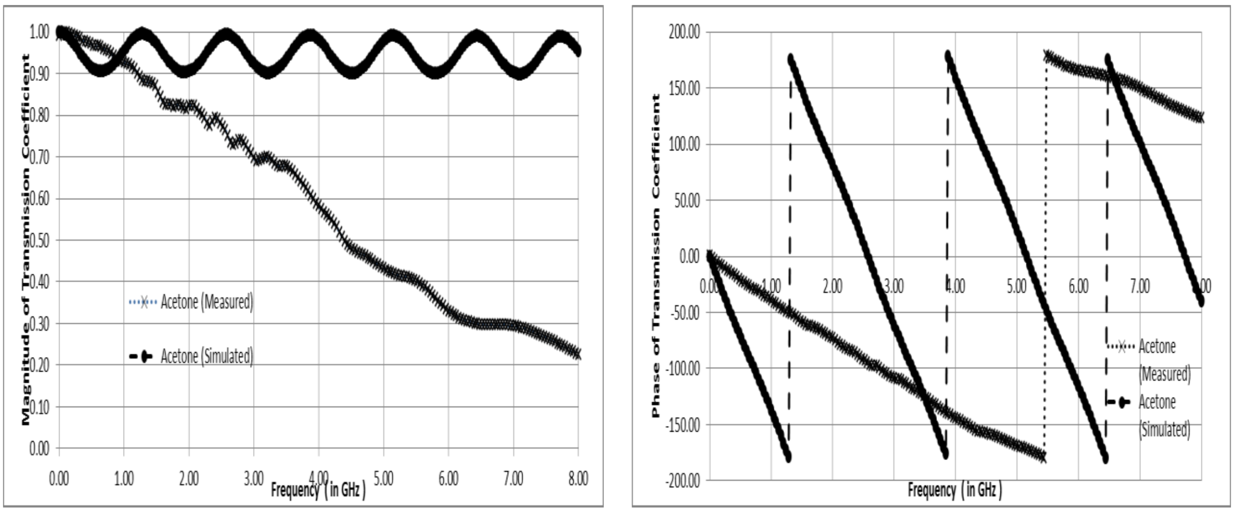

Figure 4.12.2 a) Reflection Coefficient & b) Transmission Coefficient for sample Acetone against frequency

a)

b)

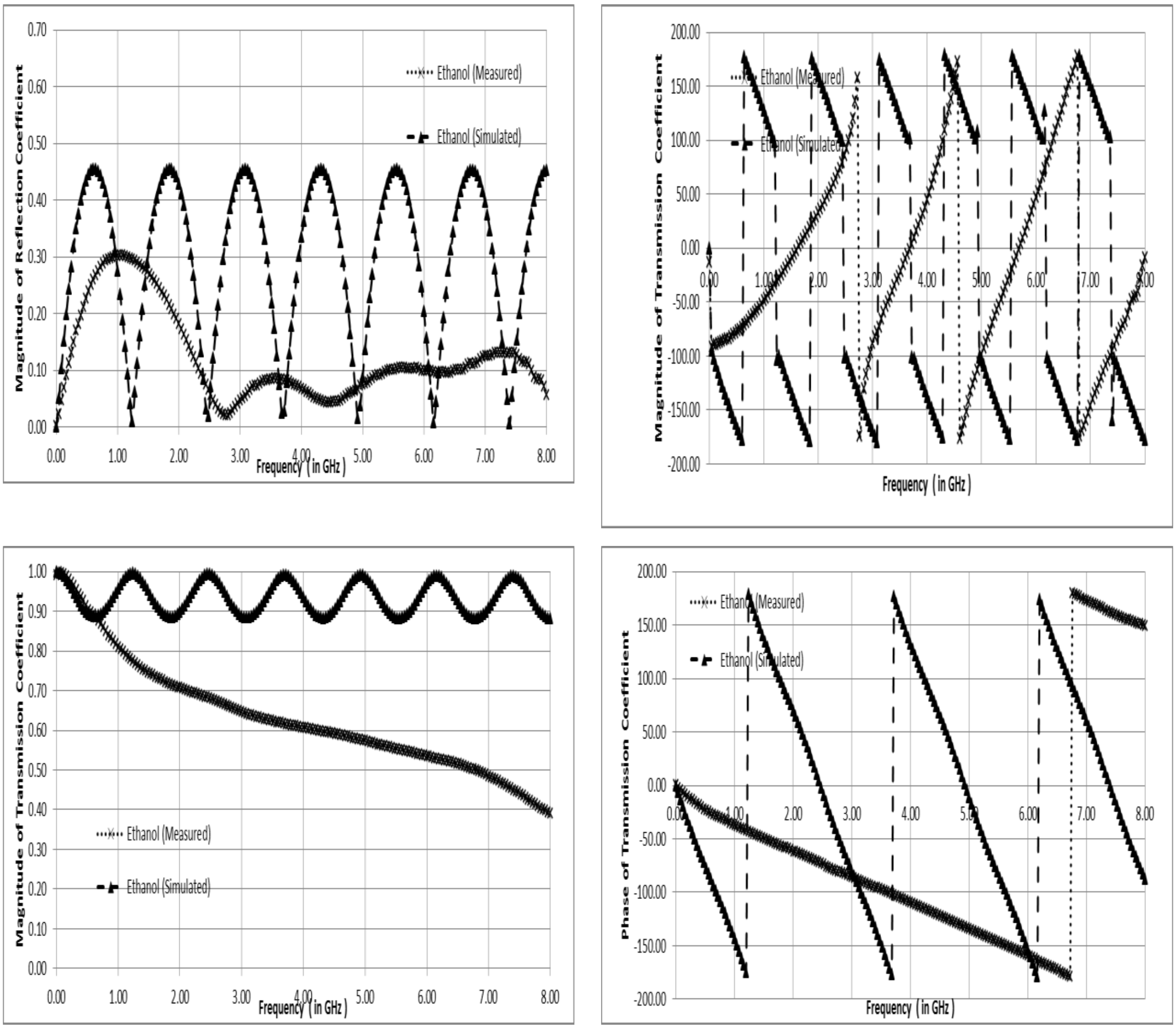

Figure 4.12.3 a) Reflection Coefficient & b) Transmission Coefficient for sample Ethanol against frequency

a)

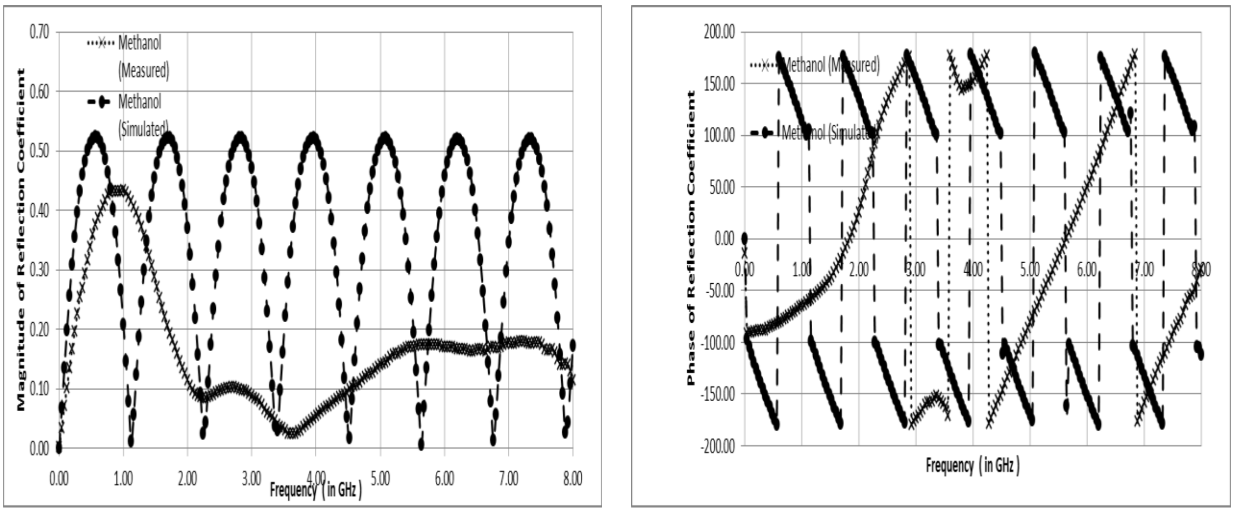

b)

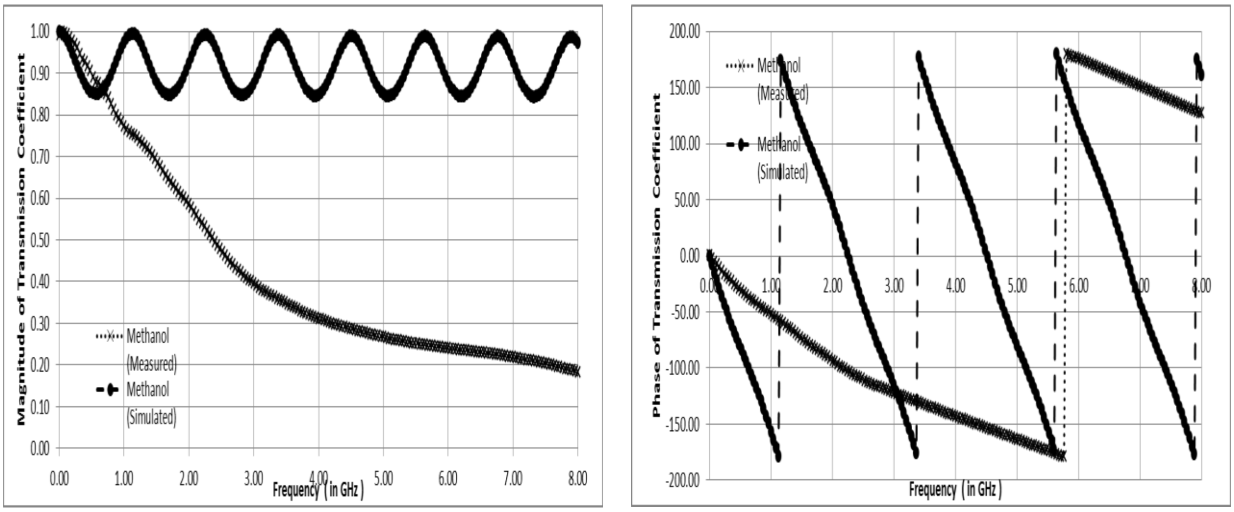

Figure 4.12.4 a) Reflection Coefficient & b) Transmission Coefficient for sample Methanol against frequency

a)

b)

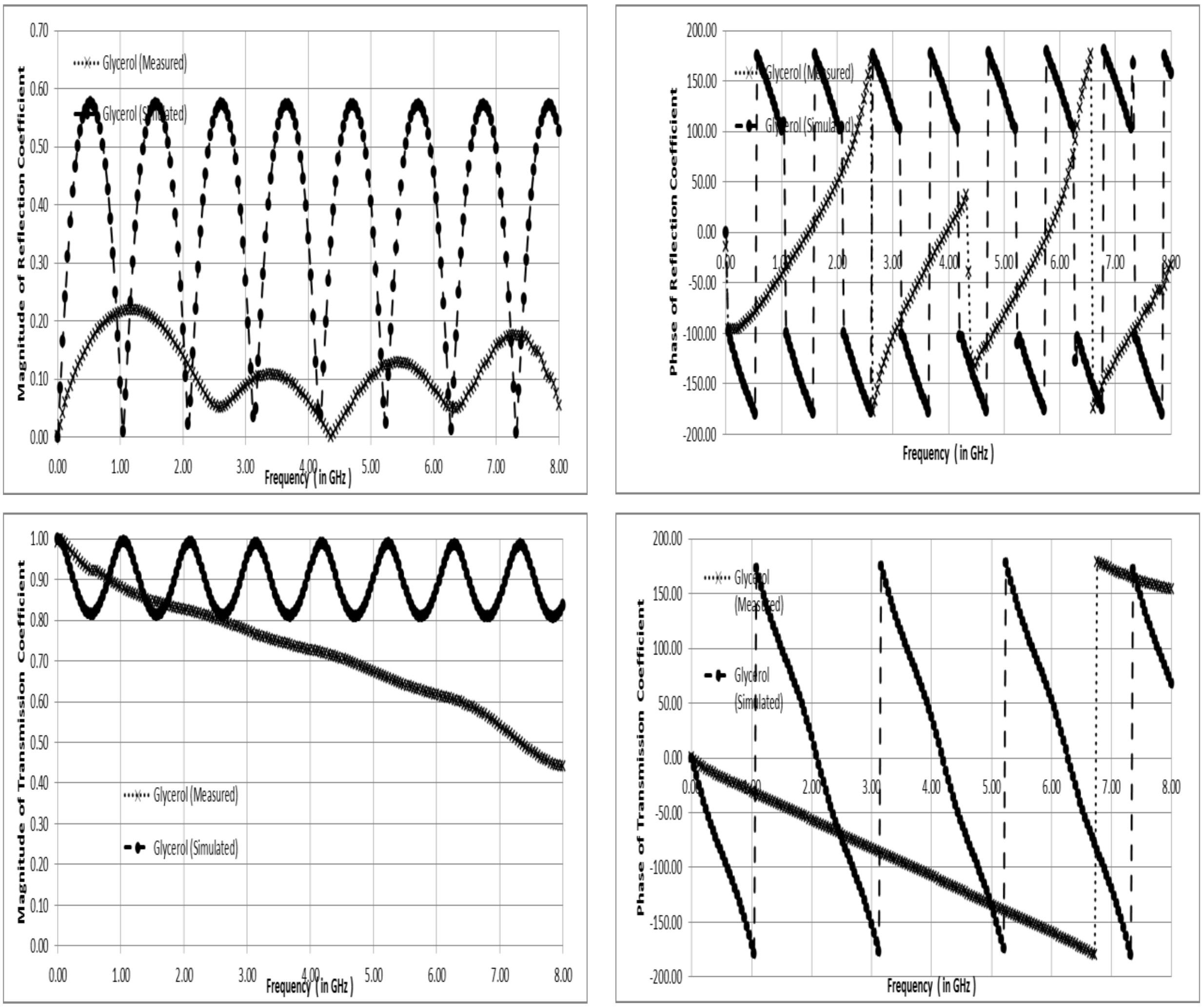

Figure 4.12.5 a) Reflection Coefficient & b) Transmission Coefficient for sample Glycerol against frequency

a)

b)

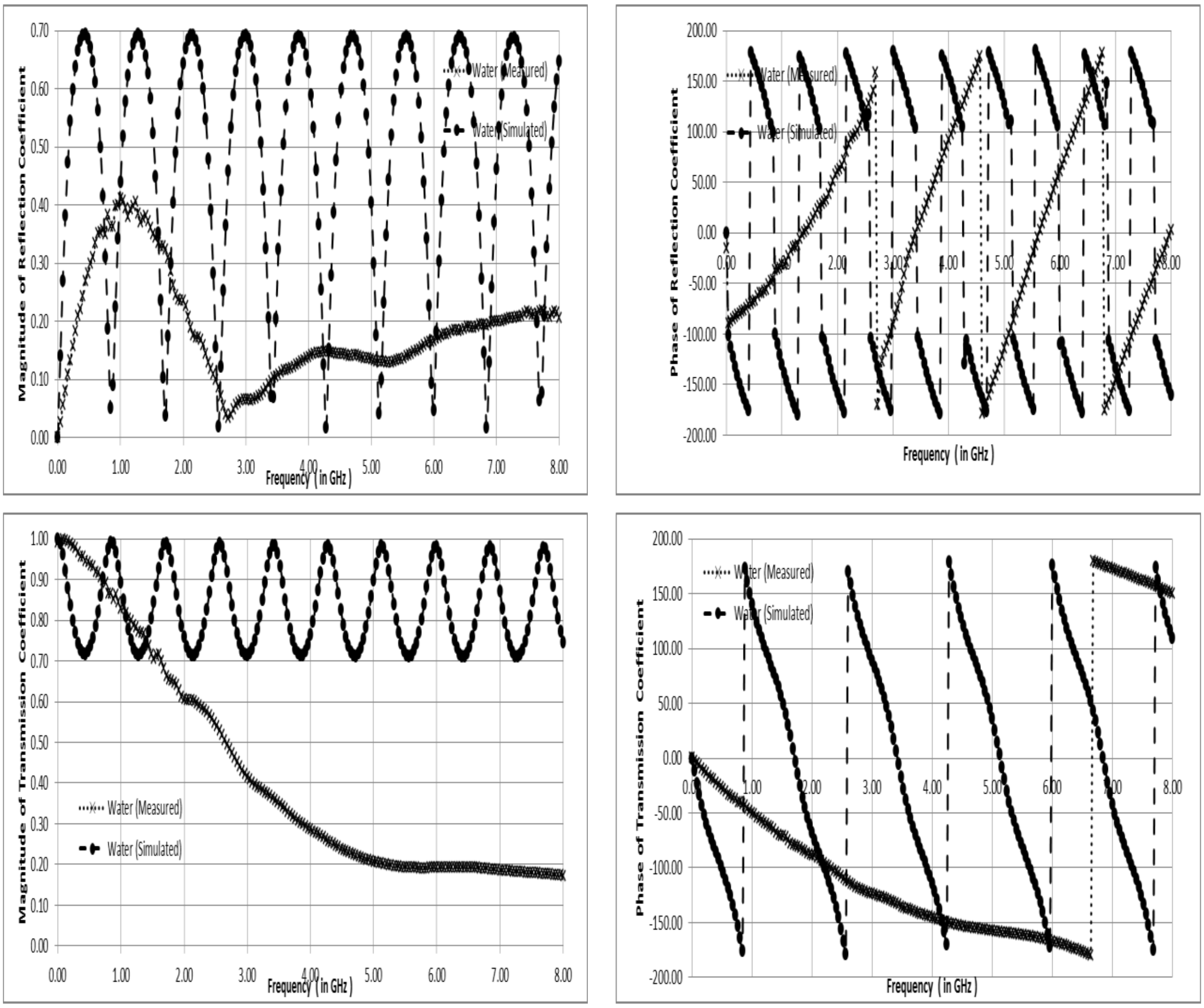

Figure 4.12.6 a) Reflection Coefficient & b) Transmission Coefficient for sample Water against frequency

4.13 Comparison of measured data and simulated data for FR - 4 substrate – 7cm

As for this section is for the line length of 7c m between the measured data and simulated data is shown in the following graphs. On top of having error in the practical design of the microstrip line, the simulated data from the software does not consider the factor of the occurrence of the energy loss over the frequency range.

a)

b)

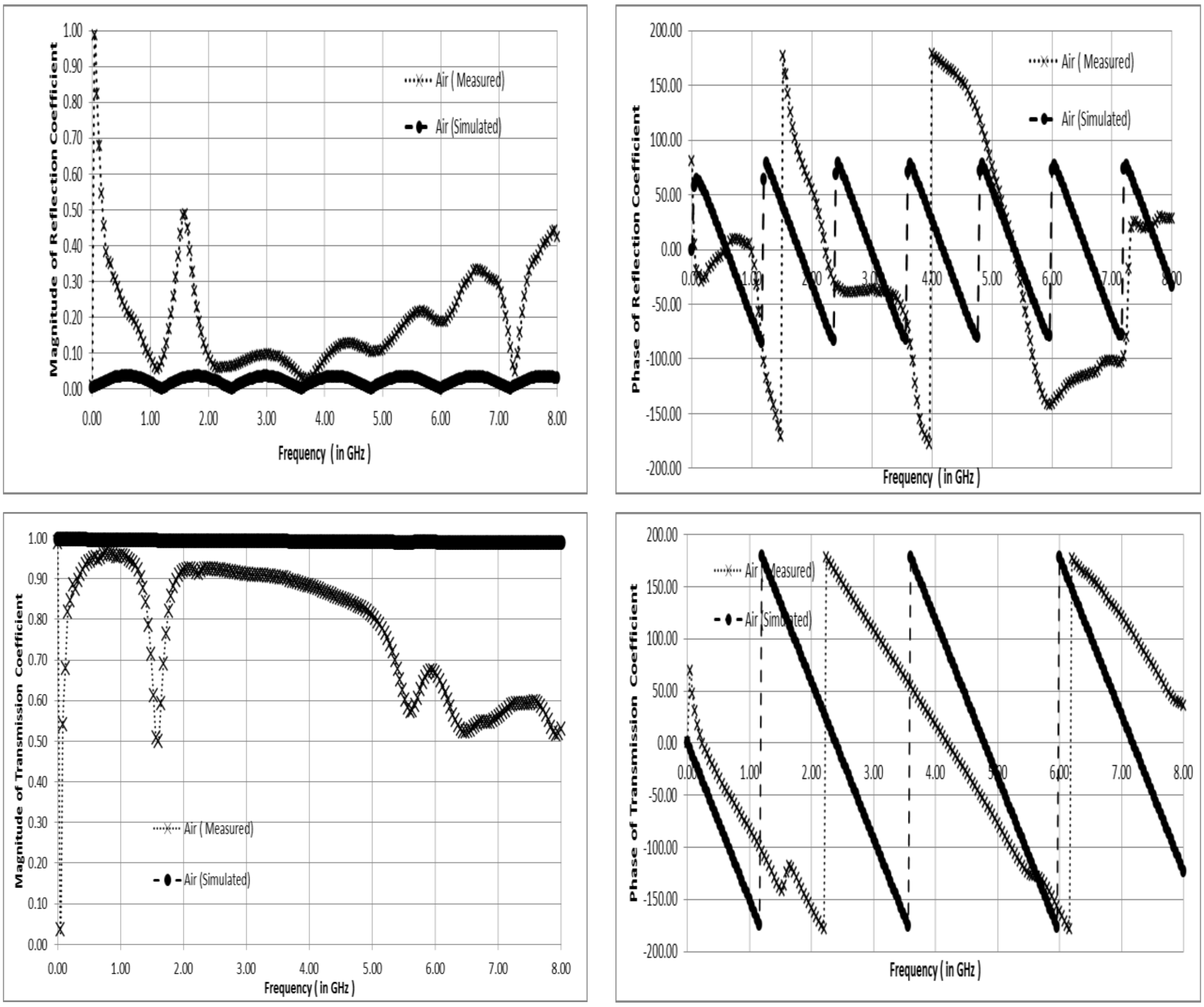

Figure 4.13.1 a) Reflection Coefficient & b) Transmission Coefficient for sample Air against frequency

a)

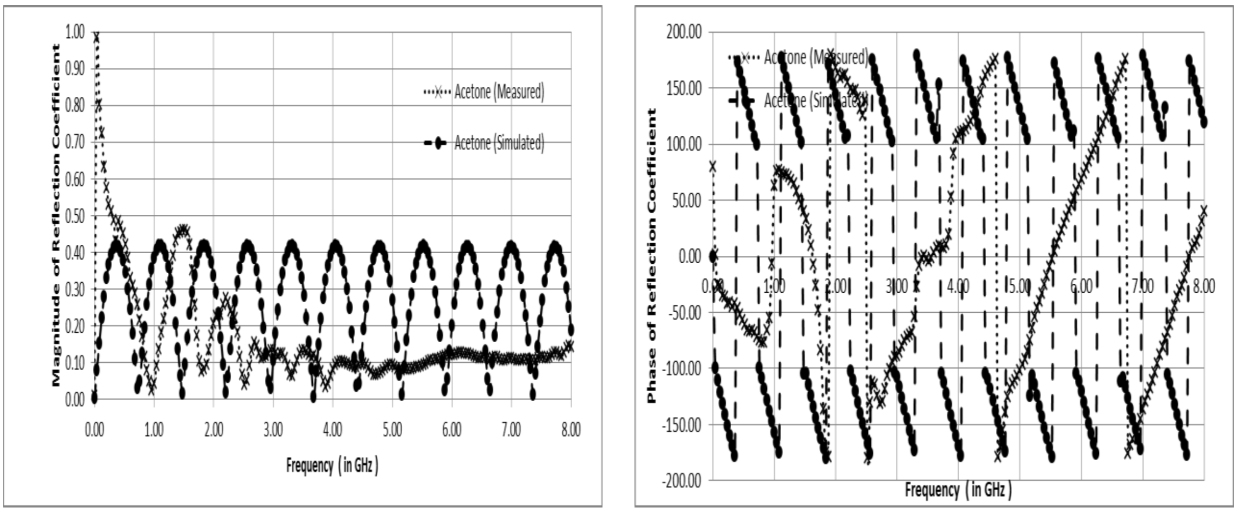

b)

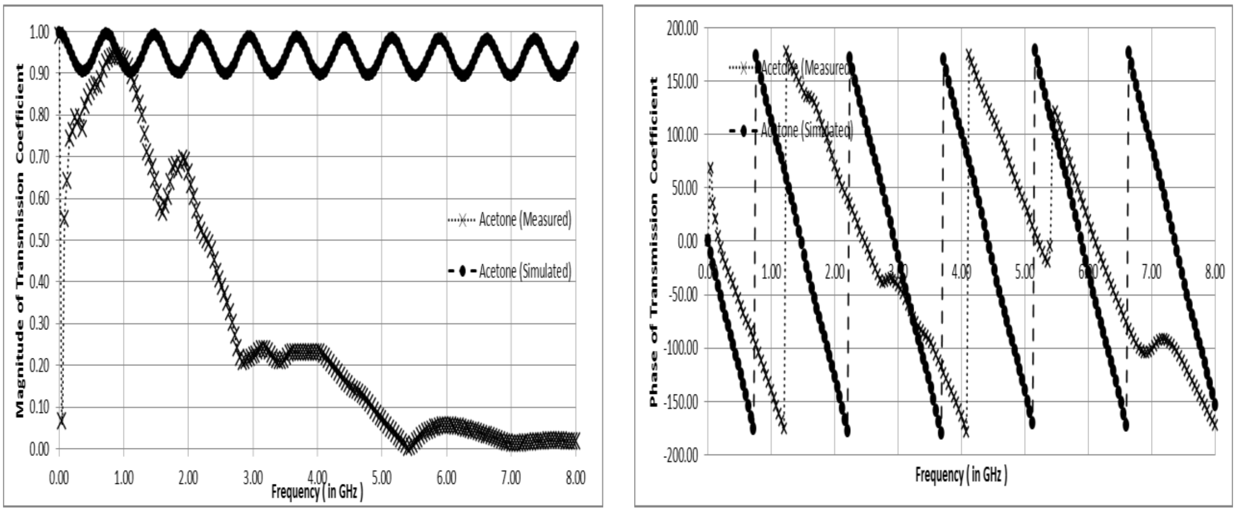

Figure 4.13.2 a) Reflection Coefficient & b) Transmission Coefficient for sample Acetone against frequency

a)

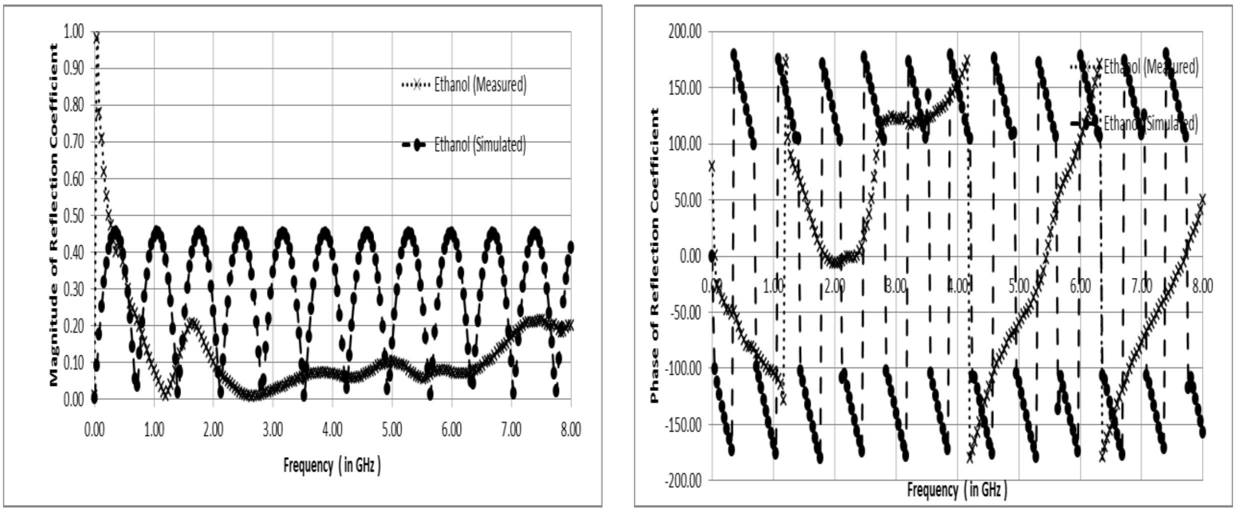

b)

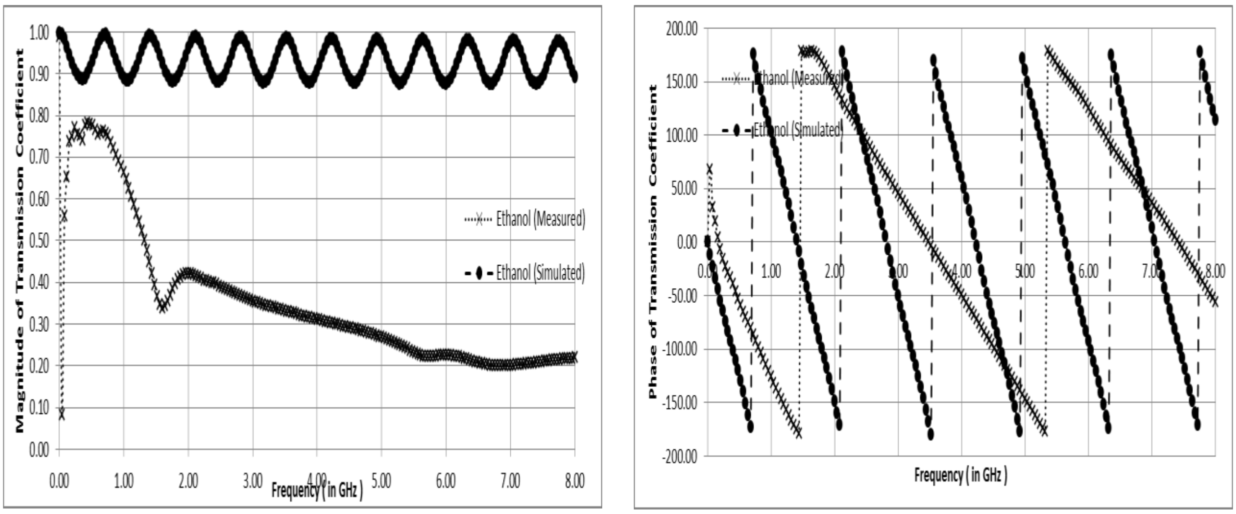

Figure 4.13.3 a) Reflection Coefficient & b) Transmission Coefficient for sample Ethanol against frequency

a)

b)

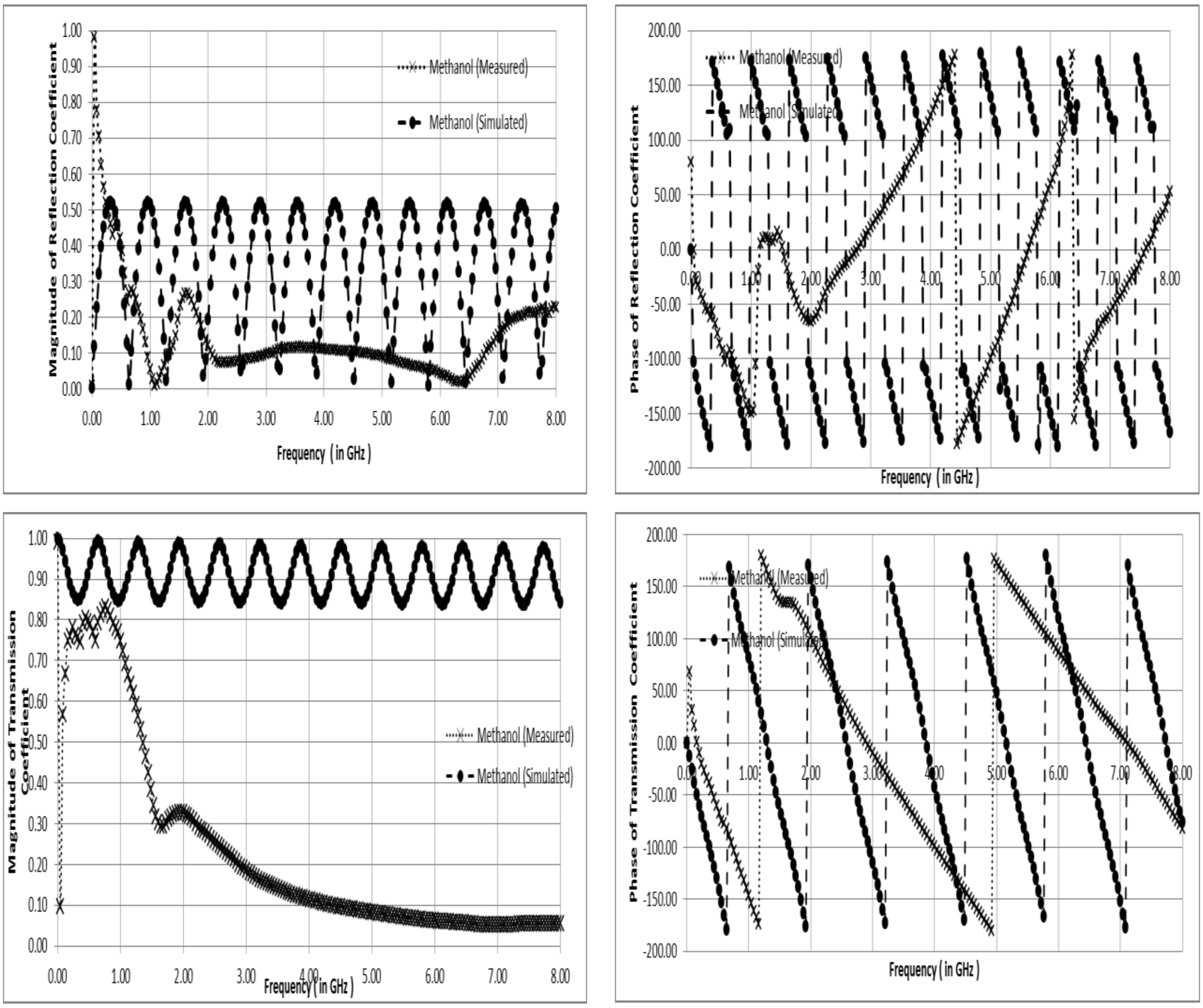

Figure 4.13.4 a) Reflection Coefficient & b) Transmission Coefficient for sample Methanol against frequency

a)

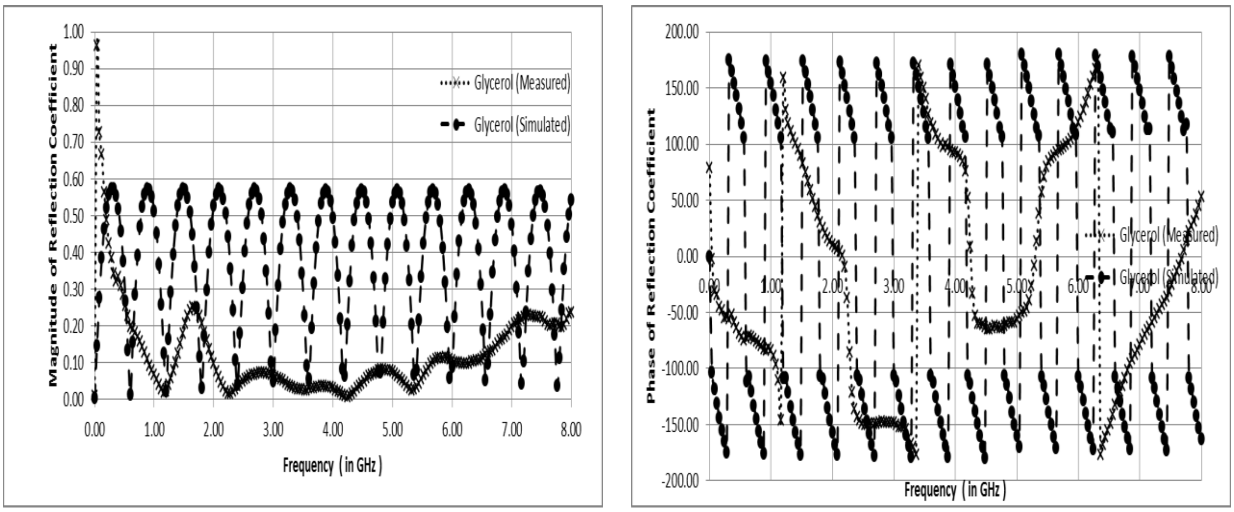

b)

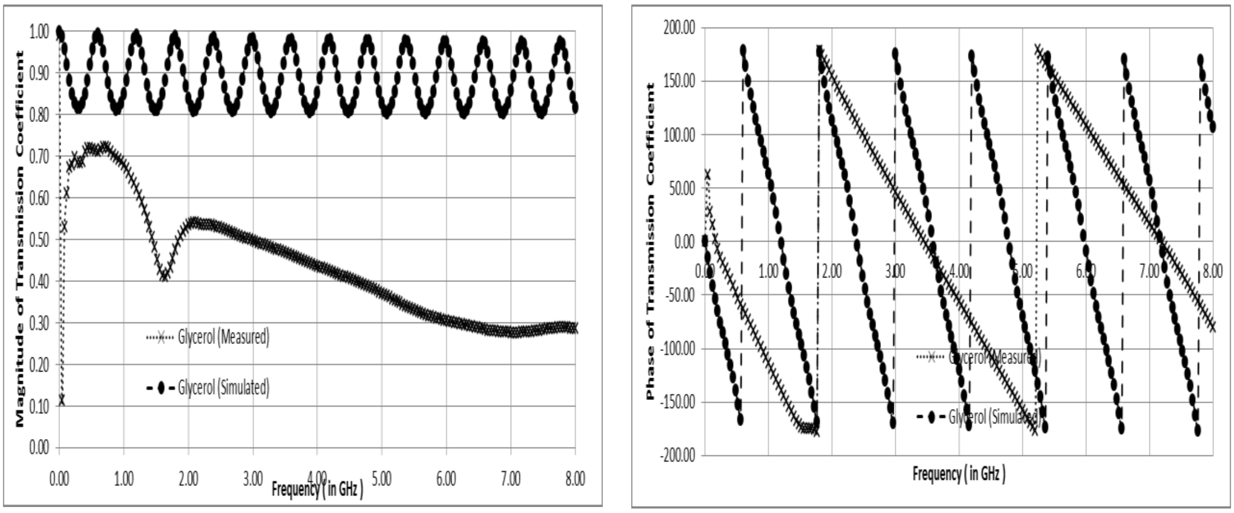

Figure 4.13.5 a) Reflection Coefficient & b) Transmission Coefficient for sample Glycerol against frequency

a)

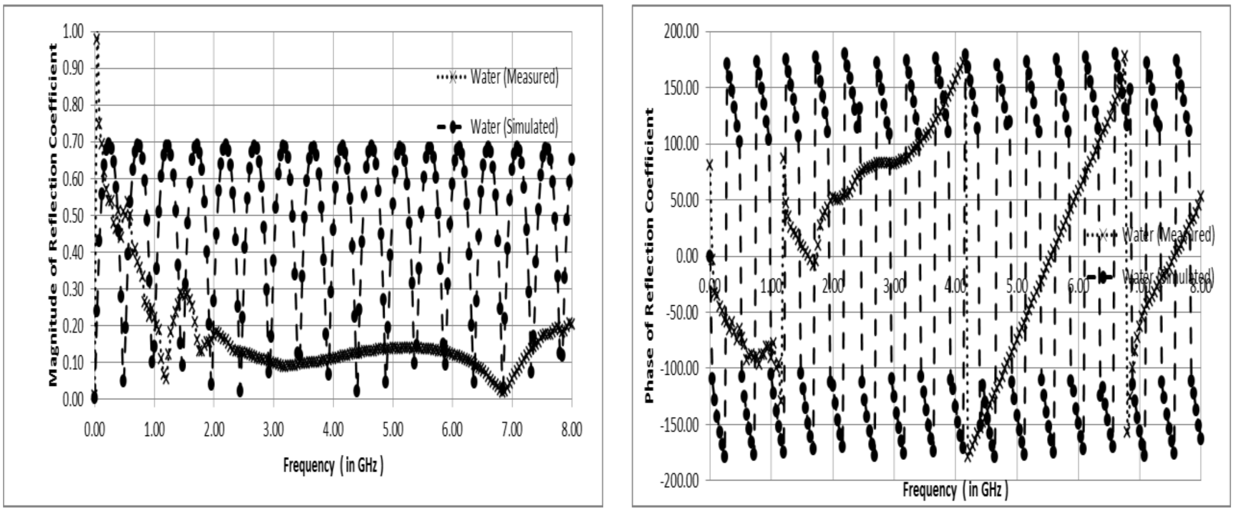

b)

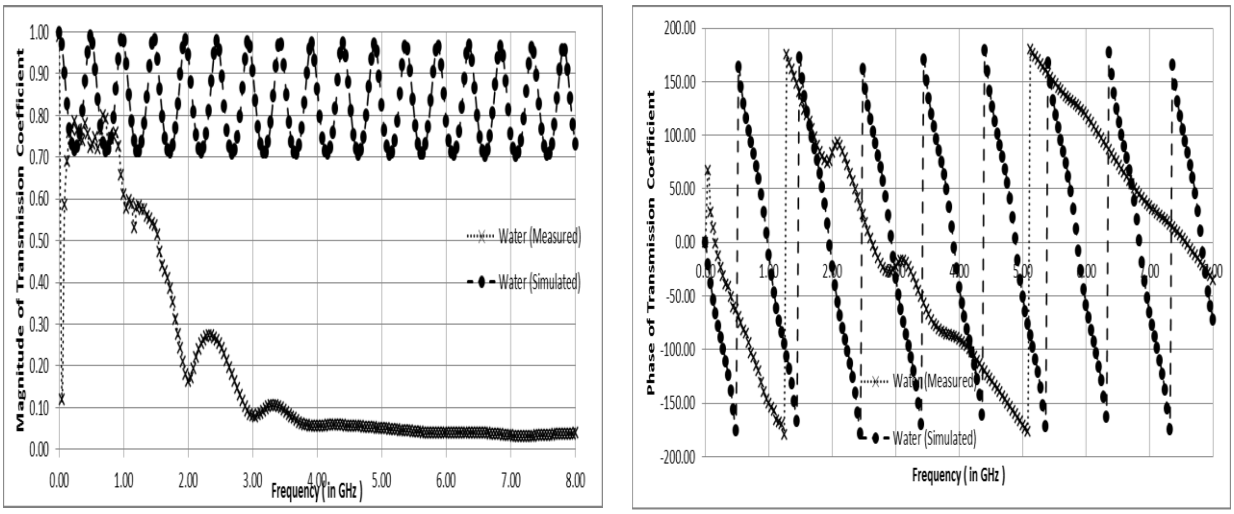

Figure 4.13.6 a) Reflection Coefficient & b) Transmission Coefficient for sample Water against frequency

4.14 Analysis Overview of Measurement Data

From overall results that been obtained, it can be observed that with the different line lengths of the microstrip line sensor shows different result in the magnitude response and phase response for transmission coefficient and reflection coefficient through the permittivity of sample that varies. On top of that, the curvature effect of the RT Duroid 6006 substrate has been added along to it.

For the different lengths being featured in the design of the microstrip line sensor, it can be perceived that the difference occurs in the rate of recurrence in the magnitude response as the EM wave that pass through the medium with wider wave being propagated. The phase response, there is presence of phase shift as the line length of the sensor increases.

As the permittivity of the sample increases, the responses given are changing due to the fact of the EM wave travelling through two different medium. This is based on the existence of the polarability in the liquid samples used. When an electric field is applied to the dielectric, then the polarization occurs in which each of the electric dipole of liquid molecules tends to align along with direction of the applied field. But as the frequency increases, the electric dipole of liquid sample delays behind the applied field.

Regarding the curvature effect of the sensor, the magnitude response and phase response given through the transmission coefficient and reflection coefficient respectively have slight difference as the frequency increases. It can be justified that the performance is obtainable despite of the shape of the sensor. The connectivity from port 1 to port 2 is present and the substrate used does not provide any defect to the transmission line on it. However, there is no sequential order of performance in association with the curvature effect of the sensor aimed at different samples permittivity and followed by the different line lengths of the sensor.

CHAPTER 5

CONLUSION AND RECOMMENDATIONS

5.1 Conclusion

For this thesis, a 50 ohm microstrip line sensor with using FR- 4 and RT Duroid 6006 substrates were used in designing for measuring permittivity of sample within the range of frequency that falls under the electromagnetic wave. At prior a simulation for both substrates used is done though AWR Design Environment alongside TX-line to obtain the optimum width of the line sensor. The attained optimum widths are 3.1370 mm and 0.9316 mm for FR -4 and RT Duroid 6006 substrates respectively to achieving matching impedance condition.

The performance of the sensors in terms of the both reflection and transmission coefficients which are presented in magnitude response and phase response individually were analysed in the chapter 4. It is observed that for each sample there is no sequential formation for from flat to different bending angle. Due to this, forming of empirical formula at a specified EM wave frequency range between the transmission coefficient, reflection coefficient and the permittivity of liquid sample is unable to achieve.

5.2 Recommendations

Emphasising on the equipment being used which is the VNA network analyser is expensive and high sensitivity. It is difficult to use more frequently as it has extreme level of prone to cause damage the equipment. Therefore, it would better to have portable version of this equipment. This idea is suggested as it would provide better convenient to carry out the experiment.

In terms of selecting the substrate to be used, it would be suggested that it is advisable to choose in regard to the sensitivity level at EM wave propagation of frequency. Consequently, it is recommended that a longer line length of the microstrip sensor as it has wider coverage followed by the several trials of the bending angle can be applied.

REFERENCES

Alexopoulos, N. & Nakatani, A., 1987. Cylindrical Substrate Microstrip Line Characterization. *IEEE Transactions on Microwave Theory and Techniques IEEE Trans. Microwave Theory Techn.*, 35(9), 843–849.

Anon, Dielectric Constants of some common Liquids. *Dielectric Constants Of Some Common Liquids*. Available from: http://www.engineeringtoolbox.com/liquid-dielectric-constants-d_1263.html [Accessed March 15, 2016].

Anon, 2014. Agilent Basics of Measuring the Dielectric Properties of Materials.

Chen, L.F., 2004. *Microwave electronics: measurement and materials characterization*, Chichester: Wiley.

Edwards, T.C., 1983. *Foundations for microstrip circuit design*, Chichester: Wiley.

Heuermann, H. & Schiek, B., 1993. The in-fixture calibration procedure line-network-network-LNN. *23rd European Microwave Conference, 1993*.

Hinojosa, J., 2001. S-parameter broad-band measurements on-microstrip and fast extraction of the substrate intrinsic properties. *IEEE Microwave and Wireless Components Letters IEEE Microw. Wireless Compon. Lett.*, 11(7), 305–307.

Konaka, T. et al., 1991. Relative permittivity and dielectric loss tangent of substrate materials for high-T c superconducting film. *Journal of Superconductivity J Supercond*, 4(4), 283–288.

Medina, F. & Horno, M., 1990. Spectral and variational analysis of generalized cylindrical and elliptical strip and microstrip lines. *IEEE Transactions on Microwave Theory and Techniques IEEE Trans. Microwave Theory Techn.*, 38(9), 1287–1293.

Narayanan, P.M., 2014. Microstrip Transmission Line Method for Broadband Permittivity Measurement of Dielectric Substrates. *IEEE Transactions on Microwave Theory and Techniques IEEE Trans. Microwave Theory Techn.*, 62(11), 2784–2790.

Nesimoglu, T. & Sabah, C., 2014. Characterization of metamaterials using a new design and measurement technique for microstrip circuit applications. *Proceedings of 2014 Mediterranean Microwave Symposium (MMS2014)*.

Nesimoglu, T., Karaali, M. & Sabah, C., 2014. Tuning the electric resonance of a metamaterial based single-sided S-Shaped resonator. *2014 20th International Conference on Microwaves, Radar and Wireless Communications (MIKON)*.

Pozar, D.M., 2005. *Microwave engineering*, Hoboken, NJ: J. Wiley.

Queffelec, P., Floc'h, M.L. & Gelin, P., 1998. Broad-band characterization of magnetic and dielectric thin films using a microstrip line. *IEEE Trans. Instrum. Meas. IEEE Transactions on Instrumentation and Measurement*, 47(4), 956–963.

Rolfes, I., 2007. Obstacle-based self-calibration techniques for the determination of the permittivity of liquids. *Adv. Radio Sci. Advances in Radio Science*, 5, 29–35.

Roy, R., Paulraj, A. & Kailath, T., 1986. ESPRIT--A subspace rotation approach to estimation of parameters of cisoids in noise. *IEEE Transactions on Acoustics, Speech, and Signal Processing IEEE Trans. Acoust., Speech, Signal Process.*, 34(5), 1340–1342.

Sheen, J., 2005. Study of microwave dielectric properties measurements by various resonance techniques. *Measurement*, 37(2), 123–130.

Sheng, X., Yung, E. & Chan, C., Effect of finite-width curved substrate to microstrip transmission line. *1999 Asia Pacific Microwave Conference. APMC'99. Microwaves Enter the 21st Century. Conference Proceedings (Cat. No.99TH8473)*.

Solomons, G. & Fryhle, C., 2000. *Organic Chemsitry*, New York: John Wiley & Sons

Veselago, V.G., 1968. THE ELECTRODYNAMICS OF SUBSTANCES WITH SIMULTANEOUSLY NEGATIVE VALUES OF ϵ AND μ. *Soviet Physics Uspekhi Sov. Phys. Usp.*, 10(4), 509–514.

Weisshaar, A. & Tripathi, V., 1990. Perturbation analysis and modeling of curved microstrip bends. *IEEE Transactions on Microwave Theory and Techniques IEEE Trans. Microwave Theory Techn.*, 38(10), 1449–1454